NASA Contractor Report 185185

A Radiological Assessment of Nuclear Power and Propulsion Operations near Space Station Freedom

Wesley E. Bolch, J. Kelly Thomas, K. Lee Peddicord, Paul Nelson,
David T. Marshall, and Donna M. Busche
Texas A & M University
College Station, Texas

March 1990

Prepared for
Lewis Research Center
Under Grant NAG 3-944

National Aeronautics and
Space Administration

Contractor Report,
(Texas A&M Univ.)
Unclas

NASA Contractor Report 185185

A Radiological Assessment of Nuclear Power and Propulsion Operations near Space Station Freedom

Wesley E. Bolch, J. Kelly Thomas, K. Lee Peddicord, Paul Nelson,
David T. Marshall, and Donna M. Busche
Texas A & M University
College Station, Texas

March 1990

Prepared for
Lewis Research Center
Under Grant NAG 3-944

National Aeronautics and
Space Administration

ACKNOWLEDGEMENTS

The authors would like to gratefully acknowledge the assistance and guidance of several individuals at NASA's Lewis Research Center (LeRC) and Johnson Space Center (JSC). In particular, the authors would like to thank Steve M. Stevenson (LeRC), the Project Manager for this study, and Alan J. Willoughby of the Analex Corporation, Cleveland, Ohio. Additional thanks are extended to Kurt Hack (LeRC) for verification of vehicle trajectories, Stan Borowski (LeRC) for NTR mission parameters, Alva Hardy (JSC) for information on geomagnetic fields, Stuart Nachtwey (JSC) for information on doses from natural space radiations, and Tom Marcille of the General Electric Company, San Jose, for SP-100 reactor source terms. This work was supported by the Advanced Space Analysis Office, NASA Lewis Research Center, under Grant NAG 3-944 with the Texas Engineering Experiment Station, Texas A&M University.

PRECEDING PAGE BLANK NOT FILMED

PAGE iii INTENTIONALLY BLANK

TABLE OF CONTENTS

PRECEDING PAGE BLANK NOT FILMED

PAGE iv INTENTIONALLY BLANK

CHAPTER 1

INTRODUCTION

INTRODUCTION

The chief purpose of this project was to identify scenarios involving the use of nuclear power systems in the vicinity of the Space Station Freedom (SSF) and quantify their radiological impact on the SSF crew. Several of the scenarios developed relate to the use of SSF as an evolutionary transport node for lunar and Mars missions. The use of nuclear power on co-orbiting platforms and the storage and handling issues associated with radioisotopic power systems were also explored as they relate to SSF.

In general, the analysis methods employed in this work are simplified and the results are intended to aid mission planners and identify operational and design constraints on SSF associated with the use of nuclear power sources. However, the analysis procedures developed in this work can be extended to provide more rigorous results and this will be pursued in a follow-on project.

RADIATION DOSE LIMITS

A central philosophy in these analyses was the utilization of a dose budget concept. The radiation source terms and resulting dose from the natural space environment at SSF were first analyzed and determined as discussed in Chapter 2. Guidelines provided by a committee of the National Council on Radiation Protection and Measurements (NCRP) were employed to set a limit on the total dose to the SSF crew from both the natural radiation sources and nuclear systems. As described in Chapter 3, the difference between the total dose limit and the dose from natural sources defines the dose budget for the SSF crew. Given the radiation source terms associated with the nuclear power system in any given scenario, the dose budget may then be employed to identify and quantify constraints on the interaction of the system with SSF. Chapter 4 describes the radiation source terms associated with the nuclear reactor systems examined in this work and Chapter 8 defines those for the radioisotopic systems analyzed. This approach was found to be extremely useful and its application to other mission classes, such as lunar and Mars bases, is highly recommended.

SCENARIOS EXAMINED

The scenarios developed and examined in this work are believed to span the range of likely interaction between nuclear power systems and SSF. The values for the design and operational variables associated with these scenarios were selected based on consultation with the project staff at the NASA Lewis Research Center. When possible, sensitivity analyses were carried out to explore the effect of these variables on the radiological impacts of the system under study.

One of the chief interactions between SSF crew and nuclear systems will be with nuclear propulsion systems for lunar and Mars missions. Both nuclear thermal rockets (NTRs) and nuclear electric propulsion (NEP) vehicles were studied. The NERVA reactor was employed for the NTR missions and a scaled SP-100 class reactor was assumed for the NEP missions. The launch and return of these craft are addressed in Chapters 5 and 6, respectively. It was determined that reasonable separation distances between the vehicle and SSF and, for the return scenarios, reactor shutdown times prior to approaching SSF, would limit the dose to the SSF crew to acceptable limits. In fact, for the launch of Mars vehicles, it is likely that these separation distances will be smaller than those required to meet collision avoidance criteria.

As discussed in Chapter 7, operating reactors on co-orbiting platforms could also interact with SSF. Such reactors might, for example, be employed for electrolysis of water or for materials processing. As with the reactors on Mars vehicles, it was found that reasonable separation distances between the vehicle and SSF could be defined in order to limit the dose to the SSF crew. It was also determined that optimized platform construction could drastically reduce these distances. In the case of an electrolysis platform, placing the water tanks between the reactor and SSF would decrease the dose received by the SSF crew substantially.

Lastly, as described in Chapter 8, the storage of radioisotopic power systems on SSF was examined. Based on the results from this work, it appears that this would have very little radiological impact on the SSF crew and the only minor constraints are necessary to insure adequate radiation protection.

PORTABLE SHIELD CONCEPT

In all the scenarios examined, it appears that a portable shield located at SSF could serve to reduce the dose received from the nuclear system under study (see Chapter 9). Most nuclear systems that interact with SSF will not require a 4π man-rated shield to meet the radiation protection requirements of their own mission. For instance, the propellant tanks on the NTR Mars vehicle provide a large fraction of the crew shielding. Most of the reactors only utilize shadow or disk shields for the protection of the personnel and/or electronics associated with them. Thus, there may be little, if any, shielding between the reactor and SSF crew. The operational constraints reported in this work were developed under this assumption. Although these operational constraints are not unacceptable, if shielding were available they could be relaxed. It would be redundant and prohibitively expensive to place this additional shielding on each of the systems that will interact with SSF. Rather, this additional shielding should be kept at SSF and utilized during periods of interaction with nuclear systems. All the scenarios examined in this work would derive a benefit from this approach.

Furthermore, there will be periods when there are not any nuclear systems in the vicinity of SSF. During such periods of time, the portable shield could be placed around the SSF crew habitat module(s) in order to reduce the dose from natural sources. This would serve to increase the dose budget available for interaction with nuclear systems and is consistent with the radiation protection philosophy called ALARA which emphasizes that radiation exposures, regardless of their source, should be kept as low as reasonably achievable.

The principal investigators for this project are currently carrying out scoping studies of the portable shield concept with the support of NASA's Office of Exploration (OEXP). It is recommended that these studies be extended in the near future to include complete engineering analyses of the shield design and further definition of its role in reducing the SSF crew doses from natural sources.

CONCLUSIONS

The results from this study indicate that realistic scenarios do not exist which would preclude the use of nuclear power sources in the vicinity of SSF. The radiation dose to the SSF crew can be maintained at safe levels solely by implementing proper and reasonable operational procedures. These consist primarily of constraints on separation distances between the radiation source and the SSF crew and on reactor shutdown times prior to the approach of vehicles utilizing nuclear propulsion. These constraints are not severe and do not significantly impair the functionality of an evolutionary space station. Furthermore, the use of portable multi-functional radiation shields would both relax these constraints and reduce the dose to the SSF crew from the natural space environment in accordance with the ALARA radiation protection criteria.

The dose budget concept employed in this work may be applied in the analysis of nuclear systems for the lunar and Mars missions currently under consideration by NASA. This approach was found to be extremely useful in this work and its application to other mission classes is highly recommended.

Lastly, the analysis methods employed in this work are simplified and the results are intended to aid mission planners and identify operational and design constraints on SSF associated with the use of nuclear power sources. However, the analysis procedures developed in this work can be extended to provide more rigorous results and this will be pursued in a follow-on project.

CHAPTER 2

NATURAL SOURCES OF RADIATION EXPOSURE AT SPACE STATION FREEDOM

INTRODUCTION

Even without man-made radiation sources in the vicinity of Space Station Freedom, radiation exposures are unavoidable due to the presence of natural space radiations. This natural space environment will deliver an average daily radiation dose to SSF crew members equal to what they would receive in one year from natural terrestrial sources other that indoor radon (NCRP 1989). Fortunately, both natural sources of radiation deliver annual doses below recommended limits designed to protect individuals from various radiation health effects. Nevertheless, man-made radiation exposures in space must always be placed in context with a non-trivial space radiation background.

SOURCES OF SPACE RADIATION

Natural space radiations can be conveniently placed into three categories according to their source: (1) trapped particles, (2) galactic cosmic rays (GCR), and (3) solar particle events (SPE) (NCRP 1989).

The trapped particles consist of both electrons and protons which are held within the earth's magnetic field. Both particles spiral around the geomagnetic field lines, bouncing between mirror points in the Northern and Southern hemispheres. Since they are of opposite charge, the trapped electrons drift eastward and the protons drift westward. The trapped electrons are found in two partially distinct regions called the "inner zone" (< 11,500 km) and the "outer zone" (between 11,500 and 70,200 km). The electron intensities in the outer zone are ~10 times those in the inner zone. Both zones experience a 10-fold diurnal variation in intensity with a smaller variation corresponding to the 11-year solar cycle. The trapped protons occupy a more limited volume of space and are more dosimetrically important than the electrons for low earth-orbiting missions such as the space station. The most intense region of trapped protons is found between Africa and South America where the proton belt dips to lower altitudes. This region is called the South Atlantic Anomaly (SAA) and is caused by a slight off-center displacement of the earth's magnetic dipole.

Galactic cosmic rays are typically charged particles which are present isotropically in space and arise from sources outside our solar system. Due to their interactions with the "solar wind", their intensity decreases during the active part of the solar cycle (solar maximum). The maximum total particle flux of GCR at solar minimum is estimated to be about 4 cm^{-2} s^{-1}. Their distribution within the energy range of greatest flux is 87% protons, 12% helium ions, and 1% heavier ions. This latter group has been given the generic term HZE particles (High Z and Energy). Although HZE particles are found in low abundance with respect to protons and helium ions, they are much more densely ionizing and thus their contribution to the total GCR dose can be substantial.

Solar particle events are large emissions of charged particles from the sun during solar flare activity. They consist mostly of protons, with a small contribution of helium and HZE particles, and occur sporadically during the active phase of the 11-year solar cycle. SPE fall into two general categories according to their intensities: ordinary and anomalously large. Due to the shielding effect of the earth's magnetic field, ordinary SPE do not contribute substantially to radiation doses in low earth orbits. Although they occur infrequently, anomalously large SPE can contribute to radiation doses in low earth orbits (LEO) at high inclinations.

NATURAL SPACE RADIATION DOSES AT SSF

Under current flight plans, NASA proposes to place SSF at an altitude of 450 km and in an orbital inclination of 28.5°. In this orbit, the station is in the lower fringes of the trapped proton belt. As shown in Table 2.1, an estimated annual radiation dose to crew members at SSF is 400 mSv or 40 rem (NCRP 1989 and Curtis et. al 1986) (see Appendix A for definitions of radiation dosimetry quantities and units). Irradiation by trapped protons constitutes 92% of the radiation dose, while the remaining 8% is due to GCR. A majority of the proton dose is accrued during traversal of the SAA. At higher inclinations, less time in spent in the SAA, and thus the proton dose decreases. At the same time, however, the GCR dose increases as the geomagnetic field provides less natural shielding for low-energy GCR charged particles. Note that the total annual dose at 57° and at 0° is less than at a 28.5° inclination. Although the total dose is 30% greater at this lower inclination, the geomagnetic field at this point does provide protection from SPE. A single anomalously large SPE can more than double the annual dose to crew members in a polar

orbit. At present, the baseline design for space station does not include a "storm shelter" for protection against solar flare activity.

REFERENCE NATURAL DOSES AT SPACE STATION

As discussed above, dose rates at the space station will average about 400 mSv/y or 0.033 Sv/mo due primarily to the trapped-proton irradiation. The lower fringes of proton belt, however, will vary in altitude as the earth's atmosphere contracts and expands during periods of minimum and maximum solar activity, respectively. Consequently, dose rates at SSF can range from a low of 0.015 Sv/mo at 450 km during solar maximum to a high of 0.053 Sv/mo at 500 km during solar minimum (Nachtwey 1989). If the station were to vary its altitude over several years so as to achieve a constant atmospheric drag, an average 30-day radiation dose of 0.01 Sv could be achieved.

In subsequent chapters, radiation doses delivered by man-made radiation sources will be compared to doses due solely to the natural space environment at the space station. It is thus convenient at this point to define two reference natural dose rates corresponding to the extremes in its variation at SSF. We define these reference values as a "best-case" natural dose rate of 0.01 Sv/mo and a "worst-case" natural dose rate of 0.05 Sv/mo. The latter value will be used in the following chapter to derive a conservative estimate of allowable doses from man-made space radiation sources.

CONCLUSIONS

It is instructive to compare space radiation doses to natural background doses on earth. Table 2.2 gives the average annual U.S. whole-body radiation doses from five natural sources (NCRP 1987a). The total annual dose is 3.0 mSv or less than 1% of annual doses from natural space radiations at SSF. As indicated in Table 2.3, man-made radiation sources on earth contribute only an additional 0.6 mSv to an individual's annual dose (NCRP 1987b). Clearly, the radiation environment in space is not as hospitable as it is on earth. Nevertheless, crew members at SSF will receive only ~40% of their annual recommended dose limit at the end of a extended 180-day duty tour (see Chapter 3). Furthermore, radiation exposures, be they from natural or man-made sources, will constitute only one of many occupational risks inherent to manned space activity.

References

Curtis, S. B., W. Atwell, R. Beever, and A. Hardy (1986) "Radiation Environments and Absorbed Dose Estimations on Manned Space Missions," Adv. Space Res, 6 (11): 269-274.

NCRP (1987a) Exposure of the Population in the United States and Canada form Natural Background Radiation, NCRP Report No. 94, National Council on Radiation Protection and Measurements, Bethesda, Maryland, December 1987.

NCRP (1987b) Ionizing Radiation Exposure of the Population of the United States, NCRP Report No. 93, National Council on Radiation Protection and Measurements, Bethesda, Maryland, September 1987.

NCRP (1989) Guidance on Radiation Received in Space Activities, NCRP Report No. 98, National Council on Radiation Protection and Measurements, Bethesda, Maryland, July 1989.

Nachtwey, D. S. (1989) Personal Communication, NASA Johnson Space Center, Houston, Texas, September 1989.

Table 2.1 Natural Radiation Doses[a] at SSF at 450 km and at Various Orbital Inclinations. (NCRP 1989 and Curtis et. al 1986)

Radiation Source	28.5 degrees	57 degrees	0 degrees
Trapped Proton Dose:	370 mSv/y	240 mSv/y	210 mSv/y
GCR Dose:	30 mSv/y	62 mSv/y	80 mSv/y
Total:	400 mSv/y	300 mSv/y	300 mSv/y
AL SPE	0 mSv additional	50 mSv additional	370 mSv additional

[a]Doses are to the blood forming organs (BFO) and for a spacecraft with 1.0 g cm^{-2} Al shielding orbiting during solar minimum.

Table 2.2 Natural Background Doses on Earth. (NCRP 1987a)

Radiation Source	Dose Rate (mSv/y)
Cosmic	0.27
Cosmogenic	0.01
Terresterial	0.28
Inhaled (Radon)	2.0
In the Body	0.4
Rounded Total:	3.0 mSv/y

Table 2.3 Average Individual Doses on Earth from All Sources. (NCRP 1987b)

Radiation Source	Dose Rate (mSv/y)
Natural	3.0
Occupational	0.009
Nuclear Fuel Cycle	0.0005
Consumer Products	0.071
Medical	0.53
Rounded Total:	3.6 mSv/y

CHAPTER 3

RADIATION DOSE LIMITS FOR SSF PERSONNEL

INTRODUCTION

This chapter presents currently recommended dose limits for radiation exposures to space workers. Since individuals at SSF will receive a somewhat constant radiation dose from trapped protons and GCR, the difference between recommended dose limits and doses from natural space radiations can be defined as an "available radiation dose budget" to be assigned to each individual crew member. If necessary, this dose budget could then be expended through exposures to man-made radiation sources such as nuclear reactors, radioisotope sources, or even medical x-ray examinations. It is current radiation protection practice to keep such exposures "As Low As Reasonably Achievable" (ALARA) (ICRP 1977 and NCRP 1987). Nevertheless, mission planners should be cognizant of the operational limits imposed, not only by this ALARA principle, but by the use of these individual radiation dose budgets. Before introducing the radiation dose limits to space workers, the general considerations by which they are defined are discussed below.

RADIATION PROTECTION CONSIDERATIONS

Health effects of radiation exposure fall under two general classes: stochastic effects and nonstochastic effects. Nonstochastic effects are those for which severity of the effect increases with increasing radiation dose delivered above a certain threshold. This threshold dose can vary greatly between individuals. Examples of nonstochastic effects are cataracts, blood changes, and decreased sperm production in the male. Stochastic effects are those for which only the probability of occurrence increases with increasing radiation dose, the severity of the effect is dose independent, and a threshold dose level, if it exists, is close to zero. Consequently, any radiation exposure will have an associated level of risk, however small. The main stochastic effects of concern are cancer (malignant tumors and leukemia) and genetic effects.

By international agreement, the principal objectives of radiation protection are: (1) to prevent the occurrence of nonstochastic effects; and (2) to reduce the risk of stochastic effects to levels comparable to risks associated with traditionally "safe" occupations (ICRP 1977 and NCRP 1987). Three concurrent approaches are generally used to achieve these

objectives. First, all activities resulting in radiation exposures must be justified in terms of perceived benefits and projected costs. Second, all radiation exposures must be kept to as low a level as is reasonably achievable. Within the ALARA principle, it is assumed that economic and societal factors are to be used to determine what effort of dose reduction is deemed "reasonable". Finally, all individual radiation doses must be kept below recommended and/or regulatory dose limits.

NCRP RECOMMENDED DOSE LIMITS

Table 3.1 gives radiation dose limits for NASA's space workers as currently recommended by the National Council on Radiation Protection and Measurements (NCRP) (NCRP 1989). These career limits correspond to a 3% lifetime excess risk of fatal cancer where a career is assumed to be approximately 10 years. For the blood forming organs (BFO), the career limits range from 1.0 Sv for females 25 years of age at first exposure to 4.0 Sv for males 55 years of age at first exposure. Annual and 30-day limits are also specified so as to prevent the occurrence of nonstochastic radiation effects. As indicated in the table, an individual may receive 0.5 Sv to the BFO in a given year of space activity, yet cannot receive more than one-half the annual limit within any one 30-day period.

These dose limits are for total radiation exposures regardless of source. At present, they are only recommendations to NASA. However, it is expected that in the near future they will be adopted by the Occupational Safety and Health Administration (OSHA) of the U.S. Department of Labor, the organization with regulatory authority over radiation exposures to NASA personnel (Nachtwey 1989). Current OSHA regulations follow those of the U.S. Nuclear Regulatory Commission which specifies that occupational radiation workers will not receive annual whole-body radiation doses from man-made sources in excess of 0.05 Sv.

RADIATION DOSE BUDGETS FOR SSF CREW MEMBERS

Two radiation dose budgets are defined in this report: LBAD-st and LBAD-lt. The acronym LBAD stands for Lower Bound on Available Dose and the suffixes "st" and "lt" stand for short-term and long-term exposures, respectively. This approach is based upon three main considerations. First, man-made radiation sources in space predominantly emit neutron and gamma radiations. Individuals exposed to these radiation types will generally receive uniform whole-body doses; consequently, only the NCRP limits to the blood

forming organs are used to define dose budgets. Second, to be somewhat conservative, only the reference "worst-case" natural dose rate at SSF (0.05 Sv/mo) is used in their definitions. Third, in order to cover the range of scenarios by which man-made radiation exposures may occur, two exposure types and periods are considered.

The first type is a short-term, infrequent exposure occurring once during a particular 30-day period. Because the exposure is infrequent, the 30-day NCRP dose limit would apply to the individuals exposed (0.25 Sv in 30 days). An example would be exposure during extravehicular activity (EVA) near a shutdown reactor as part of the unloading of a Mars vehicle. The second exposure type corresponds to a long-term, continuous exposure to crew members during a maximum 6-month tour-of-duty at the station. Because the exposure is continuous, the annual NCRP dose limit would apply (0.50 Sv in 6 months). An example would be radiation exposure from an operating reactor on a co-orbiting platform.

The numerical values for LBAD-st and LBAD-lt are calculated as follows:

LBAD-st = (NCRP 30-day Limit) - (Worst-Case Natural Dose @ SSF Over 30 Days)
= (0.25 Sv/mo) - (0.05 Sv/mo)
= 0.20 Sv in 30 days.

LBAD-lt = (NCRP Annual Limit) - (Worst-Case Natural Dose @ SSF Over 6 Months)
= (0.50 Sv/yr) - (6 mo/yr) (0.05 Sv/mo)
= 0.20 Sv in 180 days.

It is strictly coincidental that both radiation dose budgets numerically equal 0.20 Sv. If the LBAD-lt is prorated uniformly over a full 180-day crew rotation period, only 0.033 Sv from man-made sources would be allowed within any 30-day period. Consequently, the LBAD-lt is a more restrictive dose budget than the LBAD-st.

USE OF RADIATION DOSE BUDGETS

Radiation exposure of crew members will be one of the primary factors determining the operational limits on space nuclear power sources employed in the vicinity of SSF. The range of "permissible" operations can thus be linked to a range of "permissible" man-made radiation exposures. The upper bound of this dose range will, of course, be governed by

the NCRP dose limits. The lower bound will be governed by the ALARA principle. This raises the question of what is a "reasonably achievable" radiation dose from man-made sources in space. One useful definition would be to limit such doses to levels comparable to those received by the natural background. On earth, this is generally acceptable since background doses are typically very low. Although "background" doses in low earth orbit are much greater, this definition nevertheless is still valid since natural doses over typical staytimes are below recommended limits and radiation exposure is but only one of several risks presented to space workers. For the purposes of this report, therefore, the ALARA principle when applied to LEO operations will limit man-made radiation exposures to levels equaling natural doses under best-case conditions (0.01 Sv/mo).

Table 3.2 summarizes this range of "permissible" dose levels. For infrequent exposure events occurring sometime within a given 30-day period, the most permissive space nuclear power operations would result in crew members expending their LBAD-st radiation dose budgets and thus reaching the NCRP 30-day dose limit. The most restrictive operations will result in crew doses equaling one-month exposures from natural sources under best-case conditions. Similar arguments hold for long-term, continuous exposure events near or at the space station.

In Chapters 5 through 8, a range of scenarios will be presented in which space nuclear power sources will be used either at or near SSF. For each scenario, radiation doses to SSF crew members will be calculated as a function of several operational parameters such as parking distances and reactor shutdown times. As indicated in Table 3.2, what values of operational parameters are considered "safe" will depend upon the frequency and duration of the event and upon the radiation protection criteria selected.

References

ICRP (1977) Recommendations of the International Commission on Radiological Protection, ICRP Publication 26, International Commission on Radiological Protection, Pergamon Press, New York, 1977.

Nachtwey, D. S. (1989) Personal Communication, NASA Johnson Space Center, Houston, Texas, September 1989.

NCRP (1987) Recommendations on Limits for Exposure to Ionizing Radiation, NCRP Report No. 91, National Council on Radiation Protection and Measurements, Bethesda, Maryland, June 1987.

NCRP (1989) Guidance on Radiation Received in Space Activities, NCRP Report No. 98, National Council on Radiation Protection and Measurements, Bethesda, Maryland, July 1989.

Table 3.1 Recommended Dose Limits for Space Workers. (NCRP 1989)

Time Period	Dose Equivalent (Sv)		
	Blood Forming Organs	Lens of the Eye	Skin
Career	1.0 - 4.0	4.0	6.0
Annual	0.50	2.0	3.0
30-day	0.25	1.0	1.5

Table 3.2 Bounding Radiation Dose Levels for Exposures to Man-Made Radiation Sources in Space.

Radiation Protection Criteria to be Used	Exposure Type and Period	
	Short-Term, Infrequent (1 Month)	Long-Term, Continuous (6 Months)
NCRP Dose Limits (Upper Bound)	LBAD-st (0.2 Sv in 30 days)	LBAD-lt (0.2 Sv in 180 days)
ALARA Principle (Lower Bound)	1 Mo. Nat. @ SSF (BC) (0.01 Sv in 30 days)	6 Mo. Nat. @ SSF (BC) (0.06 Sv in 180 days)

CHAPTER 4

NEUTRON AND GAMMA SOURCE TERMS FOR OPERATING AND SHUTDOWN REACTORS

INTRODUCTION

This chapter deals with the determination of the neutron and gamma source terms for both operating and shutdown reactors. NERVA- and SP100-class reactors were chosen for the Mars mission and SSF operational scenarios, described in later chapters, and the source terms for these reactors are developed in this chapter. The operating reactor neutron and gamma source terms are based upon values generated as part of the SP-100 and NERVA projects. The shutdown reactor gamma source terms are based upon an empirical relationship for gamma release rates from fission products and the operating source terms.

The methods employed in this analysis are approximate and the results are intended primarily to aid mission planning; the values predicted using these methods are probably accurate to within ±25%. It is certainly possible to perform these analyses in a rigorous fashion. A number of coupled neutron-gamma transport codes are available to compute the operating reactor source term. The ORIGEN2 code (Croff 1983 and RSIC 1987) can be employed to provide accurate estimates of the radioisotope inventory based upon a reactor's operational history. However, the level of effort required to develop the reactor models required to implement the transport codes is rather large and not justified at this time. This is an area that will be explored as part of a follow-on project.

DESCRIPTION OF REACTORS

The two reference systems employed in this study are SP-100 and NERVA-class reactors. The SP-100 reactor is currently under development as part of the U.S. space program (Armijo et al. 1989, Deane et al. 1989 and Manvi and Fujita 1987). It has a baseline thermal power of 2.4 MW_t and employs a static thermoelectric power conversion subsystem to produce 100 kW_e of power. The basic design goals of the SP-100, however, call for scalability up to an order of magnitude higher power. For the purposes of this project, it was assumed that the reactor would generate 25 MW_t and utilize an active conversion system (Rankine or Brayton cycle) in order to provide 5 MW of electrical power. The SP-100 is a small, compact, fast-spectrum reactor. It utilizes highly enriched

uranium mononitride (UN) fuel, niobium - 1% zirconium (Nb-1Zr) cladding, and lithium (Li) coolant. The core vessel and structure are composed primarily of Nb-1Zr and the other materials employed in the core are also refractory alloys. Beryllium oxide (BeO) hinged reflector panels located on the outside periphery of the core are employed as the primary control mechanism. The entire core and reflector structure is enclosed in a conical carbon-carbon reentry shield. A layered tungsten (W), lithium-hydride (LiH) shadow shield is employed to decrease the radiation field at the user interface.

The NERVA (Nuclear Engine for Rocket Vehicle Application) reactor concept was developed during the U.S. space propulsion program, which ended in 1973 (Bohl et al. 1988, Haloulakos and Boehmer 1988 and Borowski et al. 1989). A NERVA derivative reactor (NDR) concept capable of producing electrical power and being employed for propulsion is currently under study for application to the U.S. Multimegawatt reactor program (Pierce et al. 1989 and Schmidt et al. 1988). There is not a single fixed NERVA reactor design; rather NERVA was a basic reactor technology demonstration program that incorporated a number of similar reactor designs such as the NRX and XE reactor series (Angelo and Buden 1985). The basic NERVA reactor concept consists of a solid graphite core with a hydrogen coolant. A variety of fuel element designs were tested as part of the NERVA program and the most highly developed of these were uranium dicarbide (UC_2) particles with a pyrolytic carbon coating contained in a graphite matrix and a UC-ZrC-C composite fuel. A niobium or zirconium carbide (NbC or ZrC) fuel element coating was employed to reduce erosion by the hydrogen propellant. Primary reactor control was achieved through the use of rotating drums located on the outside periphery of the core. The bulk of the core vessel consists mainly of aluminum and steel. Two separate shields were employed in the NERVA design (Aerojet General 1970). The first is inside the pressure vessel and designed to protect the engine components from excessive heating. A brim or disk shield at the top of the core composed of layered lead (Pb), LiH, and Boral (a B-C-Al compound) was designed to decrease the radiation field away from the reactor for manned missions. The propellant storage tank provides a substantial amount of radiation shielding for the crew. In this work, the NERVA reactor was assumed to have a peak power of 1575 MW_t and be capable of producing low levels of electrical power (approximately 100 kW_e).

OPERATING REACTOR NEUTRON AND GAMMA SOURCE TERMS

The operating reactor neutron and gamma source terms were not directly computed as part of this project, rather the values employed in this work were developed using data from the SP-100 and NERVA projects. As mentioned previously, developing the geometric and material models required to implement neutron and gamma transport codes in a meaningful fashion is a rather time-intensive task. This topic will be explored as part of a follow-on project.

A number of common radiation analysis models (CRAM) were developed in conjunction with the NERVA project; the values employed in this work were taken from one of these models (Aerojet General 1970 and Wilcox et al. 1969). The CRAM provides values in terms of equivalent point sources for various engine components. The radiation field in a direction perpendicular to the axis of the reactor-engine assembly (i.e. radially outward) is dominated by the reactor; activation of and scattering from engine and structural components represent a second-order contribution. The neutron and gamma spectra for the operating NERVA reactor are given in Tables 4.1 and 4.2, respectively. Employing the dose response functions given in Appendix B yields specific operating NERVA dose rates at a 1 meter separation distance in the radial direction from an equivalent point source of 30.6 Sv/sec/MW_t for neutrons and 14.5 Sv/sec/MW_t for gammas.

Data on the neutron and gamma levels in and around an SP-100 operating at 2.4 MW_t for beginning-of-life (BOL) conditions were available from General Electric (Marcille 1989). The neutron and gamma fluxes on the periphery of the reactor at the axial midplane were scaled linearly with power to 25 MW_t to provide a radial source term. Values were also extracted for a location behind the shadow shield; these were not scaled with the thermal power since it was assumed that the shield thickness would be increased to achieve the same dose at the user plane. The neutron and gamma spectra for the operating SP-100 reactor are given in Tables 4.3 and 4.4, respectively. The specific operating SP-100 dose rates at a 1 meter separation distance in the radial direction from an equivalent point source were computed as 14.5 Sv/sec/MW_t for neutrons and 0.897 Sv/sec/MW_t for gammas. For locations behind the shadow shield, the specific dose rates at a 1 meter separation distance from an equivalent point source are 6.82×10^{-4} Sv/sec/MW_t for neutrons and 2.4×10^{-2} Sv/sec/MW_t for gammas.

The specific radial operating dose rates employed in this work and given above are summarized in Table 4.5. As can be seen in the table, the values for the SP-100 are substantially smaller than those for the NERVA; this is particularly true for the specific gamma dose rate. Several factors contribute to these differences. The types of materials employed in the SP-100 and NERVA reactors are quite different. The SP-100 is comprised primarily of high atomic number (Z) refractory alloys while most of the structure of the NERVA is aluminum or steel. High Z materials are much more effective in attenuating gamma radiation and this will tend to decrease and soften the gamma spectrum of the SP-100 relative to that of the NERVA. Secondly, the SP-100 is a small, compact reactor whereas the NERVA is both large and graphite-moderated. This will produce a fast (hard) neutron spectrum in the SP-100 relative to the NERVA's thermal or epithermal neutron spectrum. Gammas will be produced as a consequence of the neutron thermalization (slowing down) process and this will occur to a larger degree in the NERVA. The relative amount of structural and control materials in these reactors will also play a role. The ratio of the core to vessel (including reflectors) radius for the SP-100 is approximately 0.56 at the core axial midplane, while this value is 0.74 for the NERVA. Thus, there is proportionally more structural material, and hence radiation interaction, with the SP-100 compared to the NERVA. In addition, the energy groups selected from the SP-100 and NERVA project reports are not consistent. Those employed for the NERVA were simply the values available in the literature. For the SP-100, however, this energy structure was initially requested by the authors. GE has the capability to provide a number of different energy group structures; a set more closely matching that employed with the NERVA was not obtained due to time constraints. Lastly, the computational methods employed by the SP-100 and NERVA project teams are not the same. The SP-100 project is employing current radiation transport codes and cross section libraries and this factor could introduce some difference in the operating dose rate values. As previously mentioned, the development of "in-house" capabilities to carry out direct computation of the radiation source terms on a consistent basis will be explored in a follow-on project.

SHUTDOWN REACTOR GAMMA SOURCE TERMS

The shutdown reactor gamma source strength was computed using the simple empirical relationship shown below (LaBauve et al. 1982):

$$f(t) = \sum_{j=1}^{11} \alpha_j e^{-\lambda_j t}$$

where f is the energy release rate per fission (MeV/fission/sec), t is the time since the fission occurred, and α_j and λ_j are empirical constants. Integrating with respect to both reactor operating and shutdown time yields the gamma energy release rate at the time of exposure. There are alternate periods of full and reduced power operation in the Mars mission scenarios employed in this work; each period of operation is treated separately and the source terms are summed to compute a total source. As discussed in Appendix C, there are a large number of such relationships available which vary in complexity and accuracy.

Once the total source has been computed, the gamma dose rate is computed using the simple relationship shown below:

$$\dot{H}_{\gamma_s} = \dot{H}_{\gamma_o}\left[\frac{P_{\gamma_s}}{P_{\gamma_o}}\right]$$

where H is the gamma dose rate and P is gamma energy release rate (power), the subscripts s and o denote shutdown and operating conditions, respectively. The operating reactor dose rates were discussed in the section above. The operating gamma power is taken to be a fraction of the total reactor power, as shown below:

$$\dot{H}_{\gamma_s} = \dot{H}_{\gamma_o}\left[\frac{P_{\gamma_s}}{f_\gamma P_o}\right]$$

Prompt gammas are emitted simultaneously with a fission event and contribute about 7 MeV to the approximately 200 MeV of recoverable energy released per ^{235}U fission event. Gammas are also emitted as a result of neutron capture events and contribute another 3 to 12 MeV per fission (Lamarsh 1966). Fission product gammas are emitted after the fission event as a result of the radioactive decay of fission products. If the operating reactor dose rate corresponds to BOL conditions, then fission product gammas will make only a minor contribution to the corresponding dose rate. A value of 0.065 was taken for f_γ in this work. This method presumes that the operating and shutdown gamma spectra are identical since the conversion between flux and dose is energy dependent, as discussed in Appendix B. While this condition is not strictly met, the chief differences are in the low energy end

of the spectrum and the low energy gammas do not make a large contribution to the total dose.

CONCLUSIONS

The methodology employed to compute the neutron and gamma source terms for both operating and shutdown NERVA- and SP100-class reactors were reported. The operating reactor neutron and gamma source terms are based upon values generated as part of the SP-100 and NERVA projects. The shutdown reactor gamma source terms are based upon an empirical relationship for gamma release rates from fission products and the operating gamma dose rates. These methodologies are approximate and the results are intended primarily to aid mission planning. It is acknowledged that it would be desirable to obtain more accurate source term descriptions by employing transport and radioisotope inventory codes and this topic will be explored as part of a follow-on project. However, the procedures employed here provide sufficiently accurate values to carry out initial mission planning and trade-off studies.

References

Aerojet General (1970) NERVA Engine Reference Data, S130-CP-090290AF1, Aerojet General, Sacramento, CA, Sept. 1970.

Angelo, J.A., Jr. and D. Buden (1985) Space Nuclear Power, Orbit Book Co., Malabar, FL. pp. 177 - 96.

Armijo, J.S. et al. (1989) "SP-100, Technology Accomplishments," in Trans. of the Sixth Symposium on Space Nuclear Power Systems, CONF-890103--Summs., held in Albuquerque, NM, 8-12 January 1989, pp. 352 - 6.

Bohl, R.J., J.E. Boudreau and W.L. Kirk (1988) "History of Some Direct Nuclear Propulsion Developments since 1946," in Space Nuclear Power Systems 1987, M.S. El-Genk and M.D. Hoover, eds., Orbit Book Co., Malabar, FL, pp. 467 - 73.

Borowski, S.K., M.W. Mulac and O.F. Spurlock (1989) "Performance Comparisons of Nuclear Thermal Rocket and Chemical Propulsion Systems for Piloted Missions to Phobos/Mars," presented at the 40th Congress of the International Astronautical Federation, held in Malaga, Spain, 7-13 October 1989, paper IFA-89-027.

Croff, A.G. (1983) "ORIGEN2: A Versatile Computer Code for Calculating the Nuclide Compositions and Characteristics of Nuclear Materials," Nucl.Tech., 62: 335-52.

Deane, N.A. et al. (1989) "SP-100 Reactor Design and Performance," in Trans. of the Sixth Symposium on Space Nuclear Power Systems, CONF-890103--Summs., held in Albuquerque, NM, 8-12 January 1989, pp. 542 - 5.

Haloulakos, V.E. and C.B. Boehmer (1988) "Nuclear Propulsion: Past, Present, and Future," in Trans. of the Fifth Symposium on Space Nuclear Power Systems, CONF -880122--Summs., held in Albuquerque, NM, 11-14 January 1988, pp. 329-2.

LaBauve, R.J., T.R. England, D.C. George and C.W. Maynard (1982) "Fission Product Analytic Impulse Source Functions," Nucl.Tech., 56: 322-39.

Lamarsh, J.R. (1966) Introduction to Nuclear Reactor Theory, Addison-Wesley Publ. Co., Reading, MA, pp. 103-4.

Manvi, R. and T. Fujita (1987) SP-100 Program: Users Handbook, Basic Configurational Tradeoffs, JPLD-4154 Issue 3, Jet Propulsion Lab., Pasadena, CA, June, 1987.

Marcille, T. (1989) Personal Communication, General Electric Aerospace, SP-100 Program, San Jose, CA, July 1989.

Pierce, B.L., R.R. Holman and H.D. Kulikowski (1989) "Single NERVA Derivative Reactor Design Concept for Space Nuclear Electrical Power and Direct Propulsion," in Trans. of the Sixth Symposium on Space Nuclear Power Systems, CONF-890103--Summs., held in Albuquerque, NM, 8-12 January 1989, pp. 145 - 8.

RSIC (1987) RSIC Computer Code Collection, ORIGEN2: Isotope Generation and Depletion Code - Matrix Exponential Method, CCC-371, Radiation Shielding Information Center, Oak Ridge National Laboratory, Oak Ridge, TN, Nov. 1987.

Schmidt, J.E., J.F. Wett and J.W.H. Chi (1988) "The NERVA Derivative Reactor and a Systematic Approach to Multiple Space Power Requirements," in Trans. of the Fifth Symposium on Space Nuclear Power Systems, CONF-880122--Summs., held in Albuquerque, NM, 11-14 January 1988, pp. 415 - 6.

Wilcox, A.D., B.A. Lindsey and M.A. Capo (1969) NERVA-Flight-Engine Common Radiation-Analysis Model (U), RN-TM-0583, Nuclear Division, Aerojet General, Sacramento, CA, May 1969.

Table 4.1 Operating Equivalent NERVA BOL Neutron Flux in Radial Direction.

Group	Energy Range	Flux @ 1m (neutrons/cm^2/sec)
1	E < 0.4 eV	8.4E+13
2	0.4 eV < E < 1 MeV	3.7E+14
3	E > 1 MeV	1.1E+14

Table 4.2 Operating Equivalent NERVA BOL Gamma Flux in Radial Direction.

Group	Lower Energy (MeV)	Upper Energy (MeV)	Flux at 1 meter (gammas/cm^2/sec)
1	7.50	30.00	1.2E+12
2	7.00	7.50	2.1E+12
3	6.00	7.00	6.6E+12
4	5.00	6.00	1.9E+13
5	4.00	5.00	6.8E+13
6	3.00	4.00	1.7E+14
7	2.60	3.00	1.3E+14
8	2.20	2.60	2.0E+14
9	1.80	2.20	3.3E+14
10	1.35	1.80	5.5E+14
11	0.90	1.35	1.0E+15
12	0.40	0.90	2.4E+15
13	0.00	0.40	3.6E+15

Table 4.3 Operating Equivalent SP-100 BOL Neutron Flux.

Group	Lower Energy (MeV)	Upper Energy (MeV)	Flux at 1 meter (neutrons/cm^2/sec)	
			Radial Direction	Behind Shield
1	2.23	20.00	5.32E+11	1.24E+06
2	1.35	2.23	4.93E+11	7.22E+05
3	0.82	1.35	3.45E+11	6.82E+05
4	0.50	0.82	4.77E+11	6.37E+05
5	0.30	0.50	3.95E+11	4.68E+05
6	0.11	0.30	9.39E+11	7.54E+05
7	4.09E-02	1.11E-01	9.90E+11	4.60E+05
8	5.53E-03	4.09E-02	1.88E+12	9.21E+05
9	1.67E-04	5.53E-03	1.76E+12	1.50E+06
10	4.14E-07	1.67E-04	3.83E+11	1.80E+06
11	1.39E-10	4.14E-07	2.96E+10	9.92E+04

Table 4.4 Operating Equivalent SP-100 BOL Gamma Flux.

Group	Lower Energy (MeV)	Upper Energy (MeV)	Flux at 1 meter (gammas/cm^2/sec)	
			Radial Direction	Behind Shield
1	2.50	30.00	4.05E+11	4.14E+08
2	0.75	2.50	1.32E+12	1.08E+09
3	0.30	0.75	9.34E+11	1.07E+09
4	0.01	0.30	1.40E+12	5.86E+09

Table 4.5 Operating Equivalent SP-100 and NERVA Specific Dose Rates.

Reactor Type	Specific Dose Rate at 1 meter (Sv/sec/MWt)			
	Radial Direction		Behind Shadow Shield	
	Neutrons	Gammas	Neutrons	Gammas
NERVA	30.6	14.5	n/a	n/a
SP-100	14.5	0.897	2.85E-04	1.00E-02

CHAPTER 5

LAUNCH OF MARS VEHICLES FROM LOW EARTH ORBIT

INTRODUCTION

In this set of scenarios, a nuclear powered vehicle is launched from SSF orbit en route to the planet Mars. We consider two types of nuclear vehicles which would make this journey. One is an NEP cargo vehicle utilizing an SP-100 reactor scaled to 25-MW_t (Armijo et al. 1989 and Deane et al. 1989). The second is an NTR personnel vehicle with two stages. The first or Trans-Mars Insertion (TMI) stage is powered by a 5000-MW_t Phoebus-class reactor (Borowski et al. 1989 and Bohl et al. 1989). The second NTR stage utilizes a 1575-MW_t NERVA-class reactor (Pierce et al. 1989 and Schmidt et al. 1988) and is used during the remainder of the round trip to Mars.

For both the NEP and NTR vehicles, we calculate the cumulative radiation doses received by SSF crew members as a function of the vehicle's initial separation distance from SSF. Two directions of initial separation are considered: one whereby SSF initially lags the vehicle at launch and one in which SSF initially leads the vehicle. In all cases, the vehicle's reactor is treated as an point source of neutron and gamma radiation with the radiation fields falling off as the inverse square of the vehicle-to-SSF separation distance. In our calculations, no provisions were made for inherent shielding by either the vehicle or space station structures.

Four FORTRAN computer codes were written to perform the dose calculations for these launch scenarios. The program NEPTRAJ calculates the radius and travel angle of the NEP cargo vehicle as a function of time. A second code, NEPDOSE, uses this trajectory information to calculate NEP-to-SSF separation distances and incremental radiation doses received at SSF during the NEP escape spiral. Cumulative doses are then tabulated as a function of the vehicle's initial distance from SSF at launch. The codes NTRTRAJ and NTRDOSE make similar calculations for the NTR personnel vehicle leaving SSF orbit. Program listings of all these codes are given in Appendix D.

TRAJECTORY CALCULATIONS

The two-dimensional trajectory of each vehicle is obtained by solving the following five equations of motion as given in Zimmerman et. al (1963):

$$\dot{u} = -\frac{\mu}{r^2} + \omega^2 r + \frac{V_j \beta}{m} \sin \psi \tag{5.1}$$

$$\dot{\omega} = -\frac{2u\omega}{r} + \frac{V_j \beta}{m} \frac{\cos \psi}{r} \tag{5.2}$$

$$\dot{r} = u \tag{5.3}$$

$$\dot{\phi} = \omega \tag{5.4}$$

$$\dot{m} = -\beta \tag{5.5}$$

where u = radial velocity (m s^{-1})

μ = gravitational constant = GM_E = 3.986 x 10^{14} m^3 s^{-2}

r = vehicle radius from Earth's center (m)

ϕ = polar travel angle (radians)

ω = polar angular velocity (radians s^{-1})

V_j = engine exhaust velocity = g I_{sp} = 9.80665 I_{sp} (m s^{-1})

I_{sp} = engine specific impulse (s)

β = propellant mass flow rate (kg s^{-1})

m = vehicle mass (kg)

ψ = vehicle thrust angle measured from normal to radius (radians)
(assumed zero for tangential thrust)

and r_{Earth} = 6,378,150 meters.

These ordinary first-order differential equations are solved in NEPTRAJ and NTRTRAJ using the sixth-order Runge-Kutta-Verner routine DIVPRK from the IMSL MATH/LIBRARY scientific subroutine package (IMSL 1989). The solutions for both vehicle trajectories were advanced with a time step of one minute.

As a measure of quality assurance, the trajectory of the NEP cargo vehicle as calculated by NEPTRAJ was verified against calculations made by the technical staff in NASA LeRC's Advanced Space Analysis Office. The results are shown in Table 5.1. Excellent agreement is shown out to a total time of 50 days.

LAUNCH OF NEP CARGO VEHICLE

In our reference mission scenario, the NEP cargo vehicle departs from SSF orbit (450 km altitude and 28.5° inclination) with a tangential thrust of 138 N, a specific impulse of 5000 s, and a propellant flow rate of 0.0028 kg/s. The total mass of the vehicle at launch is 897.7 metric tons. As detailed in Chapter 4, the total neutron and gamma dose rate at one meter from the operating NEP reactor is 385 Sv/s. Since the reactor is treated as a point source of radiation, this dose rate decreases as the inverse square of the separation distance from the reactor.

Our results for the NEP cargo vehicle are summarized in Figure 5.1. Here we plot the cumulative dose received by SSF crew members as a function of the vehicle's initial separation at launch. The circles and triangles correspond to launch configurations where SSF either lags or leads the NEP vehicle, respectively. A total dose integrated over a 10-day period is calculated; however, the vast majority of this dose is received in the first several hours of launch.

Due to the relatively low thrust and subsequent deceleration of the NEP cargo vehicle as it climbs in altitude, the space station quickly outpaces the NEP vehicle in its orbit about the earth. Consequently, greater separation distances are maintained over time for launch configurations in which SSF initially leads the NEP vehicle. Figure 5.1 shows that for initial separation distances of at least 10 km, an order-of-magnitude reduction in cumulative doses to SSF crew is achieved if SSF initially leads rather than lags the NEP vehicle at launch. Figure 5.1 also shows that the space station crew will not expend their short-term radiation dose budgets provided SSF lags the NEP vehicle by at least 13 km or leads the NEP vehicle by at least 2.5 km at launch. Cumulative doses comparable to a one-month best-case natural dose of 0.01 Sv can be achieved for leading separation distances of only 16 km. It is interesting to note that the command and control zone for SSF extends ± 37 km in the orbital direction. Consequently, factors other than the concern for radiation exposure would dictate launch separation distances.

It is instructive to visualize the intermediate values which are needed to calculate each of the dose points in Figure 5.1. Consider launching the NEP vehicle with SSF initially leading by 10 km. Figure 5.2 plots the altitude of the NEP vehicle as a function of time, while Figure 5.3 gives the cumulative number of revolutions made by both the NEP vehicle and the SSF. Note that as the NEP vehicle climbs in altitude, it decelerates and its orbital period becomes longer. The resultant NEP-to-SSF separation distance is then plotted in Figure 5.4. Finally, the time history of cumulative radiation dose to SSF crew members is shown in Figure 5.5 on a logarithmic time scale. Even though the NEP vehicle makes a relatively slow ascent, the vast majority of the radiation doses to SSF crew is received within the first 6 hours of launch.

LAUNCH OF NTR PERSONNEL VEHICLE

In our second reference mission scenario, an NTR personnel vehicle is launched from SSF orbit with a tangential thrust of 1.112×10^6 N, a specific impulse of 900 s, and a propellant flow rate of 126 kg s^{-1}. The initial mass of the vehicle at launch is 456 metric tons. The radiation source term during launch is the Phoebus-class reactor of the TMI stage. We obtain an estimate of this source term by scaling the NERVA source terms given in Chapter 4 by the ratio of Phoebus-to-NERVA operating thermal power levels [5000 MW_t / 1575 MW_t]. The reactor is thus treated as an point source delivering approximately 225,500 Sv/s at a distance of one meter. The total burn time for trans-Mars insertion is 22.5 minutes.

Our results for the NTR vehicle are summarized in Figure 5.6. Here we plot the cumulative dose received by SSF crew members over the full 22.5 min TMI burn. In contrast to the departing NEP vehicle, cumulative doses are lower at a given separation distance if SSF initially lags rather than leads the NTR vehicle at launch. This shift in launch strategy is easily explained. The lighter NTR vehicle departs with a thrust ~8000 times that of the NEP vehicle and thus maximum separation distances are maintained if the NTR is launched ahead of SSF. If the vehicle is launched behind SSF, it will quickly pass the station at a slightly higher altitude resulting in greater cumulative doses. This latter trajectory is of particular concern since the first-stage NTR reactor delivers dose rates ~600 times that of the operating NEP reactor at the same distance. Figure 5.6 also indicates that short-term radiation dose budgets at SSF will not be exceeded if the NTR personnel vehicle is launched either at least 7 km ahead or at least 23 km behind the space station. If the radiation protection criterion to be meet is that cumulative doses at SSF should not exceed a

one-month worst-case natural dose (0.05 Sv), then the NTR should be launched either at least 20 km ahead or at least 73 km behind SSF. Finally, if the cumulative dose at SSF is not to exceed a one-month best-case natural dose (0.01 Sv), then the NTR should be launched either at least 62 km ahead or several hundred kilometers behind the space station.

As in the case of the NEP cargo vehicle, we can better understand these results by looking at intermediate values for a particular launch scenario. For example, consider the launch of the NTR vehicle with SSF initially lagging by 10 km. As shown in Figure 5.7, the NTR attains an altitude of almost 2800 km at the end of its TMI burn. The number of revolutions made by both the NTR and SSF during this time is shown in Figure 5.8, while the separation distance between the two objects is shown in Figure 5.9. Finally, the time history of cumulative radiation dose at SSF is shown in Figure 5.10. Whereas cumulative doses peak within a few fours during the launch of the NEP vehicle, the NTR becomes a negligible radiation source at SSF after only 2 to 3 minutes.

CONCLUSIONS

The dosimetry results for the two vehicles can be summarized by tabulating the minimum separation distances required to meet the radiation protection criteria derived in Chapter 3. These distances are shown in Table 5.2 for both vehicles. Cumulative doses of 0.05 and 0.01 Sv correspond to a one-month dose at SSF due to natural sources under worst-case and best-case conditions, respectively. Based upon radiation protection considerations only, it is advisable to have SSF lead the NEP and to have SSF lag the NTR vehicle during launch operations. The actual vehicle separation distance employed will depend upon the radiation dose criteria selected. For NEP vehicle, distances of at least 20 km can satisfy even the most restrictive dose limit. For the NTR vehicle, separation distances are more sensitive to the dose criteria selected. The NCRP dose limits can be meet for separation distances less than 10 km; however, the ALARA principle would suggest distances exceeding 60 km.

References

Armijo, J.S. et al. (1989) "SP-100, Technology Accomplishments," in Trans. of the Sixth Symposium on Space Nuclear Power Systems, CONF-890103--Summs., held in Albuquerque, NM, 8-12 January 1989, pp. 552 - 6.

Bohl, R.J., J.E. Boudreau and W.L. Kirk (1988) "History of Some Direct Nuclear Propulsion Developments since 1946," in Space Nuclear Power Systems 1987, M.S. El-Genk and M.D. Hoover, eds., Orbit Book Co., Malabar, FL, pp. 467 - 73.

Borowski, S.K., M.W. Mulac and O.F. Spurlock (1989) "Performance Comparisons of Nuclear Thermal Rocket and Chemical Propulsion Systems for Piloted Missions to Phobos/Mars," presented at the 40th Congress of the International Astronautical Federation, held in Malaga, Spain, 7-13 October 1989, paper IFA-89-027.

Deane, N.A. et al. (1989) "SP-100 Reactor Design and Performance," in Trans. of the Sixth Symposium on Space Nuclear Power Systems, CONF-890103--Summs., held in Albuquerque, NM, 8-12 January 1989, pp. 542 - 5.

IMSL (1989) MATH/LIBRARY Fortran Subroutines for Mathematical Applications, Version 1.1, MALB-USM-PERFCT-EN8901-1.1, IMSL, Inc., Houston, TX.

Pierce, B.L., R.R. Holman and H.D. Kulikowski (1989) "Single NERVA Derivative Reactor Design Concept for Space Nuclear Electrical Power and Direct Propulsion," in Trans. of the Sixth Symposium on Space Nuclear Power Systems, CONF-890103--Summs., held in Albuquerque, NM, 8-12 January 1989, pp. 542 - 5.

Schmidt, J.E., J.F. Wett and J.W.H. Chi (1988) "The NERVA Derivative Reactor and a Systematic Approach to Multiple Space Power Requirements," in Trans. of the Fifth Symposium on Space Nuclear Power Systems, CONF-880122--Summs., held in Albuquerque, NM, 11-14 January 1988, pp. 415 - 6.

Zimmerman, A. V., J. S. MacKay, and L. G. Rossa (1963) Optimum Low-Acceleration Trajectories for Interplanetary Transfers, NASA TN D-1456, NASA Lewis Research Center, Cleveland, OH.

Table 5.1 Trajectory Calculations for the NEP Cargo Vehicle.

TIME (DAYS)	ALT (km) (LERC)	ALT (km) (TAMU)	DIFFERENCE	REV. (LERC)	REV. (TAMU)	DIFFERENCE
0	450.0	450.0	0.0	0.000	0.000	0.000
1	473.7	473.6	0.1	15.347	15.347	0.000
2	497.6	497.9	-0.3	30.614	30.614	0.000
3	521.6	521.9	-0.3	45.801	45.802	0.000
4	545.8	545.9	-0.1	60.910	60.910	0.000
5	570.0	570.1	-0.1	75.939	75.940	-0.001
6	594.5	594.6	-0.2	90.889	90.890	-0.001
7	619.0	619.3	-0.3	105.761	105.762	-0.001
8	643.7	643.9	-0.2	120.555	120.556	-0.001
9	668.5	668.3	0.2	135.271	135.272	-0.001
10	693.5	693.6	-0.1	149.909	149.910	-0.001
11	718.5	718.6	-0.1	164.469	164.470	-0.001
12	743.8	743.9	-0.1	178.952	178.954	-0.001
13	769.2	769.1	0.1	193.358	193.360	-0.002
14	794.7	795.0	-0.3	207.688	207.690	-0.002
15	820.3	820.4	-0.1	221.941	221.943	-0.002
16	846.2	846.0	0.1	236.118	236.119	-0.002
17	872.1	871.9	0.2	250.218	250.220	-0.002
18	898.2	898.0	0.2	264.243	264.245	-0.002
19	924.5	924.3	0.2	278.193	278.195	-0.002
20	950.9	950.8	0.1	292.067	292.069	-0.002
21	977.4	977.6	-0.2	305.867	305.869	-0.002
22	1004.1	1004.4	-0.3	319.591	319.594	-0.002
23	1031.0	1030.8	0.2	333.241	333.244	-0.003
24	1058.0	1058.3	-0.3	346.817	346.820	-0.003
25	1085.2	1085.0	0.1	360.319	360.322	-0.003
26	1112.5	1112.8	-0.3	373.747	373.750	-0.003
27	1140.0	1139.8	0.1	387.102	387.105	-0.003
28	1167.6	1167.6	0.0	400.383	400.386	-0.003
29	1195.4	1195.7	-0.3	413.592	413.595	-0.003
30	1223.4	1223.7	-0.3	426.728	426.731	-0.003
31	1251.5	1251.8	-0.3	439.791	439.794	-0.003
32	1279.8	1280.1	-0.3	452.782	452.785	-0.003
33	1308.2	1308.6	-0.3	465.701	465.704	-0.003
34	1336.8	1337.1	-0.2	478.548	478.551	-0.003
35	1365.6	1365.5	0.1	491.324	491.327	-0.003
36	1394.6	1394.6	0.0	504.028	504.032	-0.003
37	1423.7	1424.1	-0.3	516.662	516.665	-0.003
38	1453.0	1452.9	0.2	529.225	529.228	-0.003
39	1482.5	1482.9	-0.4	541.717	541.720	-0.004
40	1512.2	1512.0	0.1	554.139	554.142	-0.004
41	1542.0	1542.1	-0.1	566.491	566.494	-0.004
42	1572.0	1572.3	-0.3	578.773	578.777	-0.004
43	1602.2	1602.2	0.0	590.986	590.989	-0.004
44	1632.5	1632.4	0.1	603.129	603.133	-0.004
45	1663.1	1662.9	0.2	615.203	615.207	-0.004
46	1693.8	1693.6	0.2	627.209	627.213	-0.004
47	1724.7	1724.6	0.1	639.146	639.149	-0.004
48	1755.8	1755.8	0.0	651.014	651.018	-0.004
49	1787.1	1787.4	-0.3	662.815	662.819	-0.004
50	1818.6	1818.8	-0.2	674.547	674.551	-0.004

Table 5.2 Minumum Launch Separation Distances (km) Required to Meet Various Radiation Dose Criteria.

	Cumulative Radiation Dose to SSF Crew		
	LBAD-st (0.2 Sv)	0.05 Sv	0.01 Sv
NEP Vehicle			
SSF Lagging @ Launch	13	44	>>100
SSF Leading @ Launch	2.5	6	16
NTR Vehicle			
SSF Lagging @ Launch	7	20	62
SSF Leading @ Launch	23	73	>>100

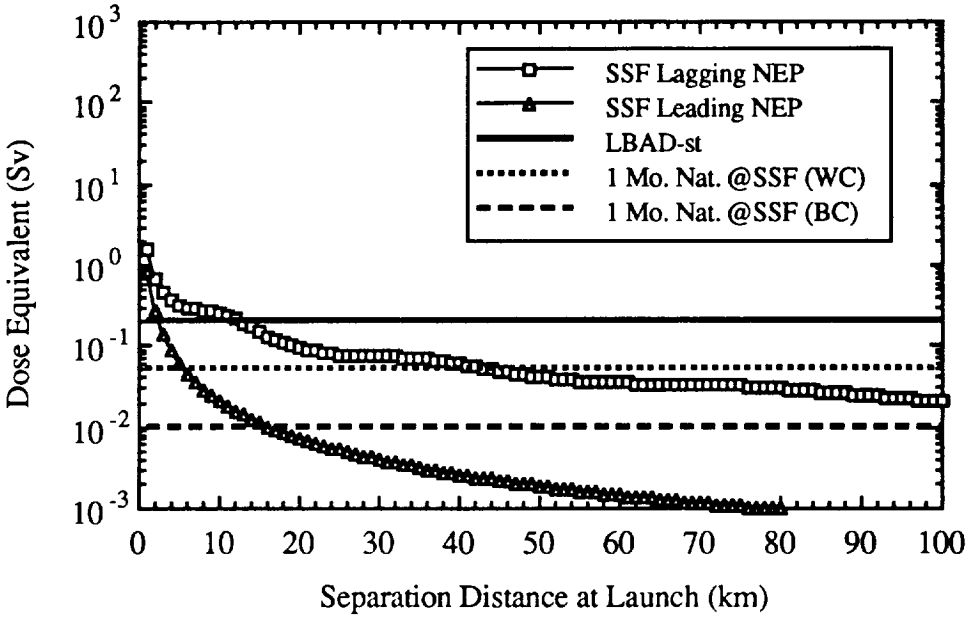

Figure 5.1 Cumulative Doses to SSF Crew Members during NEP Vehicle Launch.

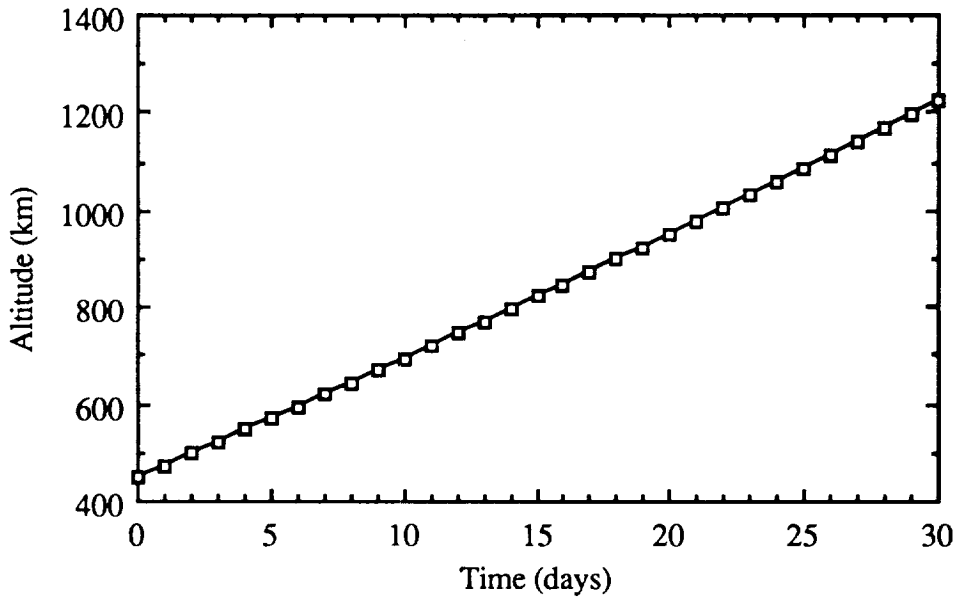

Figure 5.2 Altitude of NEP Cargo Vehicle during Launch.

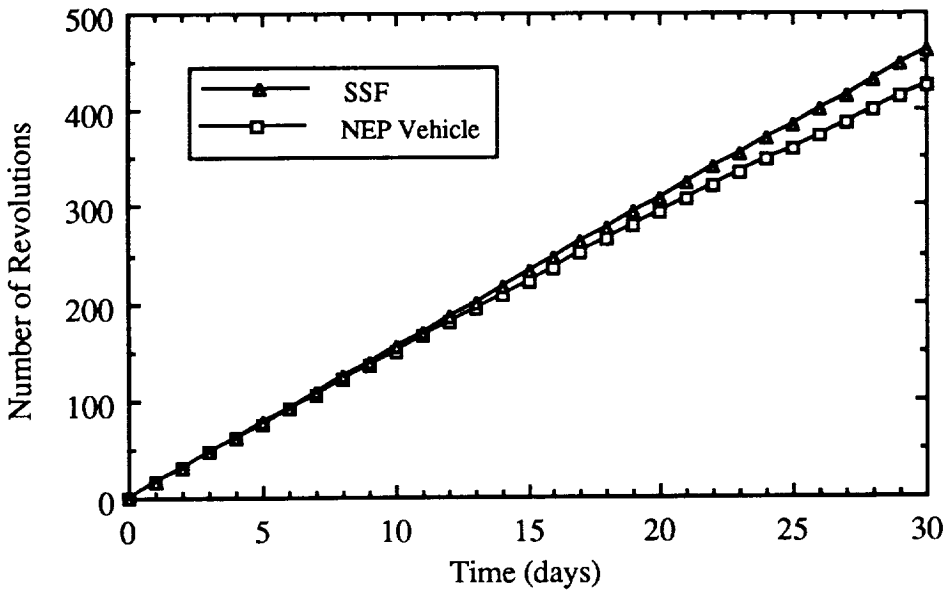

Figure 5.3 Revolutions made by the NEP Cargo Vehicle and SSF (SSF Leading NEP by 10 km at Launch).

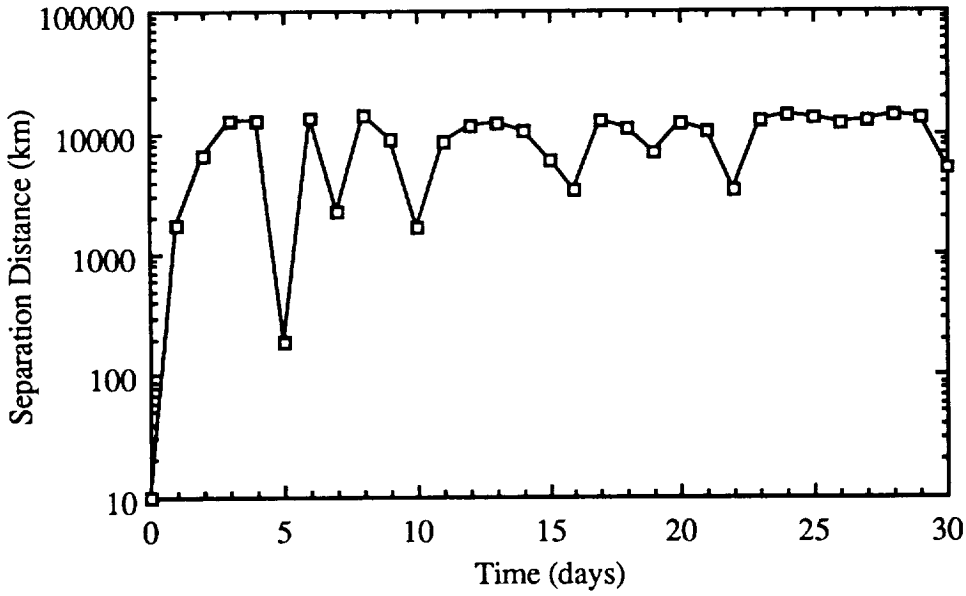

Figure 5.4 NEP-to-SSF Separation Distance during Launch (SSF Leading NEP by 10 km at Launch).

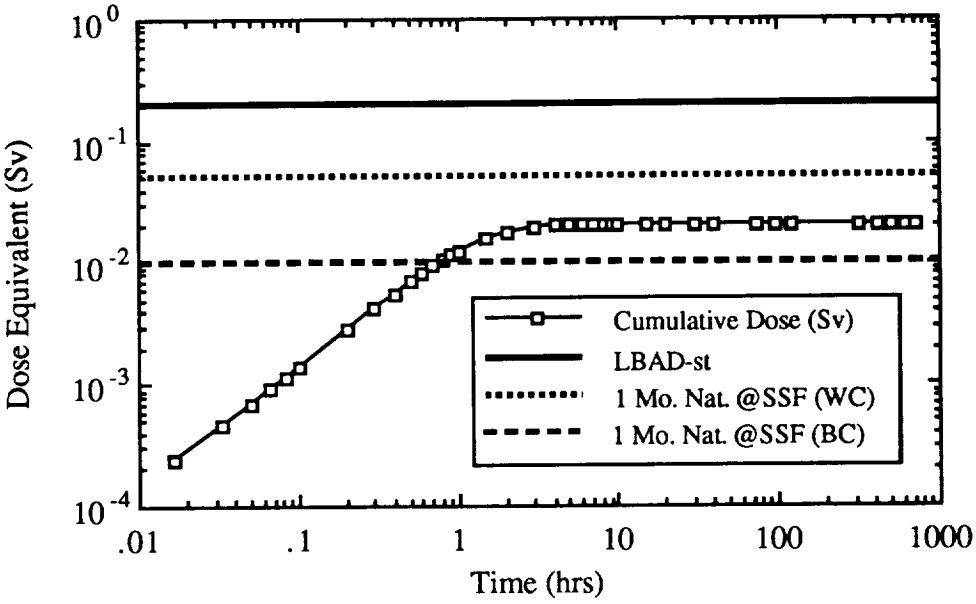

Figure 5.5 Cumulative Dose at SSF during Launch of NEP Vehicle (SSF Leading NEP by 10 km at Launch).

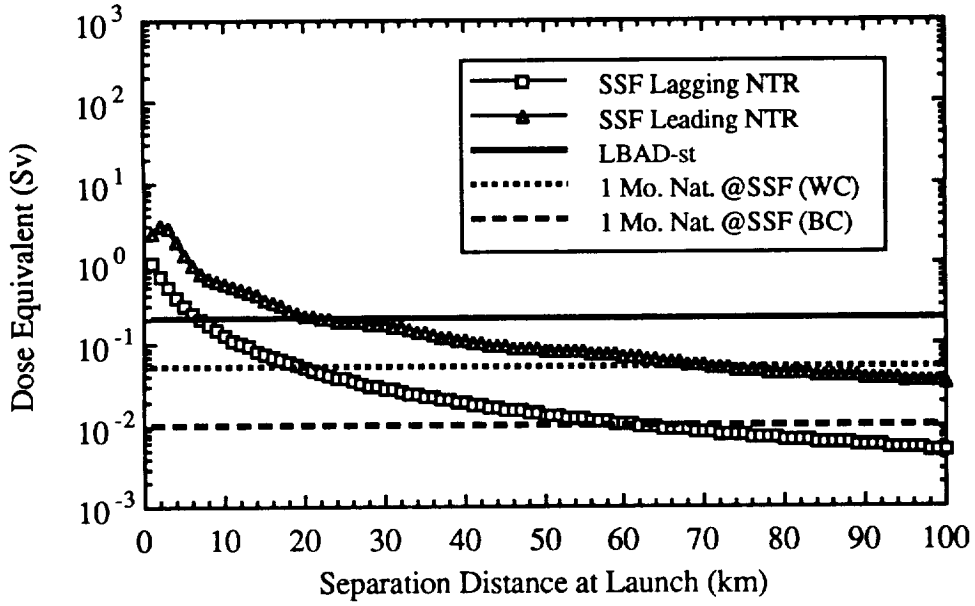

Figure 5.6 Cumulative Doses to SSF Crew Members during NTR Vehicle Launch.

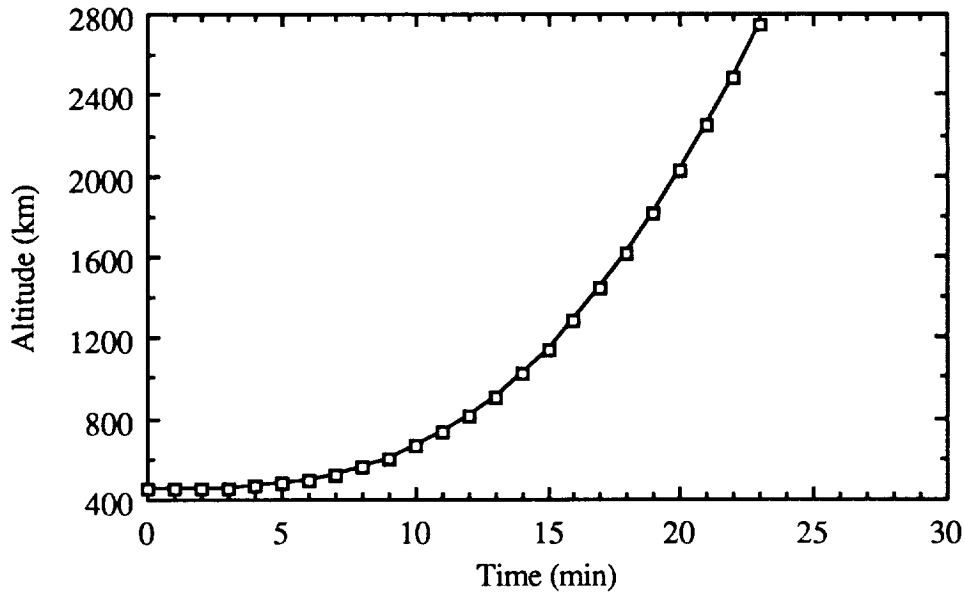

Figure 5.7 Altitude of NTR Personnel Vehicle during Launch.

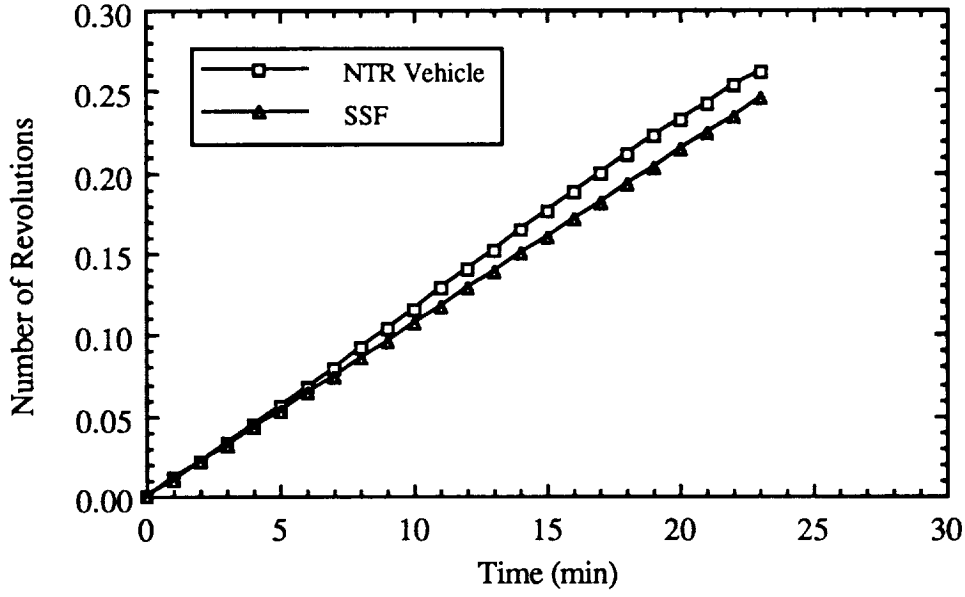

Figure 5.8 Revolutions made by the NTR Personnel Vehicle and SSF (SSF Lagging NTR by 10 km at Launch).

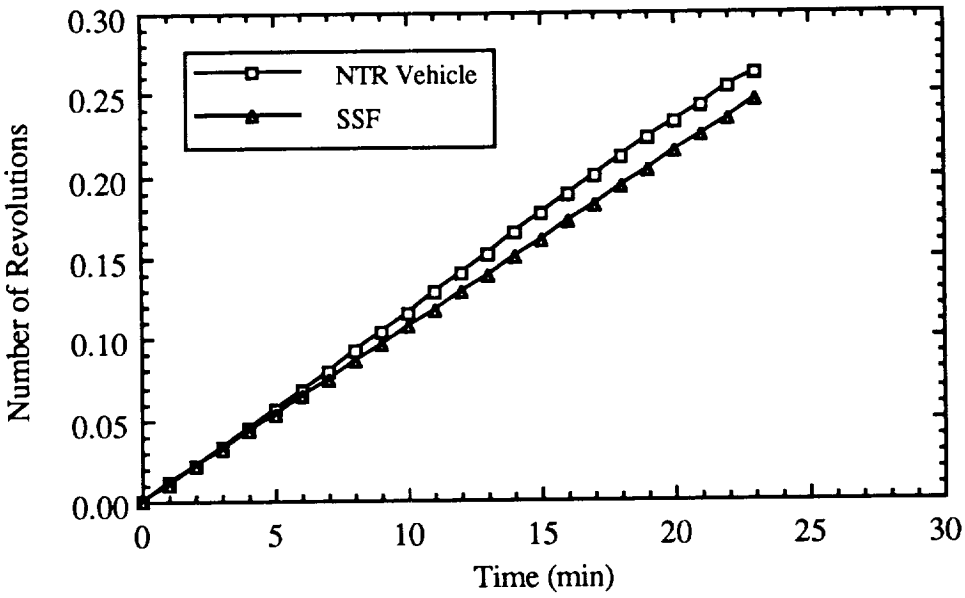

Figure 5.9 NTR-to-SSF Separation Distance during Launch (SSF Lagging NTR by 10 km at Launch).

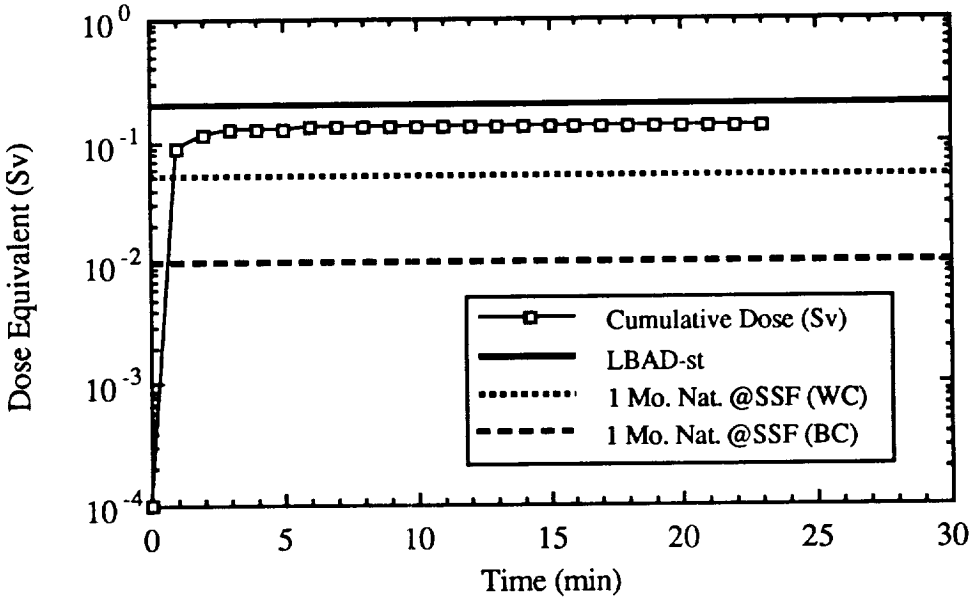

Figure 5.10 Cumulative Dose at SSF during Launch of NTR Vehicle (SSF Lagging NTR by 10 km at Launch).

CHAPTER 6

RADIOLOGICAL IMPACT OF RETURNING MARS VEHICLES

INTRODUCTION

This chapter describes the methodologies employed and results obtained from analyses of the radiological impact of returning Mars vehicles. The basic process employed was to identify and characterize likely Nuclear Electric Propulsion (NEP) and Nuclear Thermal Rocket (NTR) operational parameters, compute the shutdown gamma source terms, and employ these along with operational gamma dose rates to compute shutdown gamma dose rates. Parking distances and shutdown times required to keep the dose received by the SSF crew within the allowable dose budget were determined based on these computed shutdown gamma dose rates.

The methods employed in this analysis are approximate and the results are intended primarily to aid mission planning. However, the basic methodology is sound and the procedures employed could be refined, if necessary, to provide more accurate dose estimates. It is important to bear in mind that the dose to SSF crew is inversely proportional to the square of the separation distance from the reactor. For example, if the dose at a separation distance of 10 km is underpredicted by 50%, the separation distance need only be increased by about 22%. Similarly, since the gamma source from a shutdown reactor decreases exponentially with time, relatively short increases in reactor shutdown time can significantly decrease the dose received by SSF crew. Thus, the uncertainties associated with the source terms employed will not have a large impact on the computed required separation distances and shutdown times.

MARS MISSION AND SSF OPERATIONAL SCENARIOS

The two reference Mars mission scenarios employed in this work were developed based on discussions with the project staff at NASA Lewis Research Center (Stevenson and Willoughby 1989). The first consists of an NEP Mars cargo craft on a 1810 day round-trip to Mars departing from low earth orbit (LEO). It was assumed that an SP100-class reactor (Armijo et al. 1989 and Deane et al. 1989) would be employed. The reference SP-100 reactor currently under development has a baseline thermal power of 2.4 MW_t and

employs a static thermoelectric power conversion subsystem to produce 100 kW_e of power. The basic design goals of the SP100, however, call for scalability up to an order of magnitude higher power. In the scenario employed here, it was assumed that the reactor would generate 25 MW_t and utilize a dynamic system (Rankine or Brayton cycle) in order to provide 5 MW of electrical power. The vehicle was assumed to spend 150 days in Mars orbit with the reactor operating at 0.4 MW_t and 373 days coasting with a housekeeping power level of 0.2 MW_t; for the remainder of the mission, the reactor was assumed to be operating at its full rated power of 25 MW_t. The housekeeping power, 0.2 MW_t, was assumed to be available throughout the voyage.

The second Mars mission scenario consists of an NTR craft on a 486 day round-trip to Mars starting from LEO. The first portion of the mission, the trans-Mars insertion (TMI), is to be powered by a Phoebus-class reactor that would be discarded after Earth escape (Borowski et al. 1989 and Bohl et al. 1989). It was assumed that a NERVA-class reactor (Pierce et al. 1989 and Schmidt et al. 1988) operating at 1575 MW_t would be employed for the remainder of the mission. The NERVA-class reactor was assumed to be bimodal, providing both thermal power for propulsion and electrical power for housekeeping and mission requirements. The vehicle was assumed to spend 30 days in Mars orbit with the reactor operating at 0.4 MW_t and 456 days coasting at a housekeeping power level of 0.2 MW_t; for the remainder of the mission the reactor is to operate at its full rated power of 1575 MW_t. As with the NEP scenario, the housekeeping power is to be provided for the entire mission. The thermal power levels and duration of the mission phases for each of the mission scenarios are summarized in Tables 6.1 and 6.2.

The reactors were treated as point sources and no shielding from the vehicle structure, cargo, or reactor shields was considered. This represents a "worst-case" scenario and is conservative. In all likelihood, the craft itself or temporary shielding would be employed to reduce dose values below those reported here. Activated core and vehicle components would also make a minor contribution to the shutdown gamma source strength, but were neglected in this work.

GAMMA DOSE RATE FROM RETURNING MARS VEHICLES

The total integrated thermal power, or burnup, values for the NEP and NTR reactors are 32,310 and 210 MW-days (MWD), respectively. Thus, while the NTR has a rated thermal power more than 60 times that of the NEP, its burnup is less than 1% of the NEP's. This is a direct result of the very short duration of the full-power NTR burns. In contrast, the NEP operates at full power for over 70% of the mission. The gamma source term is directly dependent upon the magnitude of the fission product inventory, which in turn is governed by burnup. However, the fission product gamma source decays exponentially with time so that the operational history of the reactor also impacts the strength of the shutdown gamma field. In general, the NTR source term will be higher than that of the NEP shortly after reactor shutdown due to the presence of a large number of short-lived fission products produced during the Earth orbital capture (EOC) phase. These will die off shortly, within a matter of days, and the NEP and NTR source terms will be roughly equal. For longer periods of time, the higher burnup of the NEP reactor will dominate and its source term will be larger than that of the NTR. Both source terms will, however, die off exponentially with time.

The gamma source terms and decay heat model employed in this work were described in some detail in Chapter 4. These were employed to compute the gamma energy release and dose rate after shutdown for the mission scenarios described above. Figure 6.1 gives the NTR shutdown gamma energy release rate, or power, due to the decay of fission products; both the contribution from each mission phase and the total gamma heating rate are shown. Figure 6.2 presents this same information, but with a limited power scale in order to more clearly illustrate the curves. The most recent burn dominates all others during the first month after any shutdown. The inventory of short-lived isotopes produced during the EOC burn represents a relatively strong gamma source term. The short-lived radioisotopes produced during the other mission phases have already decayed away; those that remain have much longer half lives and are comparatively weak gamma sources. The housekeeping power produced during the coast to Earth also produces an inventory of radioisotopes that contributes significantly after that produced during the EOC burn has cooled off slightly. At two months after reactor shutdown, radioisotopes from the EOC phase comprise about 50% of the total source strength while those built up during the coast to Earth represent approximately 25%. At much longer shutdown times, on the order of a year, most of the phases contribute equally to the total.

The NEP gamma energy release rate after shutdown is less complicated than that for the NTR. The contribution from the propulsive power completely dominates that from housekeeping and Mars operations for all reactor shutdown times. The NEP gamma source strength is initially less than that of the NTR, but it does not decrease nearly as fast as that of the NTR since it has been operated at full power for over 300 days prior to shutdown. The gamma energy release rate from the NTR has fallen to 1/3 of that for the NEP after only one day. The time at which the source term for the NTR becomes the lesser of the two is, of course, dependent on the mission scenario.

As discussed in Chapter 4, the dose rate from each reactor is directly proportional to the gamma energy release rate, although the constant that relates these two quantities is different for the two reactors. The total gamma dose rates for both the NTR and NEP are compared in Figure 6.3. The behavior of these curves is governed by the same factors that determine the gamma energy release rates described above. The dose rates are shown on a more limited scale in Figure 6.4. The dose rate for the NTR falls below that of the NEP at about 10 days after shutdown.

INTEGRATED GAMMA DOSE FROM RETURNING MARS VEHICLES

The reactors on the returning Mars craft are assumed to be shutdown for some time period after arrival in LEO at a relatively large distance from SSF. The craft are then towed or drift to within some variable distance of SSF; it is at this time that the calculation of the dose to SSF crew begins. As explained in Chapter 4, the relationships employed to compute the dose rates discussed in the section above can be integrated over exposure time to yield absorbed dose values.

Three basic SSF operational scenarios were examined and it is believed that these encompass the range of possible interactions between returning Mars vehicles and SSF crew. The first is a 4-hour EVA in close proximity to the reactor. This is intended to model an operation involving unloading of the returning vehicle. In this case, it is likely that only a few crew members would be exposed. The next two are 30- and 180-day parking scenarios in which the vehicles are positioned at a relatively large distance from SSF. These represent periods during which the craft may be refurbished for another voyage, and the entire SSF crew would receive the calculated dose.

The 4-hour EVA and 30-day parking scenario cases were examined using the maximum recommended 30-day dose (one-half the annual dose) while the entire annual dose budget was allowed in the 180-day case. The selection of these dose budgets is discussed in Chapter 3.

Figure 6.5 illustrates the the six-month parking dose for the NEP reactor at distances of 1, 5, and 10 km along with the long-term lower bound on available dose (LBAD-lt = 0.2 Sv) and the six-month natural space dose under worst-case (0.3 Sv) and best-case (0.06 Sv) conditions, respectively. The point at which any dose curve crosses the LBAD-lt line gives the minimum shutdown time required to meet the radiation protection guidelines. Thus, for a parking distance of 1 km, a reactor shutdown time of about 180 days is required to insure that the dose to the SSF crew is less than LBAD-lt. Conversely, the craft can be brought immediately to parking distance in excess of approximately 4 km without exceeding this limit. The worst-case natural dose is higher than LBAD-lt and at 1 km a shutdown time of only 135 days is required for the dose from the reactor to equal this value. At a parking distance of 5 km, a reactor shutdown time of less than 8 days is required to lower the dose to the same level as the best-case natural dose. At parking distances in excess of 6 km, the parking dose is always less than the natural dose. In this case, the reactor need not be shutdown far from SSF and towed to its parking position, but rather could arrive there under its own power.

Figure 6.6 illustrates the the 30-day parking dose for the NEP reactor at the same parking distances as for the six-month case. The short-term lower bound on available dose (LBAD-st = 0.2 Sv) and one-month natural dose under worst-case (0.05 Sv) and best-case (0.01 Sv) conditions are also given. A reactor shutdown time of 75 days is required to yield a dose to the SSF crew less than LBAD-lt for a parking distance of 1 km. At parking distances of only a few kilometers, the vehicle can be delivered immediately after shutdown without exceeding the LBAD criterion. Comparing figures 6.5 and 6.6 shows that the craft may be brought much closer to SSF if it will only be in the vicinity for 30 days. This is because half of the annual dose may be received if the exposure period is limited to 30 days. A more detailed discussion of the relationship between the 30-day and 6-month parking restrictions is given later in this chapter.

Figure 6.7 gives the 4-hour EVA dose outside the shadow shield of a NEP reactor at distances of 50, 100, and 200 m along with the same LBAD-st and natural values given above. A separation distance of at least 50 m is required to meet LBAD-st constraints for a

shutdown time of 150 days. For this same shutdown time, separation distances of 100 and 200 m give approximately the same dose to the EVA crew as the one-month natural dose under worst-case and best-case conditions, respectively. At a separation distance of 200 m, a 4-hour EVA would be permissible outside the shadow shield after a shutdown period of only a few days. The results for an 4-hour EVA inside the shadow shield are shown in Figure 6.8; note that the scale on the y-axis (dose) is shifted one order of magnitude lower than those discussed above. As can be seen, a 50 m EVA could be performed almost immediately without exceeding the tightest criterion. The EVA may be performed within 13 m of the reactor without exceeding LBAD-st.

Figures 6.9, 6.10, and 6.11 give the results for the NTR vehicle. The results are similar to those discussed above with the exception that the NTR gamma dose rate is higher at very short shutdown times (less than 10 days) due to the recent EOC burn and decreases faster than that of the NEP due to a lower integrated reactor power (burnup). The results for the NTR will be discussed mainly from the standpoint of their differences with respect to the NEP cases outlined above.

The six-month parking dose for the NTR is shown in Figure 6.9. A reactor shutdown time of just under 90 days is required to meet the LBAD-lt criterion at a 1-km separation distance; the corresponding shutdown time for the NEP is about 180 days. Nevertheless, to allow parking distances greater than a few kilometers, a shutdown time of only one day is needed to allow the short-lived fission products produced during the EOC burn to decay sufficiently.

Figure 6.10 gives the 30-day parking dose for the NTR. A separation distance of only 1 km is required for a shutdown time of about 25 days in order to meet the LBAD-st requirements. As with the six-month NTR parking dose, a shutdown time of only about 1 day is required for parking distances of more than a few kilometers. The required shutdown time for the NEP with a parking distance of 1 km is 75 days.

The 4-hour EVA dose outside the disk shield of a NTR reactor is presented in Figure 6.11. A separation distance of at least 50 m is required to meet LBAD-st constraints for a shutdown time of 90 days; 150 days were required for the NEP at this distance. A shutdown time of only 6 days is required at a separation distance of 200 m.

Some of the data illustrated above were tabulated to provide a more concise set of results. Table 6.3 summarizes the shutdown times necessary to satisfy the LBAD-st criterion (0.2 Sv) for a 4-hour EVA at the separation distances discussed above.

For relatively small separation distances, the NEP reactor requires a longer shutdown time than the NTR, however, the situation is reversed for larger separation distances. This is a direct result of the variation of the gamma source terms for these reactors with shutdown time. As previously discussed, the NTR gamma source strength is initially larger than that of the NEP due to the recent full-power operation of the NTR during EOC phase, but it decreases more quickly with shutdown time due to its much smaller total integrated power. Larger separation distances allow the shutdown time to be decreased and this places more weight on the initially large source term of the NTR. Short separation distances require longer shutdown periods and this tends to emphasize the larger long-term source strength of the NEP.

The shutdown time required to satisfy the LBAD-st criterion for 30-day parking scenarios at distances of 1 km are 75 and 21 days, respectively, for the NEP and NTR. Those for the NEP and NTR 6-month cases are 183 and 91 days, respectively. For the 5- and 10-km parking distances, either vehicle may be brought to its parking position immediately after shutdown without exceeding the LBAD limit.

The other limit employed in this analysis, a dose component from the reactor equal to that from the natural background, requires some degree of illustration before the tabulated results can be easily interpreted. This guideline is fundamentally different form the LBAD concept. A graphical representation of the integration of the dose rate at some arbitrary parking distance is shown in Figure 6.12. The area under the dose rate curve for a given exposure period starting at a specified reactor shutdown time yields the dose received during that exposure period. In the figure, 1- and 6-month exposures are given for cases where the exposure period begins (a) immediately after shutdown, (b) at a moderate shutdown time, and (c) at a long shutdown time. At short shutdown times, the dose for the first month would be substantially larger than the average monthly dose for the 6 month exposure since the dose rate curve is dropping off relatively sharply during this time. The total 6-month exposure dose would be roughly 3 times larger than that from the one-month case. As shown in part (b) of Figure 6.12 for moderate shutdown times, the slope of the dose rate curve is quite a bit less since the short-lived radioisotopes have decayed away. At this point, the dose for the 1-month exposure would be only 10 to 20% larger than the

average monthly dose for the 6-month exposure, and the total 6-month exposure dose would be about 5 times larger. Finally, at long shutdown times, the dose rate curve is dominated by long-lived isotopes and is relatively flat. The average monthly dose for the 6-month exposure is only slightly less than the dose received during the 1-month exposure and the total for the 6-month exposure is almost 6 times that value. The factors discussed above govern the 1- and 6-month natural dose limit parking distance curves. If the parking distance is determined by a natural dose limit, the craft may be parked closer if it is to stay there for 6-months, relative to the 1-month stay, since the integration of the reactor dose rate curve yields a lower average monthly dose. This is simply the result of a reactor dose rate that decreases with exposure time. At very long shutdown times and/or relatively flat dose rate curves, the parking distances determined by the 1-and 6-month natural levels will be almost equal.

As discussed above, the parking distances for 1-and 6-month exposure periods for which the accumulated dose is to be equal to the natural dose are related directly to the time at which the exposure begins and the reactor gamma dose rate curve. Figure 6.13 illustrates a scenario where the returning Mars vehicle is to be parked (a) for 6 months at a distance determined by the 6-month natural dose and (b) parked at 6 successive locations for a duration of 1 month per location, each determined by the 1-month natural dose. The total dose for these two cases will be the same at the end of 6 months and equal to that from 6 months natural exposure at SSF. The parking distance for the first few months of case (a) are larger than those for case (b). Again, this is a direct result of the decreasing reactor dose rate curve and the longer integration time for the 6 month exposure. In contrast, the parking distance for the last couple month parking periods are less than the 6 month distance since the dose rate curve has decreased during the previous months. As mentioned above, these parking distances will be almost equal at very long shutdown times since dose rate curves will be relatively flat.

Table 6.4 summarizes the shutdown times required to achieve a 30-day and 6-month parking gamma dose equal to the natural dose under best-case conditions (0.01 and 0.06 Sv, respectively). As discussed above, the parking distance for the 30-day case is larger than that for 6 months if the equivalent natural dose guidelines are employed.

The results presented above give the reactor shutdown time necessary to satisfy a given dose criterion at some separation or parking distance. This is useful for the case where the separation or parking distance is a fixed mission parameter and the length of time

the reactor has been shutdown is the chief mission parameter that may be varied. However, it may also be possible to satisfy mission requirements by altering both the parking distance and shutdown time. To facilitate mission planning for the parking scenarios, several isodose plots were constructed which give the relationship between parking distance and shutdown time required for several dose limits.

Figures 6.14 and 6.15 give the isodose curves for the NEP and NTR for 1- and 6-month exposures governed by LBAD and the natural dose at SSF. Several features discussed previously in this section can be seen. The NEP isodose curves are flatter than those for the NTR; this is dictated by the shape of the dose rate curves for the two reactors. The one-month natural isodose curve is more restrictive than the six-month limit, and they approach one another at long shutdown times. The LBAD-st isodose curve is less restrictive than that determined by LBAD-lt since half of the annual dose limit is taken during the one-month exposure. It is vital that all the factors discussed above be kept in mind when interpreting these curves. Finally, Figure 6.16 gives a direct comparison of the isodose curves for the NTR and NEP.

MISSION SCENARIO SENSITIVITY STUDY

Some of the parameter values employed in this work were somewhat arbitrary, particularly the thermal power levels employed during the Mars operations and coasting phases. These were subjected to a sensitivity analysis to explore their impact on the predicted dose values. The most direct method to accomplish this is to examine the impact of these variables on the total integrated thermal power. The ratio of each power level (propulsion, Mars operations, and housekeeping) to its reference value was varied independently from 0 to 2 and a ratio of the total integrated thermal power for this alternative to the reference point calculated. Figures 6.17 and 6.18 illustrate the results of this analysis for the NEP and NTR scenarios, respectively. The effect of varying the housekeeping and Mars operations power on the total integrated thermal power is negligible for the NEP. Thus, only the level of propulsive power will have a significant impact on the results presented here; furthermore, the dose will scale approximately linearly with this power level. For the NTR, the effects of changing the propulsive and housekeeping power levels are roughly equal and the total integrated power is relatively insensitive to the Mars operations power level.

Figure 6.19 illustrates the LBAD-lt isodose curves for the baseline NTR and the same mission scenario without any housekeeping power production. The NEP LBAD-lt isodose curve is also given for comparison. As can be seen, this decreases the parking distance by about 25% at long shutdown times. Shorter shutdown times are strongly influenced by the short-lived radioisotopes produced by the EOC burn and will be less sensitive to the housekeeping power level.

MULTIPLE-EVENT SCENARIOS

The results given in this section were derived under the assumption that the dose from the event under consideration and the natural dose are the only SSF crew radiation exposures. This can be denoted as a single-event scenario. However, it is quite possible that some or all of the SSF crew will receive radiation doses from multiple events. Consider, for example, the case where a returning Mars vehicle is brought to the 30 day parking distance and left for 10 days in order to unload the crew and freight. The dose received by the entire SSF crew during this time would be roughly half of LBAD-st, or about 0.1 Sv. Some members of the crew would be involved in EVA near the vehicle and thus would have an additional exposure term. Their EVA would be restricted so that the combined dose from the 10 day parking exposure and that from their EVA trip(s) would be less than LBAD-st (0.2 Sv). After this time, the craft is to be placed at a distance selected to keep the total dose received by any crew member under LBAD-lt (0.2 Sv). An illustration of this parking scenario and its relationship to the 30 day and 6 month parking curves is illustrated in Figure 6.20. The scenario could be further complicated by the rotation of some crew members during this time period. The impact of multiple-event scenarios on mission planning and SSF operations will be explored in detail as part of a follow-on project.

CONCLUSIONS

The work performed in this study to analyze the radiological impact of returning Mars NEP and NTR mission vehicles indicates that reasonable parking and EVA distances, in conjunction with relatively short reactor shutdown periods, can be employed to meet current radiation protection guidelines or equivalent natural dose. There does not appear to be a likely operational scenario which could not be addressed in this manner. Furthermore, most of the cases presented here assume that the craft and reactor shielding are not available to reduce the dose to the SSF crew; this is very conservative. In addition, portable shielding could be employed to reduce the dose to the SSF crew for EVA and parking scenarios.

References

Armijo, J.S. et al. (1989) "SP-100, Technology Accomplishments," in Trans. of the Sixth Symposium on Space Nuclear Power Systems, CONF-890103--Summs., held in Albuquerque, NM, 8-12 January 1989, pp. 352-6.

Bohl, R.J., J.E. Boudreau and W.L. Kirk (1988) "History of Some Direct Nuclear Propulsion Developments since 1946," in Space Nuclear Power Systems 1987, M.S. El-Genk and M.D. Hoover, eds., Orbit Book Co., Malabar, FL, pp. 467-73.

Borowski, S.K., M.W. Mulac and O.F. Spurlock (1989) "Performance Comparisons of Nuclear Thermal Rocket and Chemical Propulsion Systems for Piloted Missions to Phobos/Mars," presented at the 40th Congress of the International Astronautical Federation, held in Malaga, Spain, 7-13 October 1989, paper IFA-89-027.

Deane, N.A. et al. (1989) "SP-100 Reactor Design and Performance," in Trans. of the Sixth Symposium on Space Nuclear Power Systems, CONF-890103--Summs., held in Albuquerque, NM, 8-12 January 1989, pp. 542-5.

Pierce, B.L., R.R. Holman and H.D. Kulikowski (1989) "Single NERVA Derivative Reactor Design Concept for Space Nuclear Electrical Power and Direct Propulsion," in Trans. of the Sixth Symposium on Space Nuclear Power Systems, CONF-890103--Summs., held in Albuquerque, NM, 8-12 January 1989, pp. 145-8.

Schmidt, J.E., J.F. Wett and J.W.H. Chi (1988) "The NERVA Derivative Reactor and a Systematic Approach to Multiple Space Power Requirements," in Trans. of the Fifth Symposium on Space Nuclear Power Systems, CONF-880122--Summs., held in Albuquerque, NM, 11-14 January 1988, pp. 415-6.

Stevenson, S. and A. Willoughby (1989) Personal Communication, NASA Lewis Research Center and Analex Corp., Cleveland, OH, September 1989.

Table 6.1 NEP Mission Scenario Description.

Mission Phase	Duration (days)	Power (MWth)
Earth Spiral-Out (from 450 km)	443	25
Heliocentric to Mars		
1st Portion: Thrust	253	25
2nd Portion: Coast	162	0.2
3rd Portion: Thrust	85	25
Mars Spiral-In	86	25
Mars Operations	150	0.4
Mars Spiral-Out	39	25
Heliocentric to Earth		
1st Portion: Thrust	74	25
2nd Portion: Coast	211	0.2
3rd Portion: Thrust	68	25
Earth Spiral-In (to 450 km)	239	25
Earth Orbit Arrival	Variable	Reactor Shutdown

Table 6.2 NTR Mission Scenario Description.

Mission Phase	Duration (days)	Power (MWth)
Trans-Mars Insertion (TMI)	(1st stage)	(1st stage)
Coast To Mars	286	0.2
Mars Orbital Capture (MOC)	0.028	1575
Mars Operations	30	0.4
Trans-Earth Insertion (TEI)	0.024	1575
Coast To Earth	170	0.2
Earth Orbital Capture (EOC)	0.016	1575
Earth Orbit Arrival	Variable	Reactor Shutdown

Table 6.3 Shutdown Time (days) Required to Satisfy LBAD Criterion for 4 Hour, Unshielded EVA.

Separation Distance (m)	NEP	NTR
50	150	88
100	49	22
200	2.8	6

Table 6.4 Shutdown Time (days) Required to Achieve a Dose Equal to the Natural Space Radiation Background (Best Case) for Parking Scenarios.

Parking Distance (km)	NEP 30 day	NTR 30 day	NEP 6 month	NTR 6 month
1	> 360	273	> 360	214
5	59	14	7.7	0.8
10	0	0.9	0	0

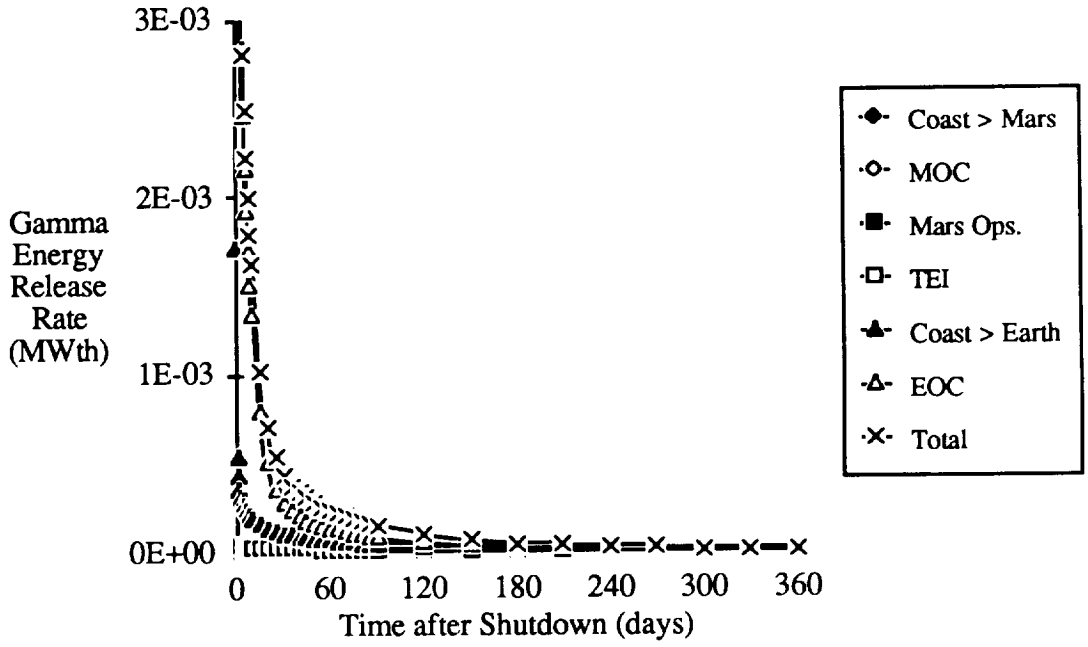

Figure 6.1 NTR Shutdown Gamma Power.

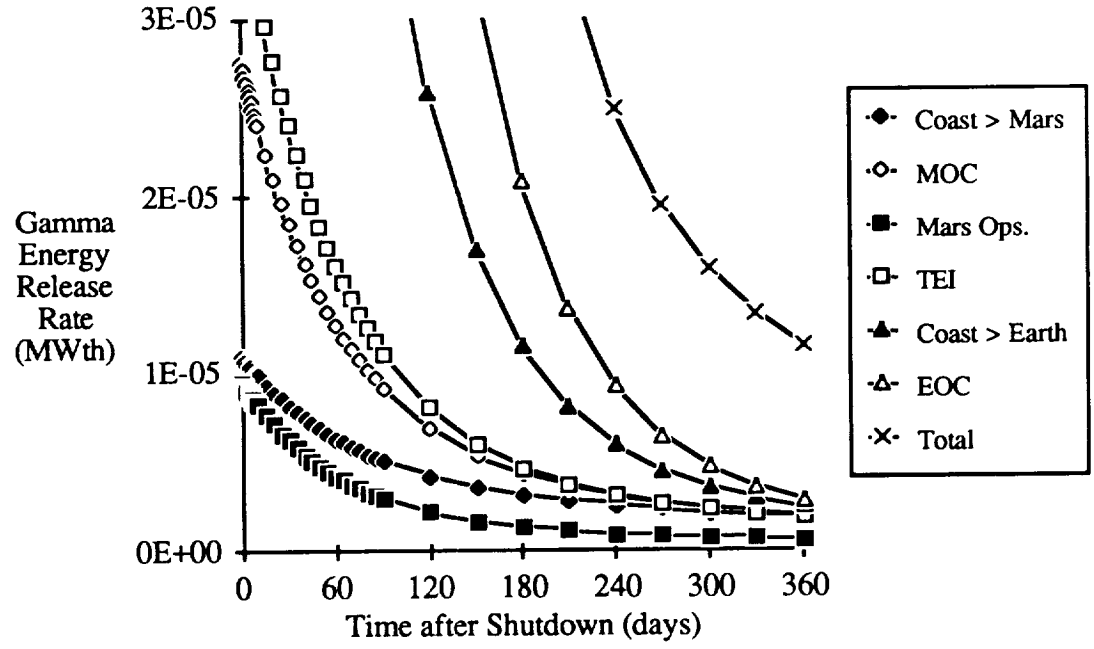

Figure 6.2 NTR Shutdown Gamma Power on a Reduced Scale.

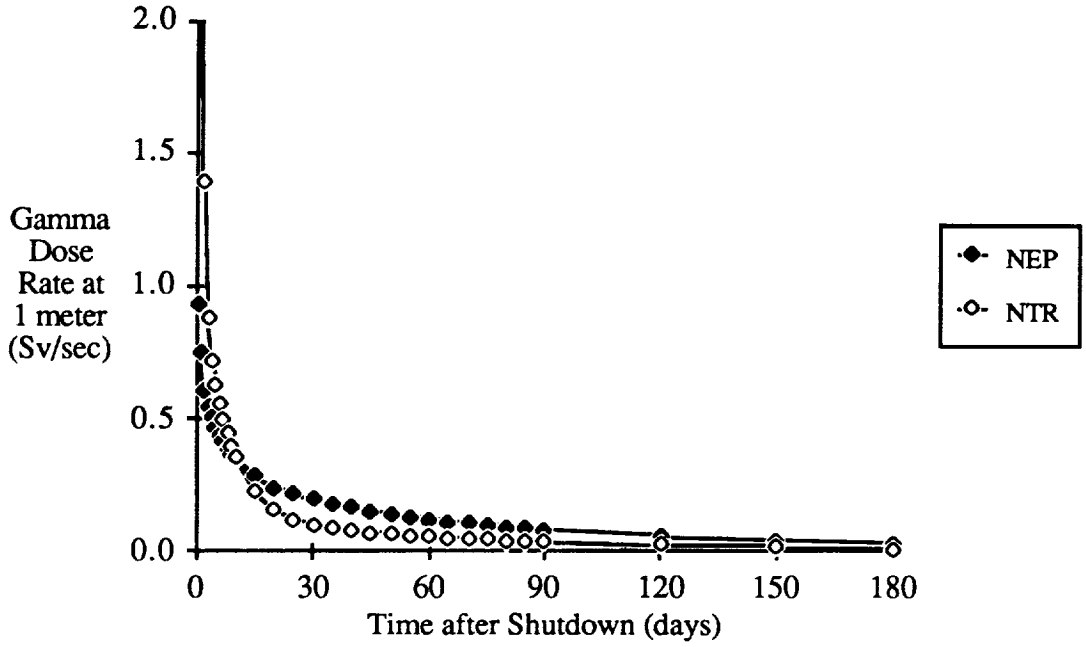

Figure 6.3 NTR and NEP Shutdown Gamma Dose Rate at 1 meter.

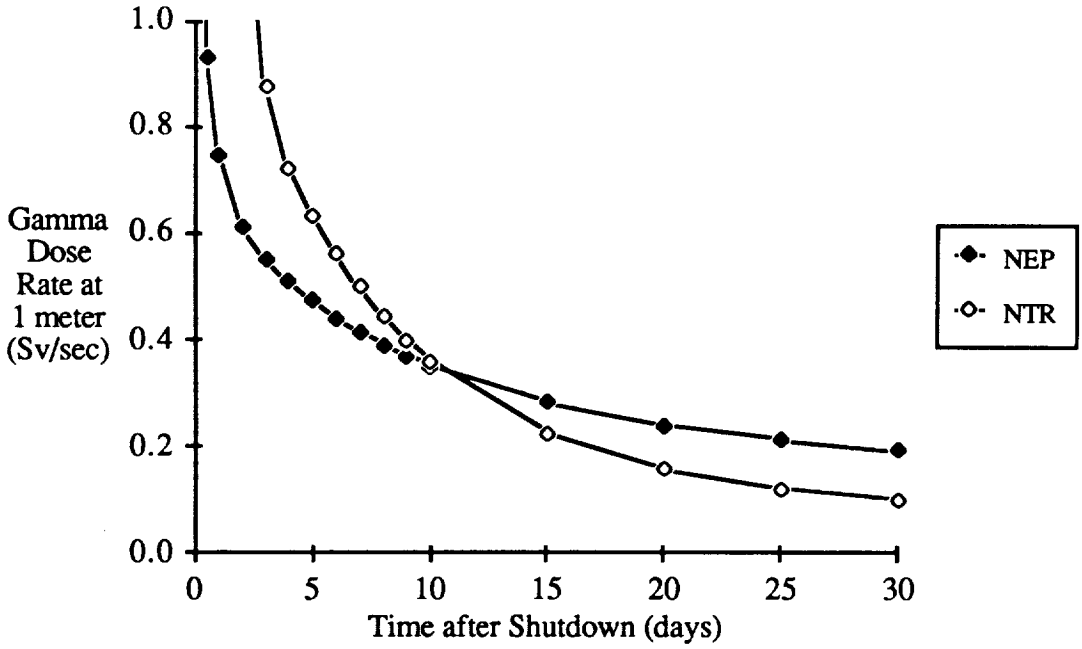

Figure 6.4 NTR and NEP Shutdown Gamma Dose Rate at 1 meter on a Reduced Scale.

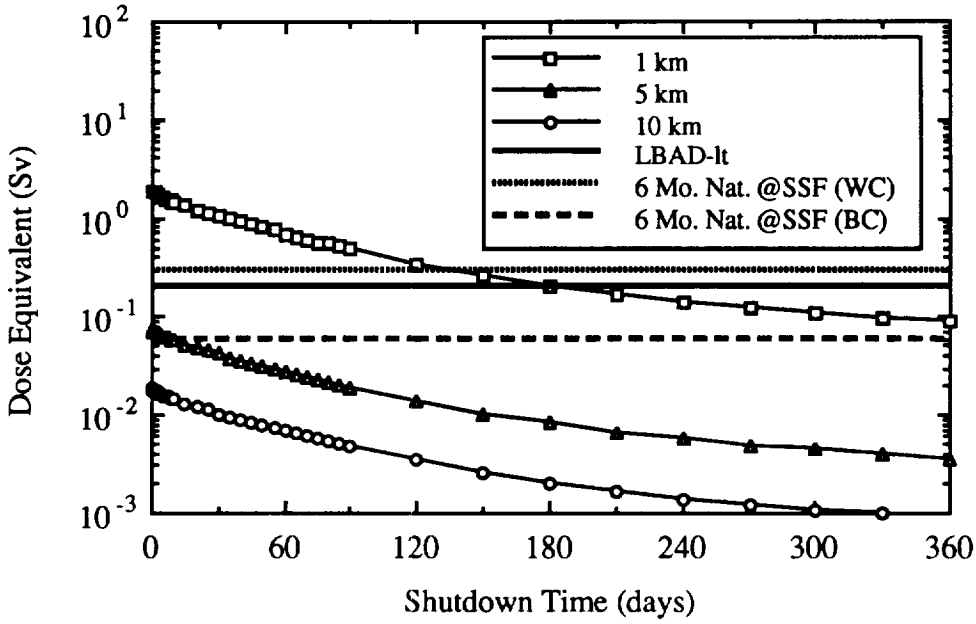

Figure 6.5 Shutdown NEP, 6 Month, Outside Shield, Parking Distance Curves.

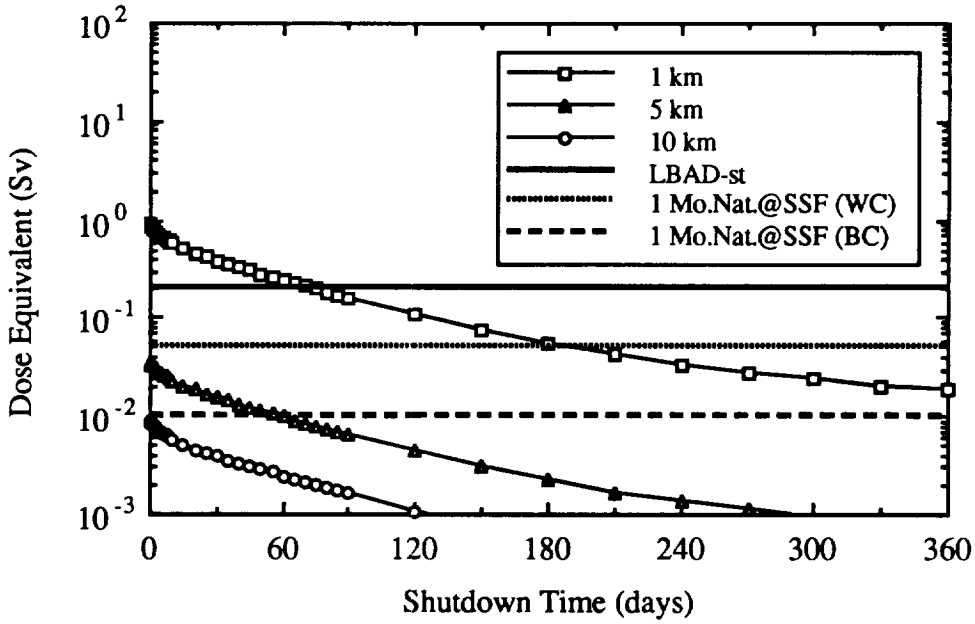

Figure 6.6 Shutdown NEP, 30 Day, Outside Shield, Parking Distance Curves.

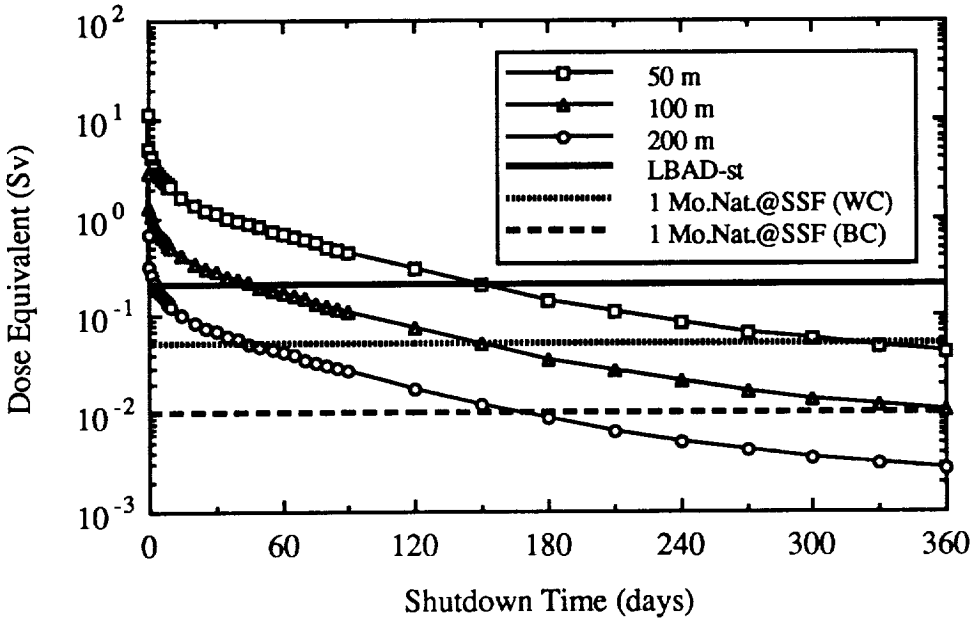

Figure 6.7 Shutdown NEP, 4 Hour EVA, Outside Shield, Separation Distance Curves.

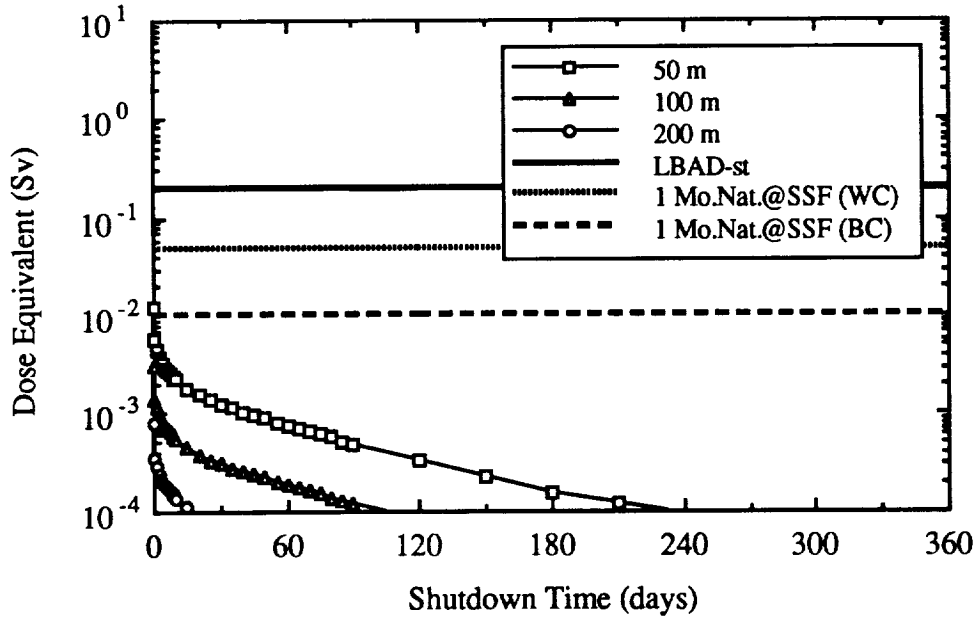

Figure 6.8 Shutdown NEP, 4 Hour EVA, Inside Shield, Separation Distance Curves.

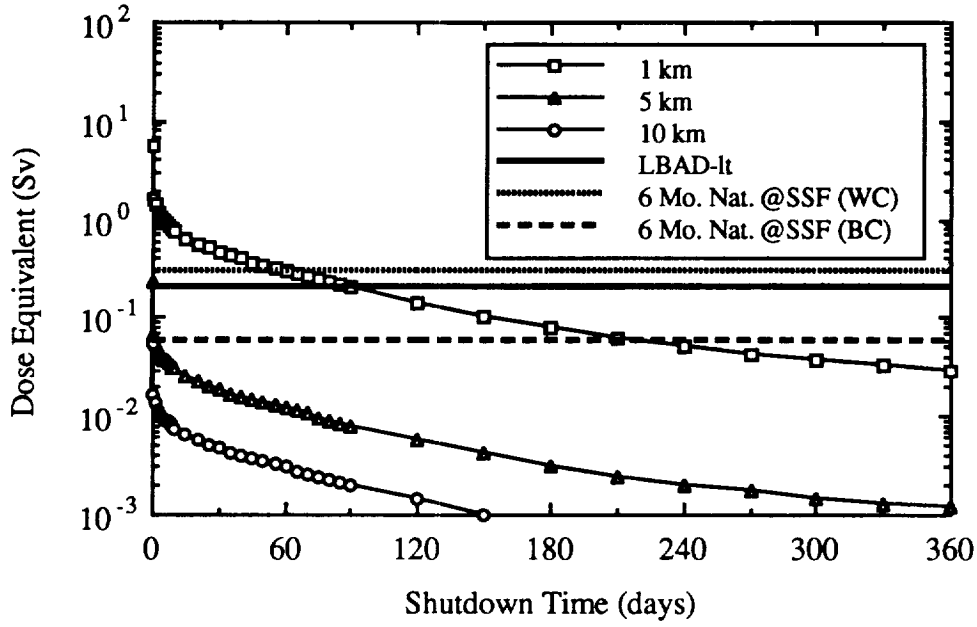

Figure 6.9 Shutdown NTR, 6 Month, Outside Shield, Parking Distance Curves.

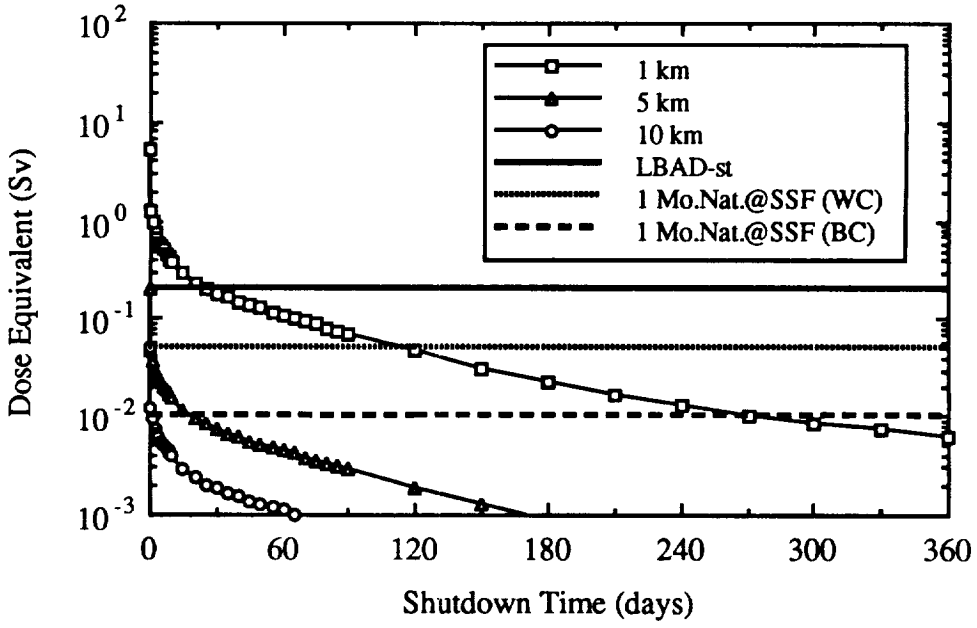

Figure 6.10 Shutdown NTR, 30 Day, Outside Shield, Parking Distance Curves.

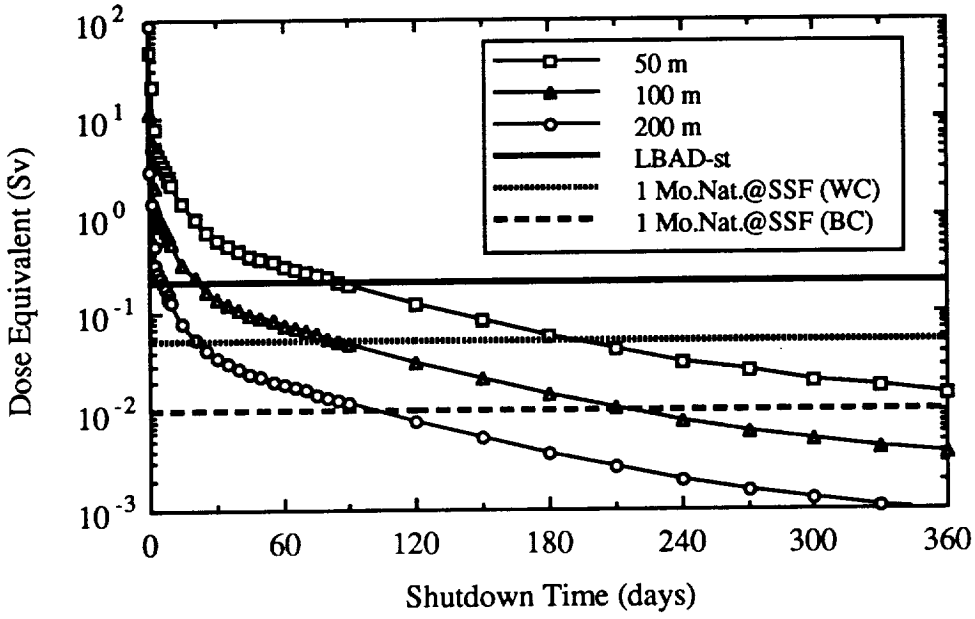

Figure 6.11 Shutdown NTR, 4 Hour EVA, Outside Shield Separation Distance Curves.

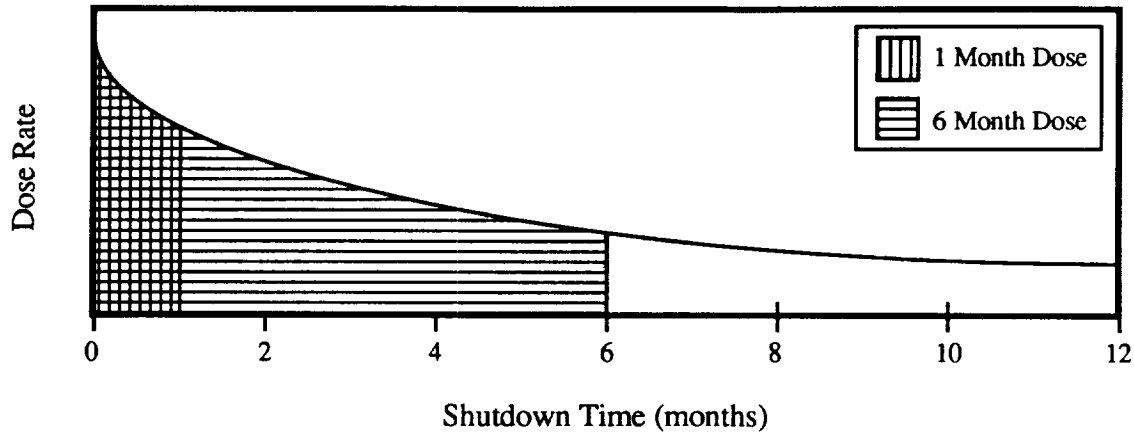

(a) Exposure Period Initiated Immediately After Shutdown.

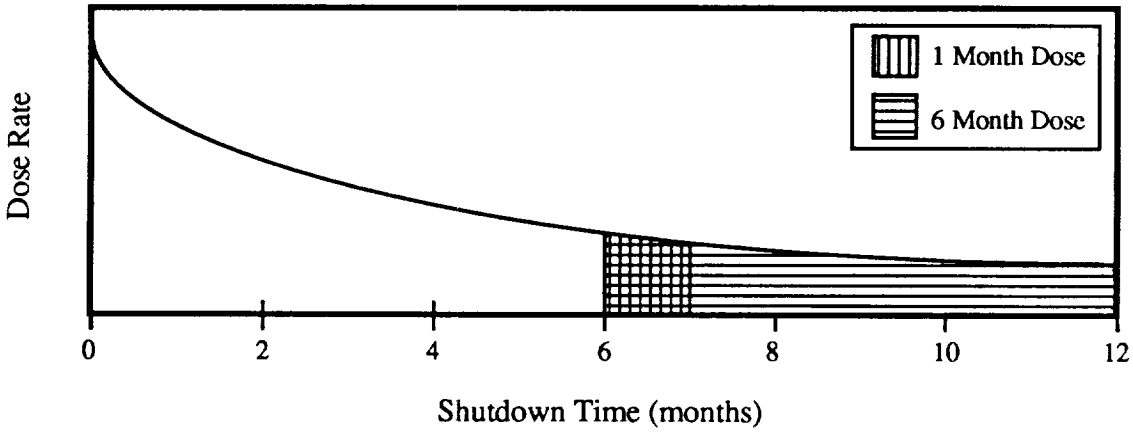

(b) Exposure Period Initiated at a Moderate Shutdown Time.

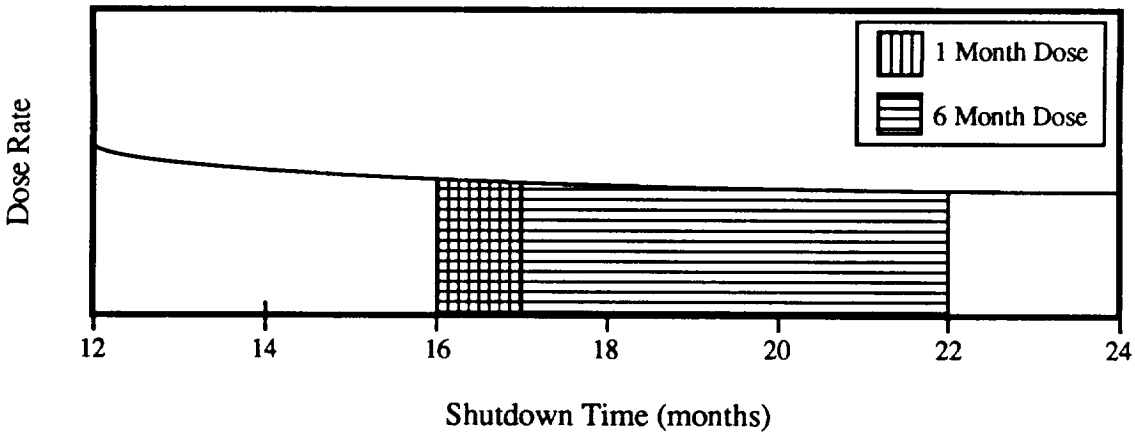

(c) Exposure Period Initiated After a Long Shutdown Time.

Figure 6.12 Variation of Backgound-Equivalent Dose with Shutdown Time.

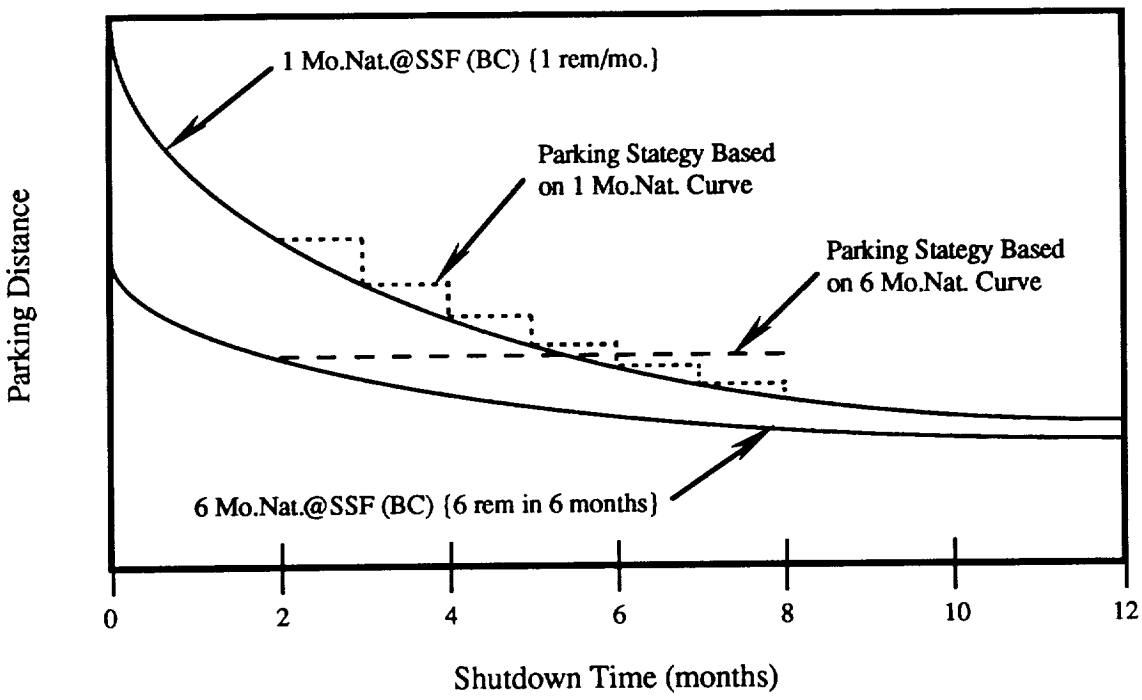

Figure 6.13 Parking Strategies Based Natural Space Radiation Isodose Curves.

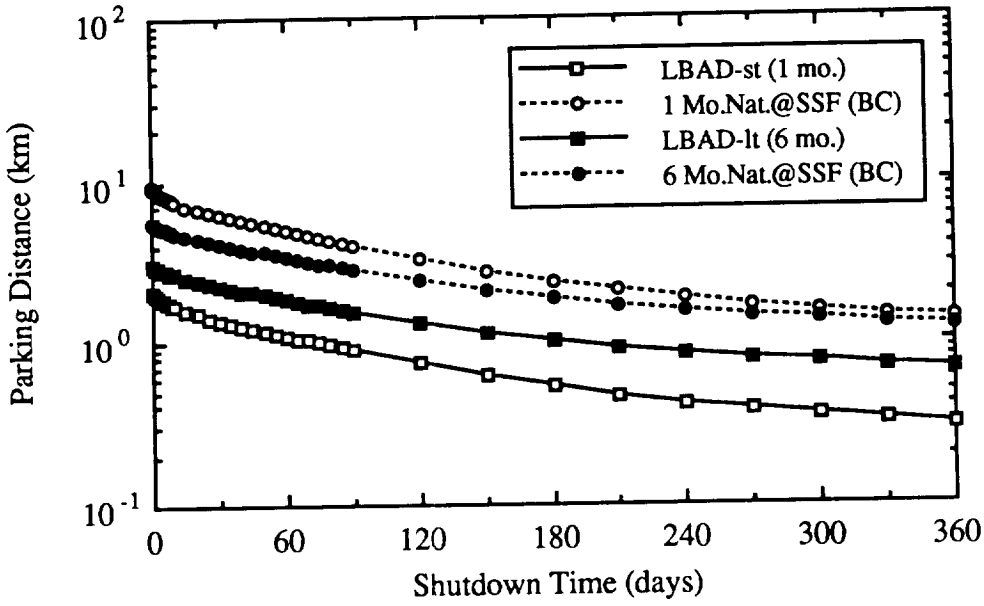

Figure 6.14 NEP LBAD and Equivalent Natural Dose Isodose Curves.

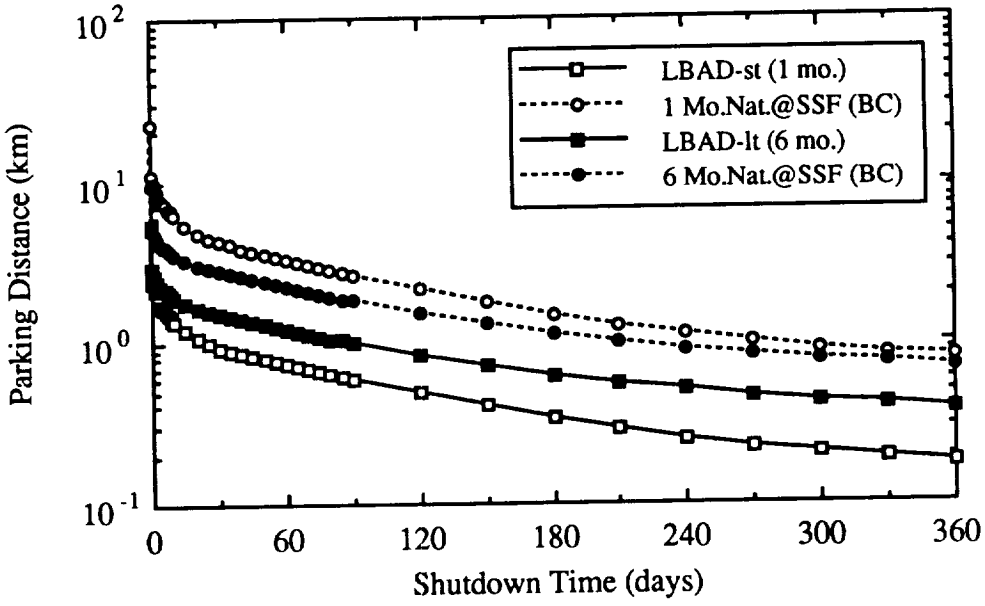

Figure 6.15 NTR LBAD and Equivalent Natural Dose Isodose Curves.

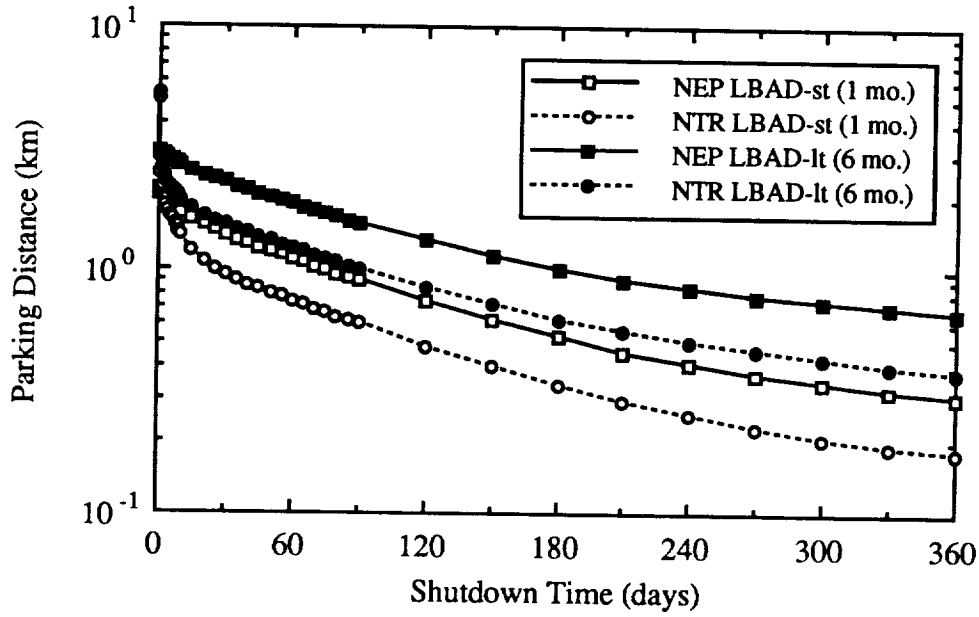

Figure 6.16 NTR and NEP LBAD-st and LBAD-lt Isodose Curves.

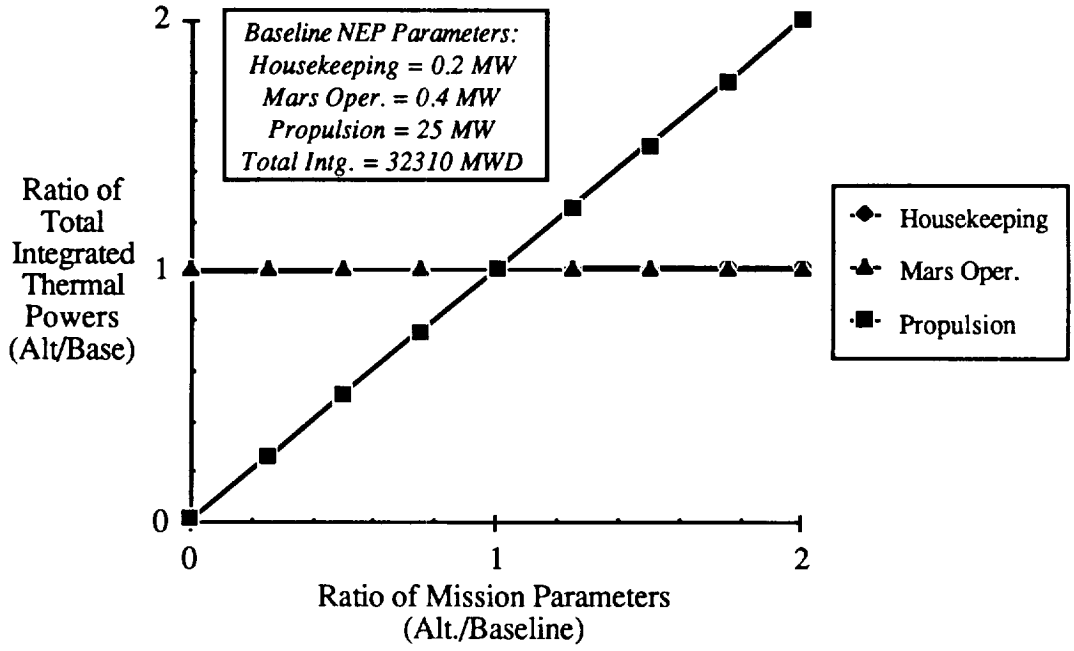

Figure 6.17 NEP Total Integrated Thermal Power Sensitivity Curves.

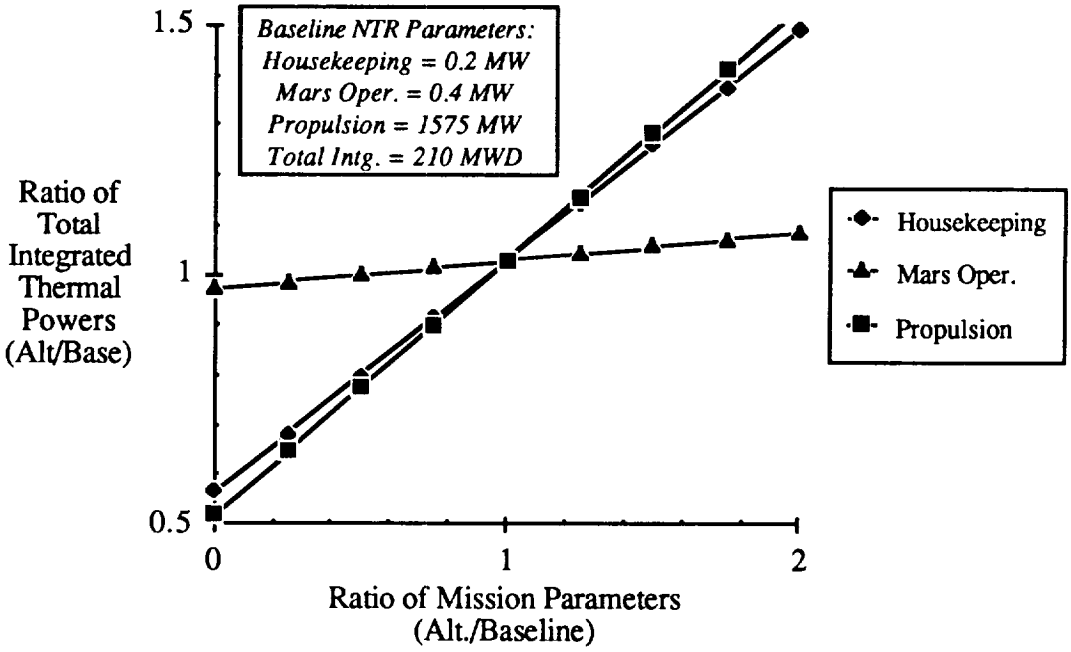

Figure 6.18 NTR Total Integrated Thermal Power Sensitivity Curves.

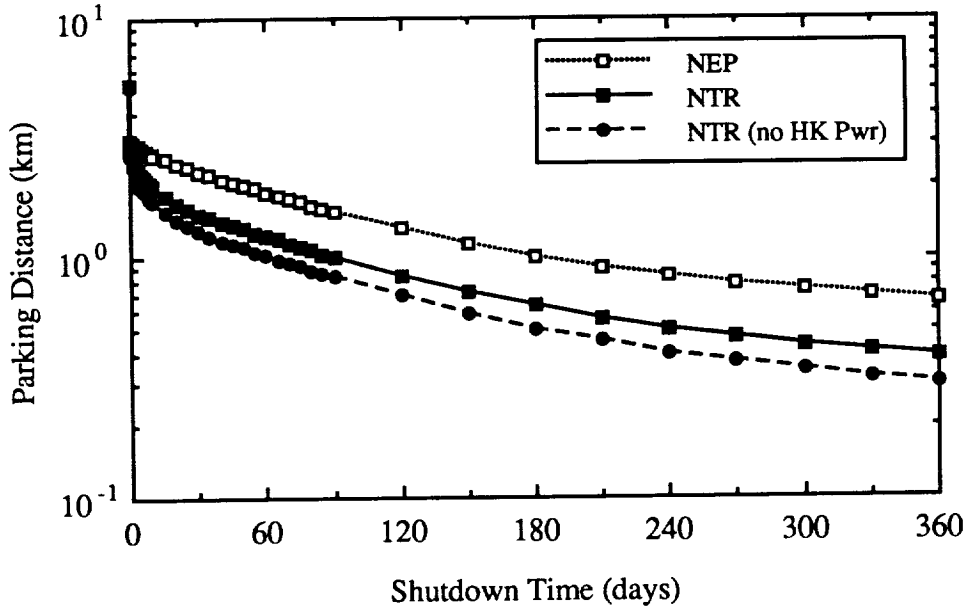

Figure 6.19 NTR Houskeeping Power Sensitivity Isodose Curves.

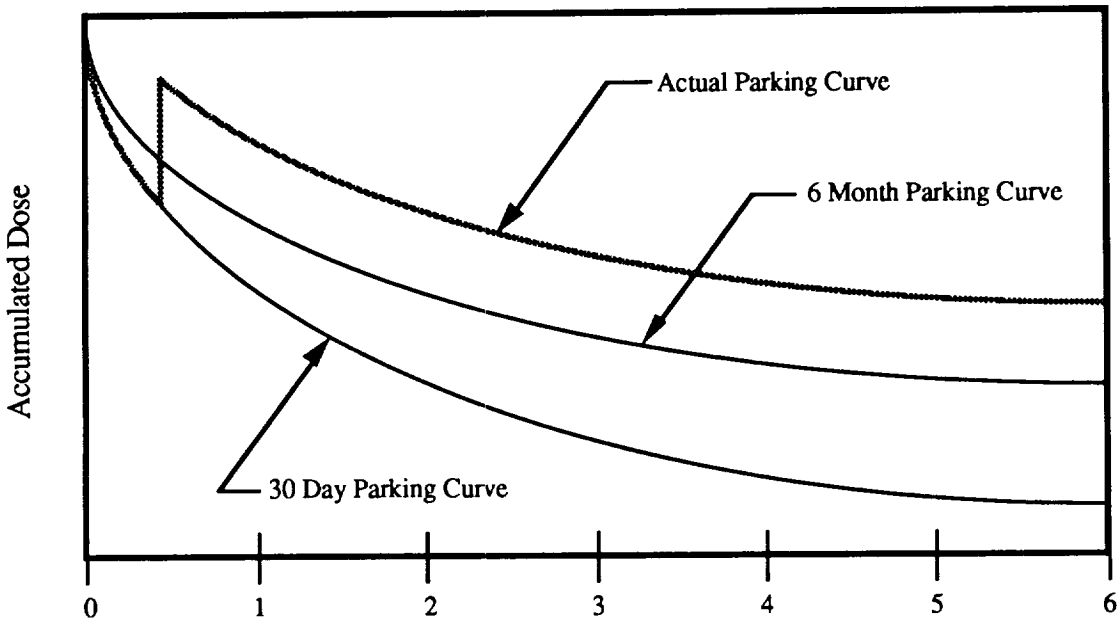

Figure 6.20 Multiple Event Parking Curve Example.

CHAPTER 7

PRESENCE OF OPERATING REACTORS ON CO-ORBITING PLATFORMS

INTRODUCTION

With the establishment of a transportation infrastructure in low earth orbit, nuclear reactors may be needed to meet the power requirements of exploration activities. To investigate the radiological impact of operating reactors to the space station, a scenario was constructed in which a single SP-100 reactor provides power for a water-electrolysis platform co-orbiting with SSF. The two key questions to be answered are: (1) at what minimum distance from SSF can such a platform be located, and (2) how far away from the reactor can a 4-hour EVA be performed on the platform itself? Clearly, prudent orientation of the structure and placement of mass and propellant on the platform can play significant roles in reducing radiation doses to SSF crew. However, until specific designs for such platforms are available, we must make the conservative assumption that radiation doses can be reduced only through geometric attenuation. The advantage of this approach is that the results are applicable to any scenario involving operating SP-100 reactors.

As with all scenarios in this report, no provisions are made for inherent shielding of the space station structure. In addition, our scenario did not directly consider placement of a nuclear reactor on SSF itself. Such a feasibility study has been previously investigated (Bloomfield et. al 1987).

RADIATION DOSES AT THE SPACE STATION

In this scenario, it was assumed that the co-orbiting platform cannot be continuously oriented to maintain SSF within the shadow of the SP-100's user-plane shield. Consequently, we conservatively treat the reactor as a point source of neutron and gamma radiation delivering 37 Sv/s at one meter (Chapter 4).

Figure 7.1 gives six-month cumulative doses at SSF as a function of the platform-to-SSF separation distance. The curve appears straight on this log-log plot since doses decrease as the inverse square of the separation distance. The solid horizontal line indicates

the long-term radiation dose budget of 0.2 Sv in six months. The two lines intersect at slightly greater than 50 km. Therefore, the reactor would have to be located at least this far away from SSF to maintain radiation doses below the NCRP guidelines for crew members on a full six-month duty tour. If cumulative doses at space station were to be kept to a level comparable to natural doses under best-case conditions, then the platform should be separated at least 100 km from the station. The command and control zone for SSF is ± 37 km in the orbital direction; consequently, it appears that radiation exposure will be a major factor dictating the proximity of operating reactors in SSF orbit.

RADIATION DOSES DURING EVA AT THE PLATFORM

Additional radiation doses to crew members may result if EVA work is required at such a platform. To assess EVA doses, it was assumed that the only shielding available to the astronaut at the platform is the existing SP-100 shadow shield. It is important to note that this shield is not designed to reduce the neutron and gamma radiation to levels acceptable for human exposure, but rather to protect electronics at the user plane. As discussed in Chapter 4, the SP-100 can be conservatively treated as a point source behind the shadow shield which delivers a dose rate of 0.0247 Sv/s at one meter.

Four-hour cumulative doses behind this shield are plotted in Figure 7.2 as a function of distance from the reactor core. At 40 m, the astronaut will expend his short-term radiation budget in four hours. He would have to be at least 200 m from the reactor in order for his cumulative dose to equal a 30-day dose from natural space radiations under best-case conditions. Again, judicious placement of mass would be highly advisable. In particular, mass of low atomic number (low-Z materials), such as liquid oxygen and hydrogen, can significantly reduce the neutron flux. Nevertheless, it appears that without any additional shielding, EVA work can be performed at reasonable distances along the structure.

MULTIPLE-EVENT SCENARIOS

Caution must be used with interpreting the results given in Figures 7.1 and 7.2. In particular, one must understand the consequences of selecting distances which deliver doses equal to the LBAD-st during EVA's and the LBAD-lt during continuous exposures at the space station.

For example, consider an individual who arrives at SSF for a six-month stay. During that time, SSF is co-orbiting with platform utilizing a single operating SP-100 reactor. If that platform is located many hundreds of kilometers away from the station, the reactor will constitute a negligible radiation source. Therefore, the only significant radiation dose he will receive will be due to the natural space environment, which under worst-case conditions will result in a cumulative dose of 0.30 Sv [0.05 Sv/mo x 6 mo]. Thus, he will be 0.20 Sv below his annual limit at the end of his stay. This "available dose" of 0.20 Sv represents our LBAD-lt dose budget which, if necessary, can be expended by additional exposures from man-made radiation sources.

Suppose that when this same individual arrives at SSF the co-orbiting platform is located only 54 km away. According to Figure 7.1, this individual will receive an additional radiation dose over six months equal to the LBAD-lt, or 0.20 Sv. Consequently, at the end of his duty tour, he will have just reached the NCRP annual dose limit and thus this individual should be excluded from any routine EVA work at the platform.

Finally, suppose that this individual were to perform a single 4-hour EVA at the platform sometime during his first of six months at the station. According to Figure 7.2, if the work was performed 40 m from the reactor, he would receive a dose equal to the LBAD-st, or 0.20 Sv, provided transit doses are negligible. Back at the station, he will receive an additional 0.05 Sv over that first month from the natural sources. Provided the platform is at a very large distance from the station and no subsequent EVA is performed, his cumulative radiation dose would be 0.25 Sv the first month and 0.50 Sv at the end of his six-month stay. If the operating reactor were not a negligible radiation source at the station, this individual would have to go home early so as not to exceed the NCRP annual limit. Furthermore, multiple reactors in SSF vicinity would require even shorter staytimes and/or larger separation distances from the station.

CONCLUSIONS

Table 7.1 summarizes our dosimetry results for operating reactors. Shown are the distances at which the various single-event dose criteria are met for both 4-hour EVAs and 6-month staytimes at SSF. For EVA work at the platform, NCRP dose limits will not be exceeded at distances greater than 40 m from the reactor. The ALARA principle, however, would suggest distances of at least 200 m. Closer distances could be allowed under this more restrictive dose criteria provided that the platform was designed to utilize propellant

tanks and support structures as additional shielding. At the space station, dose limits will not be exceeded provided that a separation distance of ~60 km was maintained. Again, these distances are only valid for situations in which additional man-made radiation exposures occur as single events. If multiple operating reactors are used in SSF vicinity, larger separation distances for each source would be necessary to insure compliance with the NCRP limits.

References

Bloomfield, H. S., and J. A. Heller (1987) A Feasibility Assessment of Installation, Operation, and Disposal Options for Nuclear Reactor Power Systems Concepts for a NASA Growth Space Station, NASA TM-89923, NASA Lewis Research Center, Cleveland, OH.

Table 7.1 Distances from an Operating SP-100 needed to Meet Various Dose Criteria.

Dose Criteria	4-Hour EVA @ Platform (behind shadow shield)	6-Month Stay @ SSF (outside of shadow shield)
LBAD-st (0.2 Sv)	40 m	
0.05 Sv	85 m	
0.01 Sv	200 m	
LBAD-lt (0.2 Sv)		54 km
0.30 Sv		44 km
0.06 Sv		100 km

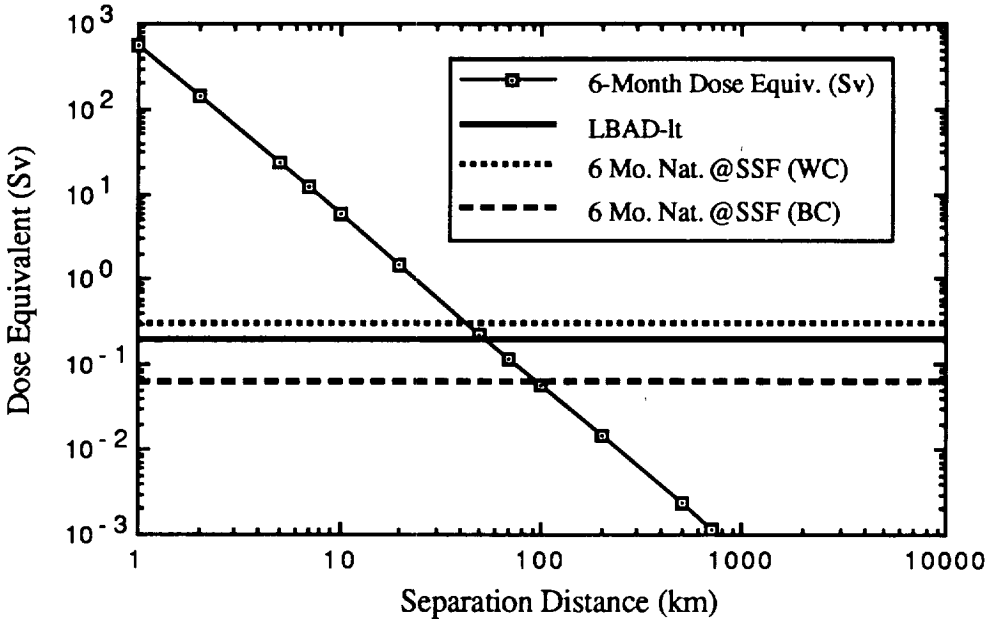

Figure 7.1 Six-Month Doses from an Operating SP-100 Reactor outside of the Reactor Shadow Shield.

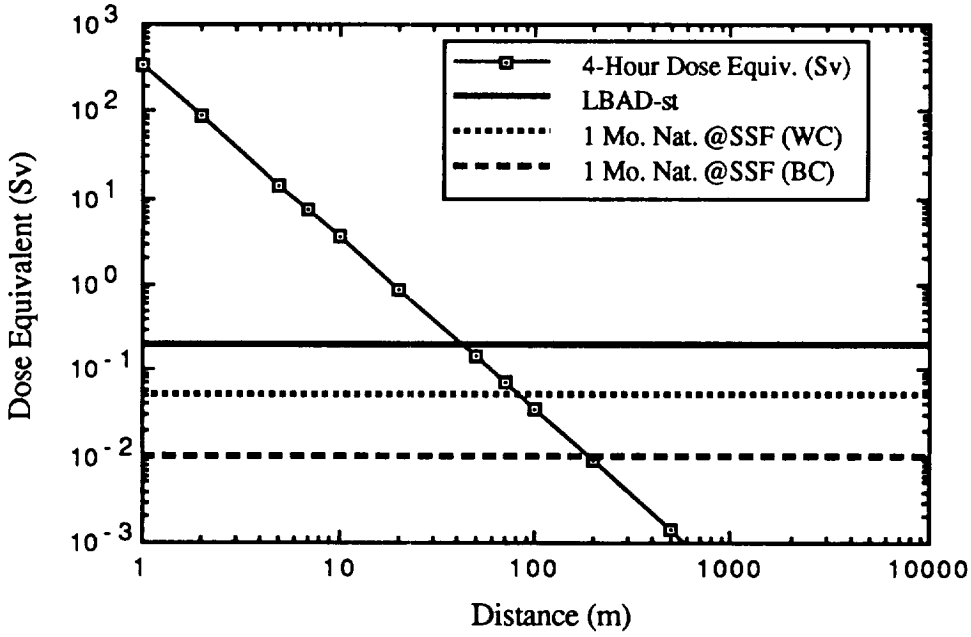

Figure 7.2 Four-Hour EVA Dose from an Operating SP-100 Reactor behind the Reactor Shadow Shield.

CHAPTER 8

PRESENCE OF RADIOISOTOPE POWER SYSTEMS ON SSF

INTRODUCTION

This chapter addresses the the radiological hazards posed by radioisotope power sources. At SSF, these sources might include the following types: Radioisotope Thermoelectric Generator (RTG), Dynamic Radioisotope Power System (DIPS), and Activated Heat Source (AHS).

Dose rates for a GPHS-RTG (General Purpose Heat Source RTG) unit were obtained from the literature. These values were employed along with the dose limits to produce separation distance curves for single and multiple RTGs stored at SSF in various orientations. The results indicate that the presence of RTGs on SSF does not represent a significant radiological hazard. This would appear to be the case for the DIPS and AHS systems as well.

DESCRIPTION OF RADIOISOTOPE POWER SYSTEMS

Three classes of radioisotope power systems could potentially be employed on or in the vicinity of SSF: RTG, DIPS, and AHS. RTGs have been employed in the U.S. space program since 1962 for a wide range of missions (Angelo and Buden 1985, Skrabek and McGrew 1988). The design currently employed for U.S. space missions is the GPHS-RTG (Bennett et al. 1987). The GPHS is fueled by plutonium dioxide (PuO_2) pellets; the Pu is comprised of about 83.5% ^{238}Pu (GE 1984). A unicouple arrangement of silicon germanium (SiGe) thermoelectric elements (TEs) is employed to produce electrical power. The advanced version of this RTG, now under development, is the MOD-RTG (Hartman et al. 1987 and Hartman 1988). The MOD-RTG also employs the GPHS as a thermal power source, but uses enhanced thermoelectric materials in a multicouple arrangement to achieve a specific power approximately 50% greater than that of the GPHS-RTG.

DIPS have not been employed to date in the U.S. space program, but are currently under active development (Davis et al. 1987, Niggemann and Lacey 1987, Bennett and Lombardo 1988 and Determan and Harty 1989). The current DIPS designs would employ

the GPHS heat source with an active power conversion subsystem, either an organic Rankine or a closed Brayton cycle. These systems are typically targeted at the 1 to 10 kW_e power range. Since they employ the same fuel as GPHS-RTGs, the radiological issues and impacts associated with DIPS are very similar.

The AHS concept is relatively new (Thomas and Peddicord 1988) and attempts to address some of the radiological concerns with the launch and reentry of systems employing ^{238}Pu. The AHS employs isotopes that are either stable or have a long half life, relative to ^{238}Pu; such isotopes include ^{209}Bi, ^{241}Am, and ^{237}Np. Once in space, the heat source material is activated using neutrons exiting a space reactor to yield an alpha emitter that produces thermal energy in the same manner as ^{238}Pu. The isotopes mentioned above (^{209}Bi, ^{241}Am, and ^{237}Np) yield ^{210}Po, ^{242}Cm, and ^{238}Pu, respectively, upon activation; these isotopes have all been employed directly in the U.S. RTG program (Angelo and Buden 1985 and Davis 1963). The thermal energy could be used directly or converted to electrical power using technology developed in the RTG and DIPS programs.

DOSE FROM RTG HANDLING AND STORAGE ON SSF

Dose rates for a GPHS-RTG were obtained from the literature (Normand et al. 1989). The GPHS-RTG initially provides approximately 4.4 kW_t of power (Bennett et al. 1987). As mentioned above, the RTG is fueled by PuO_2; thermal power is produced by the alpha decay of the ^{238}Pu isotope. About 80% of the dose is due to neutrons (Normand et al. 1989), emitted both as a result of ^{238}Pu spontaneous fission events and (α,n) reactions with ^{18}O (GE 1984). The remainder is due to gamma emission, which accompanies the alpha decay of ^{238}Pu as well as the decay of impurity isotopes and decay products. The dose rate from an RTG is dependent on the relative orientation between the exposed individual and the RTG itself. The length to diameter ratio for the GPHS-RTG is about 2.7 (Angelo and Buden 1985). If the unit is aligned axially, then a fair amount of self-shielding takes place and the dose is substantially reduced; the dose in the radial direction is over 3 times larger.

For the purposes of this work, the GPHS-RTG was treated as a point source and the axial and radial dose rates at an equivalent 1 m separation distance were taken to be 1.29×10^{-7} and 4.25×10^{-7} Sv/s , respectively. Figure 8.1 gives the 6-month dose, versus separation distance, for a single GPHS-RTG oriented in both the radial and axial directions as well as that from 5 radially oriented units. Also shown is the LBAD-lt limit (0.2 Sv) and

the dose resulting from a 6-month exposure to natural radiation sources under best- and worst-case conditions, respectively (as discussed in Chapter 3). This plot clearly shows that the storage of RTGs on SSF will not constitute a major radiological concern. For a single GPHS-RTG oriented axially, a separation distance of only 3 m is sufficient to meet the LBAD-lt criteria. Consideration of ALARA criteria would mandate that the separation distance be increased beyond this to somewhere on the order of 6 m. For a radial orientation, these distances are increased to about 6 and 10 m, respectively. Even if 5 GPHS-RTG units were stored on SSF simultaneously in a radial orientation, a 25 m separation distance from the crew habitat module would keep the dose below that from a 6-month exposure to natural sources under best-case conditions. Larger separation distances might be desirable under the ALARA criteria.

DOSE FROM DIPS AND AHS HANDLING AND STORAGE ON SSF

Since the current DIPS designs would employ ^{238}Pu as a fuel in the form of PuO_2, the same fuel used in the GPHS-RTG system discussed above, the radiological concerns associated with DIPS will be similar. The amount of ^{238}Pu in a DIPS is larger since typical DIPS thermal power levels are up to 10 times higher than that of an GPHS-RTG. The dose rate for these systems will scale approximately linearly with thermal power. DIPS systems will therefore require slightly larger separation distances than those for a single RTG, but these distances are not excessive.

A recent study (Thomas and Peddicord 1990) indicated that AHS source isotopes pose a much lower external radiological hazard prior to activation than ^{238}Pu. After activation, AHS systems fueled by ^{241}Am or ^{237}Np have roughly the same dose rate, at a given thermal power, as an RTG fueled by ^{238}Pu. AHS systems employing ^{209}Bi have a much lower dose rate. Thus, the required separation distances for AHS systems prior to activation would be even lower than those for the GPHS-RTG units discussed above. This would be the case for storage of fresh AHS units. After activation, the separation distances would be roughly the same as those for GPHS-RTGs.

CONCLUSIONS

Dose rates for a GPHS-RTG unit were obtained from the literature. These values were employed along with the dose limits to produce separation distance curves for a single RTG in various orientations and multiple RTGs. The results indicate that the presence of RTGs on SSF do not represent a significant radiological hazard. The required separation distances and operational procedures required to keep the RTG dose within reasonable limits are not restrictive. While the dose from DIPS and AHS units were not specifically calculated in this work, it appears that these conclusions will be valid for these classes of radioisotope power sources as well. As mentioned in Chapters 6 and 7, consideration must be given to multiple event scenarios in actual mission planning since the radioisotope power source dose could be just one component of the total man-made dose to the SSF crew.

References

Angelo, J.A., Jr. and D. Buden (1985) Space Nuclear Power, Orbit Book Co., Malabar, FL. pp. 133-57.

Bennett, G.L., J.L. Lombardo and B.J. Rock (1987) "Power Performance of the General Purpose Heat Source Radioisotope Thermoelectric Generator," in Space Nuclear Power Systems 1986, M.S. El-Genk and M.D. Hoover, eds., Orbit Book Co., Malabar, FL, pp. 437-50.

Bennett, G.L. and J.J. Lombardo (1988) "The Dynamic Isotope Power System: Technology Status and Demonstration Program," in Trans. of the Fifth Symposium on Space Nuclear Power Systems, CONF-8901223--Summs., held in Albuquerque, NM, 11-14 January 1988, pp. 127-30.

Davis, H.L. (1963) "Radionuclide Power for Space - Part 1: Isotope Costs and Availability," Nucleonics, 21(3): pp. 61-5.

Davis, K.A., A. Pietsch and R.D. Casagrande (1987) "Brayton Dynamic Isotope Power Systems Update," in Space Nuclear Power Systems 1986, M.S. El-Genk and M.D. Hoover, eds., Orbit Book Co., Malabar, FL, pp. 469-82.

Determan, W.R. and R.B. Harty (1989) "DIPS Spacecraft Integration Issues," in Trans. of the Sixth Symposium on Space Nuclear Power Systems, CONF-890103--Summs., held in Albuquerque, NM, 8-12 January 1989, pp. 179-83.

GE (1984) Updated Safety Analysis Report for the Galileo Mission and International Solar-Polar Mission, GESP-7186, Adv. Energy Programs, General Electric, King of Prussia, PA, April 1984.

Hartman, R.F., P.D. Gorsuch and J.R. Peterson (1987) "Technology and Hardware Status of Advanced Modular Radioisotope Generator Development," in Space

Nuclear Power Systems 1986, M.S. El-Genk and M.D. Hoover, eds., Orbit Book Co., Malabar, FL, pp. 451-60.

Hartman, R.F. (1988) "Status of Modular RTG Technology," in Trans. of the Fifth Symposium on Space Nuclear Power Systems, CONF-8901223--Summs., held in Albuquerque, NM, 11-14 January 1988, pp. 139-43.

Niggemann, R.E. and P.D. Lacey (1987) "Long-Life, Highly Survivable Rankine Cycle Dynamic Isotope Power Systems," in Space Nuclear Power Systems 1986, M.S. El-Genk and M.D. Hoover, eds., Orbit Book Co., Malabar, FL, pp. 461-7.

Normand, E., L.A. Proud, J.L. Wert, D. Oberg and T.L. Criswell (1989) "Effect of Radiation from an RTG on the Installation, Personnel, and Electronics of a Launch System," in Trans. of the Sixth Symposium on Space Nuclear Power Systems, CONF-890103--Summs., held in Albuquerque, NM, 8-12 January 1989, pp. 184-70.

Skrabek, E.A. and J.W. McGrew (1988) "Pioneer 10 and 11 Performance Update," in Space Nuclear Power Systems 1987, M.S. El-Genk and M.D. Hoover, eds., Orbit Book Co., Malabar, FL, pp. 587-95.

Thomas, J.K. and K.L. Peddicord (1988) The Activated Heat Source (AHS) Concept: Initial Report, ANFL-6-O, Internal Report - Advanced Nuclear Fuels Laboratory, Dept. of Nuclear Eng., Texas A&M Unv., College Station, TX, June 1988.

Thomas, J.K. and K.L. Peddicord (1990) "The Activated Heat Source (AHS) Concept: Scoping Analysis," to be presented at the Seventh Symposium on Space Nuclear Power Systems to be held in Albuquerque, NM, 7-11 January 1990.

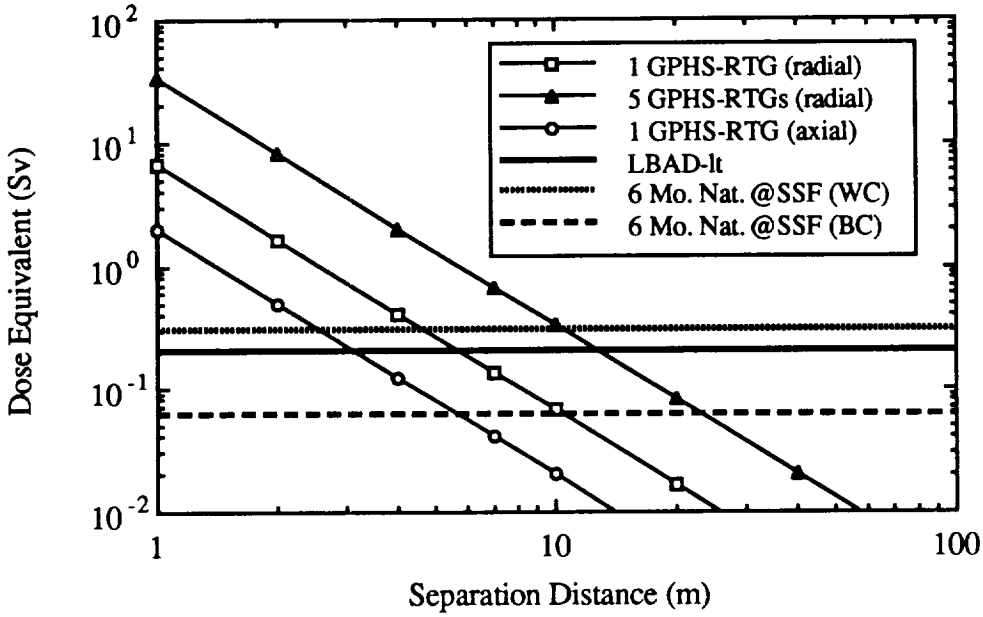

Figure 8.1 GPHS-RTG 6-Month Separation Distance Curves.

CHAPTER 9

MULTIPURPOSE PORTABLE RADIATION SHIELD CONCEPT

INTRODUCTION

This chapter briefly presents a concept for a portable radiation shield to be kept at the SSF transportation node and deployed as needed around man-made radiation sources. Such a concept represents the single major physical "scar" identified in this present study which should be accommodated within the baseline design of SSF. The principle investigators for this project are currently carrying out scoping studies for the portable shield concept under support from NASA's Office of Exploration. A more detailed design will be made as part of a follow-on project to this current study.

CONCEPT AND JUSTIFICATION

A portable shield at SSF is desirable for several reasons. First, most nuclear systems that interact with SSF will not require a 4π man-rated shield to meet the radiation protection requirements of their own missions. For instance, the propellant tanks on the NTR Mars vehicle provide a large fraction of the crew shielding. Most of reactor systems only utilize shadow or disk shields for the protection of onboard crew and/or electronic components. Consequently, there may be little, if any, shielding between the reactor and neighboring objects such as SSF. While the operational constraints on parking distance and shutdown times given in previous chapters may not be unacceptable, they could be relaxed if a portable shield were available. It would be redundant and prohibitively expensive to place such shielding on each vehicle that will interact with the station. Rather, this shield should be kept at SSF and deployed only during periods of close interaction with nuclear systems.

Second, there are specific missions for which distance and/or reactor shutdown times are clearly unacceptable and additional shielding is needed. For example, suppose that it were necessary to perform an EVA 50 m from a shutdown NEP reactor at a location outside of its shadow shield. As indicated in Figure 6.7, a reactor shutdown time of at least 150 days is necessary to ensure dose limits are not exceeded. A simple build-up factor calculation indicates that a wait time of only 10 days would be needed if a 2.4 cm tungsten shield were available.

Finally, a portable shield can be used to implement the radiation protection principle of ALARA. During periods when there are no nuclear systems in the vicinity of SSF, the

"normal" configuration of the shield could be around the habitation modules of the station. In this capacity, the shield would serve as a trapped-proton shield resulting in a reduction in crew doses from the natural sources and an increase in their radiation dose budgets. This in turn would allow either longer staytimes at the station or a greater degree of interaction with nuclear systems.

CHAPTER 10

CONCLUSIONS AND FUTURE WORK

SUMMARY

The results from this study indicate that realistic scenarios do not exist which would preclude the use of nuclear power sources in the vicinity of SSF. Radiation doses to SSF crew can be maintained at safe levels solely by implementing proper and reasonable operational procedures. These consist primarily of constraints on separation distances between the radiation source and the SSF crew and on reactor shutdown times prior to vehicle approach and final parking. For scenarios involving single man-made radiation sources, these constraints are not severe and do not significantly impair the functionality of an evolutionary space station. However, if multiple man-made radiation sources are present, each source must be controlled to the extent that total exposures from all sources are below dose limits. In this later case, significant reactor shutdown times may be required to allow EVA on returned vehicles and to allow relatively close vehicle parking distances from the station. These shutdown times may become operational unacceptable and thus supplemental shielding would be needed. It is recommended that a portable, multifunctional reactor shield be kept at SSF and deployed around the shutdown reactors of returned NEP and NTR vehicles. During periods of low vehicle activity, the shield could be deployed around the habitation modules of SSF to reduce doses from natural space radiations.

Specific conclusions from this study are summarized below. These conclusions are dependent upon the radiation protection criteria applied. The more permissive range of operations will limit total exposures to the NCRP 30-day and annual dose limits. In this case, the man-made contribution to dose will equal the LBAD-st and LBAD-lt radiation dose budgets, respectively (see Chapter 3). The more restrictive operations will limit man-made exposures to levels comparable to natural doses in LEO under best-case conditions (0.01 Sv/mo); this approach can be viewed as one implementation of the ALARA radiation protection criteria.

LAUNCH OF NEP AND NTR VEHICLES FROM LEO

If an NEP cargo vehicle is to be launched from LEO, greater separation distances are maintained and thus lower cumulative doses to SSF crew are realized if SSF initially leads the NEP within its orbit prior to launch. In this configuration, an initial launch separation distance of only 2.5 km is required to insure cumulative doses at SSF do not exceed recommended dose limits. If cumulative doses are to equal a 1-month natural dose, an initial separation of at least 16 km is needed. Clearly, factors other than the concern for radiation exposure will dictate launch separation distances for NEP vehicles.

If an NTR personnel vehicle is to be launched from LEO, lower cumulative doses result if SSF initially lags the NTR prior to launch. In this configuration, an initial separation distance of only 7 km is required to insure doses at SSF do not exceed dose limits (as discussed in Chapter 5, this result is based upon the assumption that the TMI stage of the vehicle is powered by a 5000 MW_t PHEOBUS-class reactor and not a 1575 MW_t NERVA-class reactor). If cumulative doses are to equal a 1-month natural dose, an initial separation distance of at least 62 km is required. For this criterion, radiation protection could partially dictate launch separation distances for NTR vehicles. If shorter distances are desirable, additional shielding of crew modules would be needed. This could be one of several uses for the portable shield concept discussed in the previous chapter.

6-MONTH PARKING OF RETURNED NEP AND NTR VEHICLES

A prior reactor shutdown period is not required for a returning NEP vehicle if it is to be parked no closer than 5 km from SSF. If a parking distance of 1 km is desired, the reactor must be shutdown for at least 6 months prior to towing the vehicle to this distance if cumulative 6-month doses to SSF crew are to be kept below recommended limits. If doses are to be kept comparable to natural doses, then the reactor must be shutdown for over one year. Clearly, the shutdown times for a 1 km parking distance may be operationally unacceptable and a portable reactor shield would need to be deployed around the NEP reactor.

A prior reactor shutdown period is not required for a returning NTR vehicle if it is to be parked no closer than 10 km from SSF. If a 5 km parking distance is desired, the reactor must be shutdown for one day prior to final parking. If a 1 km parking distance is desired, then a 3-month shutdown time is needed to insure doses do not exceed dose limits and a 7-month shutdown time is needed to kept doses comparable to natural doses. Again,

these restrictions on reactor shutdown times can be relaxed with the deployment of a portable shield.

4-HOUR EVA AT RETURNED NEP AND NTR VEHICLES

A prior reactor shutdown period is not required for EVAs at a returned NEP vehicle if a distance of at least 50 m within the shadow shield of the reactor is maintained. If an EVA is to be performed 50 m from the reactor outside its shadow shield, then the reactor must be shut down for at least 5 months to insure that dose limits are not exceeded. At that same location, a shutdown time of ~2 years is required if the dose received is not to exceed a 1-month dose from natural sources. Clearly, it is desirable to allow EVA at the vehicle only within the shadow of the reactor shield. If this shadow is spatially limiting, then deployment of a portable shield around the reactor is recommended.

For the returned NTR vehicle, an EVA 50 m from the reactor outside the shadow of its disk shield can be performed with a reactor shutdown time of at least 3 months. At this same location, a shutdown time of over 1 year is required to kept doses comparable to a 1-month natural dose.

OPERATING REACTORS IN THE VICINITY OF SSF

In the event that an operating SP-100 reactor is used as the power source for a electrolysis platform co-orbiting with SSF, a separation distance of at least 54 km would be needed so as to maintain crew doses below recommended limits. If the reactor were to deliver a total dose over six months comparable to that delivered by natural space radiations over the same period, then a 100 km distance would be necessary.

If EVA work was to be performed at the platform while the reactor was operating, the astronaut must be kept within the reactor's shadow shield. A potentially lethal dose would be delivered outside the shield in about 40 minutes. Within the shadow shield, the astronaut must be no closer than 40 m from the reactor to insure that his cumulative 4-hour dose would not exceed the LBAD-st dose budget. If this cumulative dose were to equal a 1-month natural dose, the EVA would have to be performed at least 200 m from the reactor. Clearly, radiation doses can be substantially reduced by having the reactor shut down prior the EVA and by prudent placement of mass and propellant at the platform. Alternatively, a portable reactor shield could be employed.

STORAGE OF RADIOISOTOPE POWER SOURCES AT SSF

In the event that RTG units are to be stored at SSF, they should be oriented in the axial direction with respect to the crew modules so as to take advantage of component self-shielding; dose rates in the radial direction are over 3-times larger. With an axial orientation, 5 RTG units can be stored as close as 7 m from the crew and still maintain doses below recommended limits. A distance of 13 m is necessary if the units were to only double the crew's dose from natural sources. If, for some reason, 5 RTGs were oriented in the radial direction, these separation distances would be 13 m and 24 m, respectively. It does not appear that RTG units at SSF would present a radiological hazard to crew members since these required separation distances are well within the ±52 m afforded by the Dual-Keel configuration of SSF (NASA 1988). Likewise, it does not appear that either DIPS or AHS radioisotope power systems will pose a serious radiological hazard.

FUTURE WORK

Several items will be addressed as part of a follow-on project. First, the analysis methodologies used in this study to calculate doses from operating and shutdown reactors will be verified and refined as necessary. As an extension of these calculations, specific vehicle designs will be incorporated so as to take into account inherent shielding of the vehicle structures. Second, scenarios will be constructed in which, not one, but several man-made radiation sources are present at or near SSF simultaneously. These scenarios will then be used to assess impacts to vehicle and SSF operations as well as to crew rotation schedules. Third, existing space radiation environment models will be obtained and implemented so that refined estimates of doses from natural space radiations can be integrated into the scenario analyses. Fourth, a detailed design for a portable, multifunctional radiation shield will be made. A scoping study of such a shield design is currently being supported by NASA's Office of Exploration. Finally, a preliminary assessment will be conducted of the radiation hazards associated with material activation and the handling of fresh and spent reactor cores.

References

NASA (1988) Space Station Freedom Technical Overview (Preliminary), National Aeronautics and Space Administration, Washington, D.C.

GLOSSARY OF TERMS

AHS	=	Activated Heat Source (p. 70).
ALARA	=	As Low As Reasonable Achievable radiation protection philosophy (p. 3).
BFO	=	Blood Forming Organs such as the red bone marrow (p. 11).
BOL	=	Beginning Of Life. BOL conditions were assumed for the operating reactor source terms (p. 18).
CRAM	=	Common Radiation Analysis Model. This model was employed in the analysis of the radiation source term for the NERVA-class reactor (p. 18).
DIPS	=	Dynamic Isotopic Power System (p. 70).
EOC	=	Earth Orbital Capture. The last (Earth-arrival) stage of the NTR Mars mission. The NERVA reactor is employed for the EOC (p. 51).
EVA	=	Extra-Vehicular Activities (p. 12).
GCR	=	Galactic Cosmic Rays (p. 5).
GPHS	=	General Purpose Heat Source. The thermal power source employed with current RTG and DIPS designs (p. 70).
GPHS-RTG	=	General Purpose Heat Source - Radioisotopic Thermoelectric Generator. The current United States RTG design (p. 70).
HZE	=	High Z and Energy. A class of GCR particles (p. 6).
ICRP	=	International Commission on Radiological Protection (p. 85).
ICRU	=	International Commission on Radiation Units and Measurements (p. 85).
LBAD	=	Lower Bound on Available Dose. The LBAD reflects the dose budget for SSF crew. Both short-term (LBAD-st) and long-term (LBAD-lt) values were developed (p. 11).
LEO	=	Low Earth Orbit. The SSF was assumed to be in LEO (p. 6).
MOC	=	Mars Orbital Capture. The second (Mars-arrival) stage of the NTR Mars mission. The NERVA reactor is employed for the MOC (p. 51).
MOD-RTG	=	Modular - Radioisotopic Thermoelectric Generator. The advanced United States RTG design (p. 70).
NCRP	=	National Council on Radiation Protection and Measurements. The NCRP radiation protection guidelines for space activities were employed in this work (p. 1).
NEP	=	Nuclear Electric Propulsion (p. 2).

NERVA	=	Nuclear Engine for Rocket Vehicle Application, the reactor system employed for the NTR analyses (p. 2).
NTR	=	Nuclear Thermal Rocket (p. 2).
OSHA	=	Occupational Safety and Health Administration (p. 11).
Phoebus	=	The reactor propulsion system assumed for the TMI stage in the NTR Mars mission analyses (p. 39).
RTG	=	Radioisotopic Thermoelectric Generator (p. 70).
SAA	=	South Atlantic Anomaly, a deformation in the Earth's geomagnetic field (p. 5).
SPE	=	Solar Particle Events (p. 5).
SP-100	=	The reactor system employed for the NEP analyses (p. 2).
SSF	=	Space Station Freedom (p. 1).
TEI	=	Trans Earth Insertion. The third (Mars-departure) stage of the NTR Mars mission. The NERVA reactor is employed for the TEI (p. 51).
TMI	=	Trans Mars Insertion. The first (earth-departure) stage of the NTR Mars mission. The Phoebus reactor is employed for the TMI (p. 25).

APPENDIX A

SUMMARY OF RADIATION DOSIMETRY QUANTITIES AND UNITS

INTRODUCTION

This appendix briefly defines the two quantities used in radiation dosimetry: the absorbed dose (D) and the dose equivalent (H). The two are related by the expression $H = \overline{Q}D$, where $\overline{Q}$ is a dimensionless weighting factor. In this report, the general term radiation "dose" will be used to specify values of dose equivalent.

ABSORBED DOSE

The primary physical quantity used in radiation dosimetry is the absorbed dose (D) and is defined as the net amount of energy deposited per unit mass of tissue or other material. Its traditional unit is the rad which is equal to 100 ergs of energy deposited per gram of material. The S.I. unit of absorbed dose is the gray (Gy) which is equal to one joule deposited per kilogram of material. Consequently, one Gy is equal to 100 rad. Absorbed dose can be measured with devices such as thermoluminescent dosimeters (TLD) or gas ionization chambers. Absorbed doses to internal organs is usually inferred from radiation transport calculations using mathematical phantoms (see Appendix B).

DOSE EQUIVALENT

Not all types of radiation produce the same amount of biological damage per unit absorbed dose. In particular, charged particles with high rates of energy loss per unit track length, such as neutron recoils and low-energy protons, are more effective in producing biological effects than those with lower rates of energy loss, such as electrons and high-energy protons. This rate of energy loss is defined as the LET, or linear energy transfer, of the particle.

To account for the greater biological effectiveness of high-LET radiations, the quantity dose equivalent (H) is defined for use in radiation protection:

$$H = \overline{Q}D ,$$

where D is the absorbed dose and $\overline{Q}$ is a dimensionless weighting parameter called the average quality factor. The traditional unit of dose equivalent is the rem and is equal to Q times the absorbed dose in rad. The S.I. unit of dose equivalent is the sievert (Sv) and is equal to Q times the absorved dose in Gy. Consequently, a dose equivalent of one Sv is equal to 100 rem.

For a given radiation field and a point of interest within the body, the average quality factor can be determined either by detailed measurement or by radiation transport calculations using the expression:

$$\overline{Q} = \frac{1}{D}\int_{L_{min}}^{L_{max}} Q_L \, D_L \, dL \, ,$$

where D is the total absorbed dose, D_L is the absorbed dose delivered by particles in the LET range L to L+dL, and Q_L is the quality factor as a function of LET as shown in Figure A.1. Note that for low-LET radiations (LET < 3.5 keV/μm), Q is always equal to one. For very high-LET radiations (LET > 175 keV/μm), Q is always equal to its maximum value of 20.

In many situations, only the type of radiation present and the total absorbed dose are known; consequently, single values of $\overline{Q}$ may be used as shown in Table A.1. Recently, however, several radiation protection organizations have issued reports recommending that $\overline{Q}$ for fast neutrons be increased from 10 to 20 (ICRP 1985, NCRP 1987) or 25 (ICRU 1986). This increased level of conservatism places a greater emphasis on making actual LET spectral measurements within radiation fields of interest.

References

ICRP (1977) Recommendations of the International Commission on Radiological Protection, ICRP Publication 26, International Commission of Radiological Protection, Pergamon Press, New York, 1977.

ICRP (1985) Statement from the 1985 Paris Meeting of the International Commission on Radiological Protection, ICRP Publication 45, International Commission of Radiological Protection, Pergamon Press, New York, 1985.

ICRU (1986) The Quality Factor in Radiation Protection, Report of the Joint Task Group of the ICRP and the ICRU, ICRU Report 40, International Commission on Radiation Units and Measurements, Bethesda, Maryland, April 1986.

NCRP (1971) Basic Radiation Protection Criteria, NCRP Report No. 39, National Council on Radiation Protection and Measurements, Bethesda, Maryland, January 1971.

NCRP (1987) Recommendations on Limits for Exposure to Ionizing Radiation, NCRP Report No. 91, National Council on Radiation Protection and Measurements, Bethesda, Maryland, June 1987.

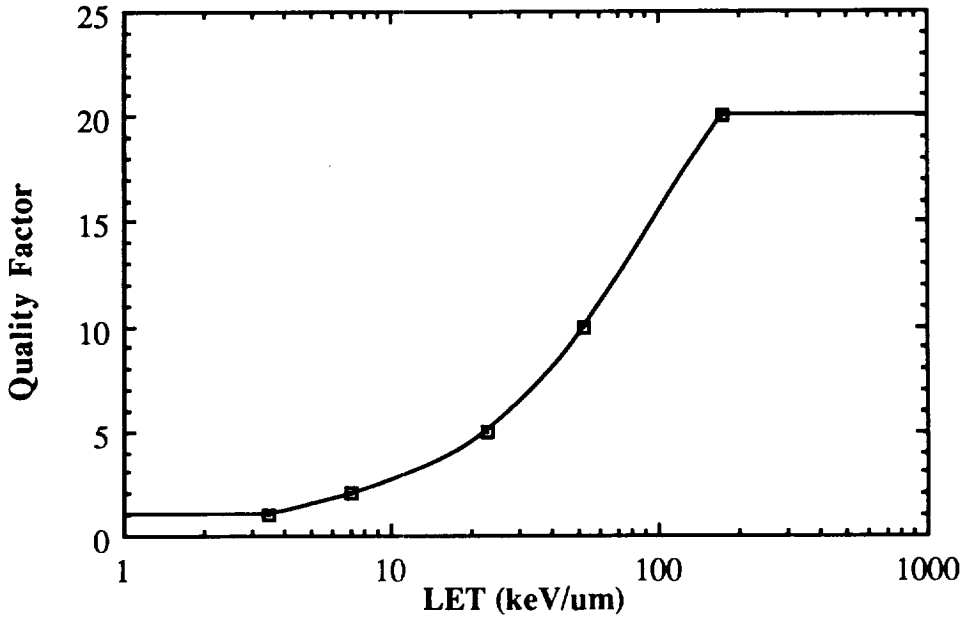

Figure A.1 Quality Factor as a Function of LET (ICRP 1977).

Table A.1 Average Values of Quality Factor for Various Radiations.
[Source: Table 5 of NCRP Report No. 39 (NCRP 1971)]

Radiation Type	Rounded Quality Factor
X-rays, Gammas, Electrons	1
Thermal Neutrons	2
Fast Neutrons	10
Protons	10
Alpha Particles	20
Fission Fragments, Recoil Nuclei	20

APPENDIX B

FLUENCE-TO-ORGAN DOSE CONVERSION FUNCTIONS

INTRODUCTION

This appendix describes the method by which radiation doses to the blood forming organs are calculated for both gamma and neutron irradiations. The term "blood forming organ" is a general term denoting the dose at a depth of 5 cm (NCRP 1989). In this report, BFO doses are specifically calculated for the red bone marrow.

CALCULATION OF ORGAN DOSES

The calculation of doses to the various organs of the body is greatly facilitated by the use of organ dose conversion functions (DCF). These functions give the organ dose delivered per unit radiation fluence as a function of particle energy incident upon the body. Thus, the dose H to a particular organ T from radiation type R is determined as:

$$H_{T,R} = \int_0^{E_{max}} \phi_{R,E} \, (DCF)_{T,R,E} \, dE \, ,$$

where $\phi_{R,E}$ is the total fluence (number of particles incident per unit area) for radiation R differential with respect to particle energy E, and $(DCF)_{T,R,E}$ is the dose conversion function for organ T and radiation R.

The radiation source terms $\phi_{R,E}$ for both operating and shutdown NEP and NTR reactors are presented in Chapter 4. Organ DCFs used in this report were take from Report 43 of the International Commission on Radiation Units and Measurements (ICRU) (ICRU 1988). These functions were generated from Monte Carlo radiation transport calculations using detailed mathematical phantoms of the human body (Kramer 1982). ICRU Report 43 graphically displays gamma and neutron dose conversion functions for 12 organs and five irradiation geometries. The five geometries are (1) a broad parallel beam from front to back; (2) a broad parallel beam from back to front; (3) a broad parallel beam from the side; (4) an isotropic field; and (5) a planar isotropic radiation field. This latter field is analogous to an individual being rotated within a broad parallel beam and is the most appropriate for

estimating radiation doses from man-made sources in space. The DCFs given in Report 43 for gamma irradiation were taken from Williams et. al 1985; those for neutron irradiation were taken from Nagarajan et. al 1981.

SELECTED DCFs FOR GAMMAS AND NEUTRONS

Dose conversion functions are given in ICRU Report 43 in the form of discrete values for 14 gamma energies and 16 neutron energies. These values for the red bone marrow are given in Tables B.1 and B.2 for planar isotropic gamma and neutron radiation fields, respectively. To facilitate the dose calculations in this report, the DCF values for gamma irradiation were fit to a third-order polynomial of the type:

$$\ln(DCF_\gamma) = a + b\ln(E_\gamma) + c[\ln(E_\gamma)]^2 + d[\ln(E_\gamma)]^3$$

where $a = -26.368453$, $b = 0.874235$, $c = -0.0468297$, $d = 0.00497059$,
E_γ is in MeV, and DCF_γ is in Sv cm^2.

This function is shown in Figure B.1 along with the tabulated values of Table B.1. The DCF values for neutron irradiation were fit to a fifth-order polynomial of the type:

$$\ln(DCF_n) = a + b\ln(E_n) + c[\ln(E_n)]^2 + d[\ln(E_n)]^3 + e[\ln(E_n)]^4 + f[\ln(E_n)]^5$$

where $a = -23.243145$, $b = 0.968684$, $c = -0.0472173$, $d = -0.0327160$,
$e = -0.00302264$, -0.0000852384, E_n is in MeV, and DCF_n is in Sv cm^2.

This function is displayed in Figure B.2. It is important to note that this functional form is only valid for neutron energies between 1 eV and 15 MeV; functional values below 1 eV are greatly overestimated and those above 15 MeV are greatly underestimated.

References

ICRU (1988) Determination of Dose Equivalents for External Radiation Sources - Part 2, ICRU Report 43, International Commission on Radiation Units and Measurements, Bethesda, Maryland, December 1988.

Kramer, R., M. Zankl, G. Williams, and G. Drexler (1982) The Calculation of Dose from External Photon Exposures using Reference Human Phantoms and Monte Carlo Methods. Part 1. The Male (ADAM) and Female (EVA) Adult Mathematical

Phantoms, GSF-Bericht S-885, Gesellschaft fur Strahlen- und Umweltforschung mbH, Munchen.

Nagarajan, P. S., A. Wittmann, and G. Burger (1981) "Fast Neutron Organ Dose Calculations using a MIRD Phantom," pp. 49-61 in Proceedings of the Fourth Symposium on Neutron Dosimetry, Vol. I, Radiation Protection Aspects, G. Burger and H. G. Ebert, Eds., Commission of the European Communities, Luxembourg.

NCRP (1989) Guidance on Radiation Received in Space Activities, NCRP Report No. 98, National Council on Radiation Protection and Measurements, Bethesda, Maryland, July 1989.

Williams, G., M. Zankl, H. Eckerl, and G. Drexler (1985) The Calculation of Dose from External Photon Exposures using Reference Human Phantoms and Monte-Carlo Methods, Part 2: The Organ Doses from Occupational Exposures, GSF-Bericht S-1079, Gesellschaft fur Strahlen- und Umweltforschung mbH, Munchen.

Table B.1 Gamma Dose to the Red Bone Marrow per Unit Fluence within a Planar Isotropic Radiation Field.
[Source: Fig. B.6 of ICRU Report 43 (ICRU 1988)]

Gamma Energy (Mev)	Dose per Unit Fluence (Sv cm^2)
2.50E-02	5.50E-14
5.00E-02	1.60E-13
6.00E-02	2.00E-13
7.00E-02	2.30E-13
8.00E-02	2.60E-13
1.00E-01	3.30E-13
1.50E-01	5.20E-13
2.00E-01	7.00E-13
3.00E-01	1.20E-12
5.00E-01	1.90E-12
1.00E+00	3.70E-12
3.00E+00	8.50E-12
6.00E+00	1.50E-11
1.00E+01	2.20E-11

Table B.2 Neutron Dose to the Red Bone Marrow per Unit Fluence within a Planar Isotropic Radiation Field.
[Source: Fig. B.33 of ICRU Report 43 (ICRU 1988)]

Neutron Energy (Mev)	Dose per Unit Fluence (Sv cm^2)
1.00E-06	2.90E-12
1.00E-05	2.70E-12
1.00E-04	2.50E-12
1.00E-03	2.40E-12
1.00E-02	2.70E-12
2.50E-02	3.40E-12
5.00E-02	5.50E-12
1.00E-01	1.00E-11
2.80E-01	2.50E-11
5.50E-01	5.20E-11
1.00E+00	9.00E-11
2.50E+00	1.70E-10
5.00E+00	2.50E-10
8.00E+00	3.10E-10
1.20E+01	3.70E-10
1.50E+01	4.00E-10

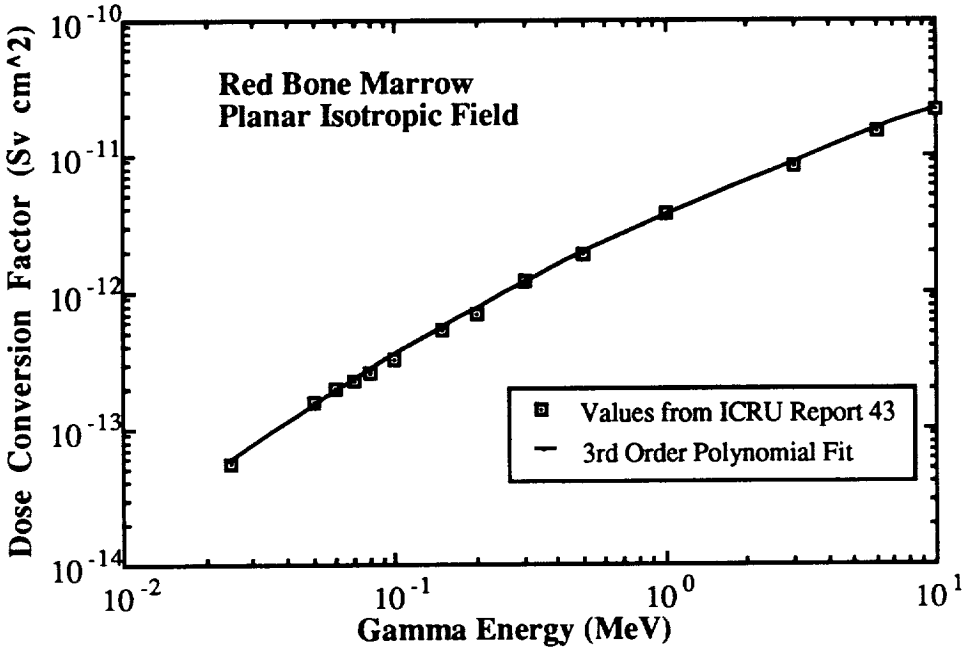

Figure B.1 Dose Equivalent (Sv) to the Red Bone Marrow, per Unit Fluence (cm^{-2}), as a Function of Photon Energy for a Planar Isotropic Radiation Field.

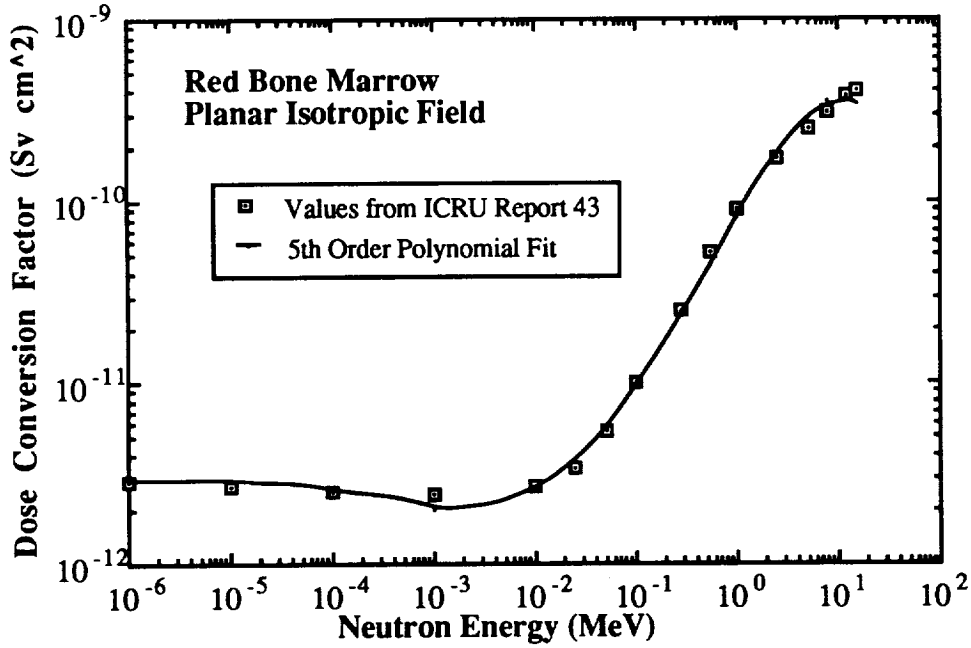

Figure B.2 Dose Equivalent (Sv) to the Red Bone Marrow, per Unit Fluence (cm^{-2}), as a Function of Neutron Energy for a Planar Isotropic Radiation Field.

C 2

APPENDIX C

DECAY HEAT CALCULATIONS FOR NUCLEAR REACTORS

INTRODUCTION

This appendix is intended to present the range of decay heat models available in the literature and discuss their advantages and disadvantages. A secondary purpose is to explain the rationale for selecting the particular model employed in this work. In addition, the expressions necessary to implement this model for the cases analyzed (i.e. the NTR and NEP reactors) are developed.

DECAY HEAT MODELS

Immediately after reactor shutdown, the reactor power level is controlled by delayed neutron emission. The power during this period may be described by the simple exponential form shown below:

$$P_s = P_o a e^{bt}$$

where 'a' (unitless) and 'b' (time^{-1}) are empirical constants, P_0 is the operating reactor power, and P_S is the power of the shutdown reactor. For a typical power reactor, 'a' and 'b' may be taken to be approximately 0.15 and 0.1 sec^{-1}, respectively (Tong and Weisman 1979, Weisman 1977). Since this behavior is only exhibited immediately after reactor shutdown, its contribution was not included in the analyses reported here.

After a few hours following reactor shutdown the reactor power is controlled by decay heat, which is primarily due to the radioactive decay of fission products. Gammas emitted from neutron capture products represent a secondary source of decay heat. The chief neutron capture products of concern for terrestrial reactors are uranium-239 (U-239) and neptunium-239 (Np-239), which result from neutron capture in U-238. This will not be of importance for most space reactor designs since their fuels are typically highly enriched in U-235 and thus contain only a small amount of U-238. Reactor structural and control materials, which are considered to be of only minor importance in terrestrial power

reactors, are usually the primary source of neutron capture products for most space reactors.

A large number of relatively simple empirical models for post-shutdown decay heat and gamma source terms have been developed and reported in the literature. These are discusses briefly in the following paragraphs.

The first class of decay heat models can be illustrated by the relationship shown below (El-Wakil 1971):

$$\frac{P_s}{P_o} = A\, t_S^{-B}\left[1 - \left(1 + \frac{t_o}{t_s}\right)^{-C}\right]$$

where A, B, and C are empirical constants, t_o is the length of time the reactor has been operated, and t_s is the reactor shutdown time. As before, P_o is the operating reactor power and P_s is the power of the shutdown reactor. El-Wakil (1971) gives these constants as 0.095, 0.26, and 0.2, respectively, for time given in seconds. The bracketed term in this expression accounts for the effect of finite reactor operation times; as this time approaches infinity, the bracketed term goes to unity. Similar expressions are also presented in ANL (1963), in this case the decay power due to gamma and beta emission are given separately and the contributions from various gamma energy groups are illustrated. It should be noted that much of the experimental work providing the foundations for these expressions was performed from the late 1940s through early 1960s. These expressions, while their simplicity is attractive, have been reported to be in error by factors greater than 2 for times in excess of a few hours (England et al. 1975).

Recently, a more accurate class of decay heat models has been developed, evaluated, and verified. These models are based on modern experimental data evaluations and employ sums of exponentials to provide a better empirical fit. An example of this type of model is shown below (Chilton et al. 1984):

$$f_k(t_f) = \sum_{j=1}^{N_k} \alpha_{jk} e^{-\lambda_{jk} t}$$

where f_k is the energy release rate per fission for gammas (or betas) in energy group k (MeV/fission/sec), t_f is the time since the fission event of interest occurred, and α_{jk} and λ_{jk} are empirical constants for energy group k. Various number of decay gamma or beta energy groups have been employed by different investigators. LaBauve et al. (1982) report formulating values for 22, 11, and 6 groups; both LaBauve et al. (1982) and ANS/ANSI (1979) give coefficient sets for a single energy group correlation. N_k is simply the number of terms used to construct the fit. LaBauve et al. (1982) employ 11 terms in their single energy group models and between 9 to 15 coefficients for their 6 energy group expressions; the ANS/ANSI (1979) model makes use of 23 terms in their single energy group model.

In the case where all contributions are lumped into a single energy group, the expression given above reduces to:

$$f(t_f) = \sum_{j=1}^{N} \alpha_j e^{-\lambda_j t}$$

Integrating with respect to both reactor operating and shutdown time yields the gamma energy release rate at the shutdown time of interest. This is discussed in more detail in the following section.

Lastly, it should be noted that a number of detailed computer codes have been developed which are capable of yielding decay heat source terms. The ORIGEN code (Croff 1973), which has been upgraded to the ORIGEN2 version (Croff 1980, Croff 1983 and RSIC 1987), is the best known and most widely utilized. The ORIGEN code series has been extensively verified and is considered a standard for this type of calculation. The CINDER code series (England et al. 1976) can also be used for this purpose. Schenter et al. (1977) provide a discussion and comparison of many of these codes; LaBauve et al. (1982) provide a short listing as well. The main advantage to employing these codes is accuracy. The simple empirical expressions given above were developed using data from terrestrial power reactors and thus will not be as accurate when applied to space reactors which employ different materials and operating conditions. Another advantage to this type of code is that neutron capture and activation effects are explicitly accounted for in the code predictions, although empirical correction factors to account for these phenomena have been developed.

SELECTION AND IMPLEMENTATION OF A DECAY HEAT MODEL

As discussed above, isotope generation and depletion codes such as ORIGEN2 yield the most accurate estimate of the decay gamma and heat source terms. However, to implement these codes requires a good knowledge of the reactor material composition and neutron flux. Since these were not readily available and the project was subject to time constraints, it was judged acceptable to employ one of the empirical exponential summation decay heat models. As noted above, the very simple decay models are not sufficiently accurate for this work. Only the decay gamma source was of interest since the betas will be absorbed within the reactor and the corresponding bremsstrahlung contribution is small compared to the decay gamma source strength.

As discussed in the section above, the gamma energy release rate per fission (MeV/fission/sec) can be expressed as:

$$f(t_f) = \sum_{j=1}^{N} \alpha_j e^{-\lambda_j t}$$

where, as before, t_f is the time since the fission event occurred, and α_j and λ_j are empirical constants. Multiplying this expression by the operating fission rate yields the total shutdown gamma energy release rate; the operating fission rate can be expressed as the reactor power divided by the recoverable energy per fission. The gamma energy release rate per unit time of reactor operation, $F(t_f)$ (in MeV/sec^2), can then be written as:

$$F(t_f) = \left(\frac{P_o}{E_r}\right) \sum_{j=1}^{N} \alpha_j e^{-\lambda_j t}$$

where P_o is the operating power in MeV/s and E_r is the recoverable energy per fission event in MeV/fission. Assuming a constant reactor power, this expression may be integrated with respect to operating time, t_o, to yield the total gamma energy release rate, or power, at some shutdown time, t_s, as shown below:

$$P_{\gamma_s}(t_s) = \left(\frac{P_o}{E_r}\right) \sum_{j=1}^{N} \alpha_j \int_{t_s}^{t_o+t_s} e^{-\lambda_j t_f}\, dt_f = \left(\frac{P_o}{E_r}\right) \sum_{j=1}^{N} \frac{\alpha_j}{\lambda_j}\left(1 - e^{-\lambda_j t_o}\right) e^{-\lambda_j t_s}$$

There are alternate periods of full and reduced power operation in the Mars mission scenarios employed in this work; each period of operation (mission phase) is treated separately and the source terms are summed to compute a total source. Denoting the operating power, operating time, and corresponding shutdown time (i.e. time since that mission phase ended) for each phase with the subscript 'm' and summing over all mission phases yields the total gamma power after reactor shutdown:

$$P_{\gamma_s}(t_s) = \sum_{m=1}^{M} \left[\left(\frac{P_{o_m}}{E_r} \right) \sum_{j=1}^{N} \frac{\alpha_j}{\lambda_j} \left(1 - e^{-\lambda_j t_{o_m}}\right) e^{-\lambda_j t_{s_m}} \right]$$

where M is the total number of mission phases. The procedure employed to compute the shutdown gamma dose using this shutdown gamma power expression is discussed in Chapter 6 of this report.

The expression given above can be integrated with respect to exposure time, t_e, to compute the total gamma energy released during a given exposure period:

$$E_\gamma(t_s, t_{exp}) = \sum_{m=1}^{M} \left[\left(\frac{P_{o_m}}{E_r} \right) \sum_{j=1}^{N} \frac{\alpha_j}{\lambda_j^2} \left(1 - e^{-\lambda_j t_{o_m}}\right) e^{-\lambda_j t_{s_m}} \left(1 - e^{-\lambda_j t_e}\right) \right]$$

As discussed in the preceding section, there are multiple coefficient sets (α_j, λ_j) available that could be employed with the expressions developed above. For the purposes of this work, the single-energy group reported by LaBauve et al. (1982) and given in Table C.1 was employed.

References

ANL (1963) Reactor Physics Constants, ANL-5800, 2nd edition, Argonne National Laboratory, Argonne, IL, pp. 634-7.

ANS/ANSI (1979) American National Standard for Decay Heat in Light Water Reactors, ANSI/ANS 5.1, American National Standards Institute, American Nuclear Society, La Grange Park, IL.

Chilton, A.B, J.K. Shultis and R.E. Faw (1984) Principles of Radiation Shielding, Prentice-Hall, Inc., Englewood Cliffs, NJ, pp. 468-77.

Croff, A.G. (1973) ORIGEN - The ORNL Isotope Generation and Depletion Code, ORNL-4628, Oak Ridge National Laboratory, Oak Ridge, TN.

Croff, A.G. (1980) ORIGEN2 - A Revised and Updated Version of the ORNL Isotope Generation and Depletion Code, ORNL-5621, Oak Ridge National Laboratory, Oak Ridge, TN.

Croff, A.G. (1983) "ORIGEN2: A Versatile Computer Code for Calculating the Nuclide Compositions and Characteristics of Nuclear Materials," Nucl.Tech., 62: 335-52.

El-Wakil, M.M. (1971) Nuclear Heat Transport, International Textbook Co., Scranton, OH, pp. 94-8.

England, T.R., R.E. Schenter and N.L. Whittemore (1976) Gamma and Beta Decay Power Following U-235 and Pu-239 Fission Bursts, LA-6021-MS, Los Alamos National Laboratory, Los Alamos, NM, July 1975.

England, T.R., M.G. Stamatelatos and N.L. Whittemore (1976) "Decay Heating, Gas Content, and Spectra Calculations for Fission Products," in Applied Nuclear Data Research and Development, January 1 - March 31, 1976, LA-6472-PR, Los Alamos National Laboratory, Los Alamos, NM, August 1976, pp. 60-63.

Keepin, G.R. (1965) Physics of Nuclear Kinetics, Addison-Wesley Publishing Co., Reading, MA, pp. 130-42.

LaBauve, R.J., T.R. England, D.C. George and C.W. Maynard (1982) "Fission Product Analytic Impulse Source Functions," Nucl.Tech., 56: 322-39.

RSIC (1987) RSIC Computer Code Collection, ORIGEN2: Isotope Generation and Depletion Code - Matrix Exponential Method, CCC-371, Radiation Shielding Information Center, Oak Ridge National Laboratory, Oak Ridge, TN, Nov. 1987.

Schenter, R.E., F. Schmittroth and T.R. England (1977) "Integral Determination of Fission Product Inventory Decay Power," Review Paper No. 15, Fission Product Nuclear Data IAEA-213, Volume 2, presented at the 2nd IAEA Advisory Group Meeting, held in Petten, Netherlands, 5-9 September 1977.

Tong, L.S. and J. Weisman (1979) Thermal Analysis of Pressurized Water Reactors, 2nd edition, American Nuclear Society, La Grange Park, IL, pp. 50-4.

Weisman, J. (1977) Elements of Nuclear Reactor Design, Elsevier Scientific Publ. Co., Amsterdam, pp. 172-4.

Table C.1 Empirical Constant Set Employed for Gamma Source Term.

Coefficient Index (j)	Alpha (unitless)	Lamda (1/sec)
1	2.808E-11	7.332E-10
2	6.038E-10	4.335E-08
3	3.227E-08	1.932E-07
4	4.055E-07	1.658E-06
5	8.439E-06	2.147E-05
6	2.421E-04	2.128E-04
7	1.792E-03	1.915E-03
8	2.810E-02	1.769E-02
9	1.516E-01	1.652E-01
10	4.162E-01	1.266E+00
11	1.053E-01	5.222E+00

APPENDIX D

FORTRAN PROGRAMS FOR CALCULATING VEHICLE TRAJECTORIES

NEPTRAJ.FOR

```
C     NEPTRAJ.FOR
C
C     THIS PROGRAM CALCULATES THE COORDINATES OF A MARS-MISSION
C     NEP CARGO VEHICLE SPIRALLING OUTWARD FROM THE SAME ORBIT AS
C     THE SPACE STATION.
C
C     INITIALIZE VARIABLES*****************************************
      IMPLICIT REAL*8 (A-H,O-Z)
      PARAMETER (MXPARM=50, NEQ=5)
      PARAMETER (PI=3.141592654, R_EARTH=6378150.0)
      DIMENSION PARAM(MXPARM), Y(NEQ)
      INTRINSIC FLOAT
      EXTERNAL  FCN, IVPRK, SSET, UMACH
C
      CALL UMACH(-2,9)
      OPEN(UNIT=9,FILE='NEPTRAJ.DAT',STATUS='NEW')
C
C     SET INITIAL VALUES ******************************************
C     NORMALIZE RADIUS AND MASS
C
C     Y1 = radial velocity
C     Y2 = anglar velocity
C     Y3 = radius from center of earth
C     Y4 = phi - the polar angle
C     Y5 = mass of vehicle
C
      R = R_EARTH + 450000.0
      M = 897700.0
      VR= 0.0
      OMEGA = 1.11899E-3
      T = 0.0
      Y(1) = VR
      Y(2) = OMEGA
      Y(3) = R
      Y(4) = 0.0
      Y(5) = M
C
      WRITE(9,50)T,Y(3),Y(4)
C
C     SET TOLERANCE  AND PARAMETERS*******************************************
C
      TOL = 0.0001
C
C     SET IVPRK PARAMETERS
C
      CALL DSET (MXPARM, 0.0, PARAM, 1)
      PARAM(2) = 1.0e-4
      PARAM(3) = 3600.0
      PARAM(10) = 2.0
      PARAM(4) = 100000.0
C
C       CALL IVPRK*************************************************
```

```
C
      IDO = 1
C
C     SHORT TIME-STEP FOR 0 < T < 30 DAYS
C
      DO 100 ISTEP= 60, 2592000, 60
         TEND= FLOAT(ISTEP)
       CALL DIVPRK (IDO, NEQ, FCN, T, TEND, TOL, PARAM, Y)
         WRITE(9,50)T,Y(3),Y(4)
100   CONTINUE
C
C     QUIT IMSL, DELETE WORK SPACE, ECT...**************************
C
      IDO=3
      CALL DIVPRK (IDO, NEQ, FCN, T, TEND, TOL, PARAM, Y)
      CLOSE(UNIT=9)
C
50    FORMAT(1X,3(1PD20.13,2X))
C
      END
C
C     SET UP EQUATIONS*************************************************
C
      SUBROUTINE FCN (NEQ, T, Y, YPRIME)
      IMPLICIT REAL*8 (A-H,O-Z)
      REAL*8 MU, IMPULSE, M
      DIMENSION Y(NEQ), YPRIME(NEQ)
C
      IMPULSE = 5000.0
      VJ = 9.80665 * IMPULSE
      MU = 3.98619E14
      BETA = 0.00280752
C
C     Y1 = radial velocity
C     Y2 = anglar velocity
C     Y3 = radius from center of earth
C     Y4 = phi - the polar angle
C     Y5 = mass of vehicle
C
      YPRIME(1) = -MU/(Y(3)**2.0) + Y(2)**2.0*Y(3)
      YPRIME(2) = -2*Y(1)*Y(2)/ Y(3) + VJ*BETA/ Y(5)
     &  / Y(3)
      YPRIME(3) = Y(1)
      YPRIME(4) = Y(2)
      YPRIME(5) = -BETA
C
      RETURN
      END
```

NEPDOSE.FOR

```
C     NEPDOSE.FOR
C
C     THIS PROGRAM READS THE TRAJECTORY DATA FOR THE NEP VEHICLE
C     AND CALCULATES SEPARATION DISTANCE BETWEEN IT AND SFF.
C
C     INITIALIZE VARIABLES**************************************
C
      IMPLICIT REAL*8(A-H,O-Z)
      PARAMETER (PI=3.141592654, R_EARTH = 6378150.0)
      CHARACTER*1 LAG
      DIMENSION TIME(0:43500),R_NEP(0:43500),PHI_NEP(0:43500)
C
C     INITIALIZE PARAMETERS FOR DOSE CALCULATION
C
      OPER_DR = 385.72                    !(Sv/s @ 1m)
      R_SS = R_EARTH + 450000.0
      OMEGA = 1.11899E-3
C
C     READ NEP TRAJECTORY DATA
C
      OPEN(UNIT=9,FILE='NEPTRAJ.DAT',STATUS='OLD')
      DO 10 I=0,43200
         READ(9,*)TIME(I),R_NEP(I),PHI_NEP(I)
10    CONTINUE
      CLOSE(UNIT=9)
C
C     READ VALUES OF INITIAL SEPARATION AT LAUNCH
C
      READ(5,*)SDINIT,SDFINAL,DELSD
      READ(5,1000)LAG        !- FOR SSF LAGGING, + FOR SSF LEADING
      SDINIT = SDINIT * 1000.
      SDFINAL = SDFINAL * 1000.
      DELSD = DELSD * 1000.
C
C     BEGIN LOOP FOR DIFFERENT INITIAL SEPARATIONS
C
      SEPDIST = SDINIT
100   PHI0 = DACOS(-(SEPDIST**2 - 2*R_SS**2) / (2.0*R_SS**2))
      DI_2 = SEPDIST**2
      CUM_DOSE = 0.0
C
      ALT_NEP = (R_NEP(0) - R_EARTH) / 1000.
      REV_NEP = PHI_NEP(0) / (2*PI)
      REV_SS = 0.0
      SD = SEPDIST / 1000.
      IF(LAG.EQ.'-')WRITE(6,1100)SD
      IF(LAG.EQ.'+')WRITE(6,1200)SD
      WRITE(6,1300)
      WRITE(6,1400)TIME(0),ALT_NEP,REV_NEP,REV_SS,SD,CUM_DOSE
C
C     PRINTOUT EVERY MINUTE FOR MINUTES 0 - 120
C
      DO 300 I=1,120
          IF(LAG.EQ.'-')THEN
            PHI_SS = OMEGA * TIME(I) - PHI0
```

```
          ELSE
            PHI_SS = OMEGA * TIME(I) + PHI0
          ENDIF
          DELX = (R_SS*DCOS(PHI_SS)) - (R_NEP(I)*DCOS(PHI_NEP(I)))
          DELY = (R_SS*DSIN(PHI_SS)) - (R_NEP(I)*DSIN(PHI_NEP(I)))
          DF_2 = DELX**2 + DELY**2
          D_2 = (DF_2 + DI_2)/2.0
          D_INCR = (OPER_DR/D_2) * 60.0
          CUM_DOSE = CUM_DOSE + D_INCR
          DI_2 = DF_2
200       CONTINUE
          ITM = I
          ALT_NEP = (R_NEP(ITM) - R_EARTH) / 1000.
          REV_NEP = PHI_NEP(ITM) / (2*PI)
          REV_SS = PHI_SS / (2*PI)
          SD = DSQRT(DF_2) / 1000.
          TM = TIME(ITM) / 3600.
          WRITE(6,1400)TM,ALT_NEP,REV_NEP,REV_SS,SD,CUM_DOSE
300     CONTINUE
C
C       PRINTOUT EVERY HOUR FOR HOURS 3 - 48
C
        DO 500 J=3,48
          DO 400 I=(60*J-59) , (60*J)
            IF(LAG.EQ.'-')THEN
              PHI_SS = OMEGA * TIME(I) - PHI0
            ELSE
              PHI_SS = OMEGA * TIME(I) + PHI0
            ENDIF
            DELX = (R_SS*DCOS(PHI_SS)) - (R_NEP(I)*DCOS(PHI_NEP(I)))
            DELY = (R_SS*DSIN(PHI_SS)) - (R_NEP(I)*DSIN(PHI_NEP(I)))
            DF_2 = DELX**2 + DELY**2
            D_2 = (DF_2 + DI_2)/2.0
            D_INCR = (OPER_DR/D_2) * 60.0
            CUM_DOSE = CUM_DOSE + D_INCR
            DI_2 = DF_2
400       CONTINUE
          ITM = J*60
          ALT_NEP = (R_NEP(ITM) - R_EARTH) / 1000.
          REV_NEP = PHI_NEP(ITM) / (2*PI)
          REV_SS = PHI_SS / (2*PI)
          SD = DSQRT(DF_2) / 1000.
          TM = TIME(ITM) / 3600.
          WRITE(6,1400)TM,ALT_NEP,REV_NEP,REV_SS,SD,CUM_DOSE
500     CONTINUE
C
C       PRINTOUT EVERY DAY FOR DAYS 3 - 30
C
        DO 700 J=3,30
          DO 600 I=(1440*J-1439) , (1440*J)
            IF(LAG.EQ.'-')THEN
              PHI_SS = OMEGA * TIME(I) - PHI0
            ELSE
              PHI_SS = OMEGA * TIME(I) + PHI0
            ENDIF
            DELX = (R_SS*DCOS(PHI_SS)) - (R_NEP(I)*DCOS(PHI_NEP(I)))
            DELY = (R_SS*DSIN(PHI_SS)) - (R_NEP(I)*DSIN(PHI_NEP(I)))
            DF_2 = DELX**2 + DELY**2
```

```
          D_2 = (DF_2 + DI_2)/2.0
          D_INCR = (OPER_DR/D_2) * 60.0
          CUM_DOSE = CUM_DOSE + D_INCR
          DI_2 = DF_2
600       CONTINUE
          ITM = J*1440
          ALT_NEP = (R_NEP(ITM) - R_EARTH) / 1000.
          REV_NEP = PHI_NEP(ITM) / (2*PI)
          REV_SS = PHI_SS / (2*PI)
          SD = DSQRT(DF_2) / 1000.
          TM = TIME(ITM) / 3600.
          WRITE(6,1400)TM,ALT_NEP,REV_NEP,REV_SS,SD,CUM_DOSE
700     CONTINUE
C
        SEPDIST = SEPDIST + DELSD
        IF(SEPDIST.LE.SDFINAL)THEN
          GO TO 100
        ELSE
          STOP
        ENDIF
C
1000    FORMAT(A1)
1100    FORMAT(/1X,'INITIAL SEPARATION DISTANCE: ',F6.1,' km'/
       $         1X,'(SSF LAGGING THE NEP VEHICLE)'/)
1200    FORMAT(/1X,'INITIAL SEPARATION DISTANCE: ',F6.1,' km'/
       $         1X,'(SSF LEADING THE NEP VEHICLE)'/)
1300    FORMAT(/1X,'  TIME (hr)',4X,'ALT (km)',4X,'REV_NEP',5X,'REV_SS',
       $         6X,'SEP DIST',3X,'DOSE (Sv)'/1X,52X,'(km)'/)
1400    FORMAT(1X,6(1PE11.4,1X))
C
        END
```

NTRTRAJ.FOR

```
C     NTRTRAJ.FOR
C
C     THIS PROGRAM CALCULATES THE COORDINATES OF A MARS-MISSION
C     NTR CARGO VEHICLE SPIRALLING OUTWARD FROM THE SAME ORBIT AS
C     THE  SPACE STATION.
C
C     INITIALIZE VARIABLES*****************************************
      IMPLICIT REAL*8 (A-H,O-Z)
      PARAMETER (MXPARM=50, NEQ=5)
      PARAMETER (PI=3.141592654, R_EARTH=6378150.0)
      DIMENSION PARAM(MXPARM), Y(NEQ)
      INTRINSIC FLOAT
      EXTERNAL  FCN, IVPRK, SSET, UMACH
C
      CALL UMACH(-2,9)
      OPEN(UNIT=9,FILE='NTRTRAJ.DAT',STATUS='NEW')
C
C     SET INITIAL VALUES ******************************************
C     NORMALIZE RADIUS AND MASS
C
C     Y1 = radial velocity
C     Y2 = anglar velocity
C     Y3 = radius from center of earth
C     Y4 = phi - the polar angle
C     Y5 = mass of vehicle
C
      R = R_EARTH + 450000.0
      M = 456000.0
      VR= 0.0
      OMEGA = 1.11899E-3
      T = 0.0
      Y(1) = VR
      Y(2) = OMEGA
      Y(3) = R
      Y(4) = 0.0
      Y(5) = M
C
      WRITE(9,50)T,Y(3),Y(4)
C
C     SET TOLERANCE  AND PARAMETERS*******************************
C
      TOL = 0.0001
C
C     SET IVPRK PARAMETERS
C
      CALL DSET (MXPARM, 0.0, PARAM, 1)
      PARAM(2) = 1.0e-4
      PARAM(3) = 3600.0
      PARAM(10) = 2.0
      PARAM(4) = 100000.0
C
C       CALL IVPRK*************************************************
C
      IDO = 1
C
```

```
C      SHORT TIME-STEP FOR 0 < T < 23 MINUTES
C
       DO 100 ISTEP= 60, 1380, 60
          TEND= FLOAT(ISTEP)
        CALL DIVPRK (IDO, NEQ, FCN, T, TEND, TOL, PARAM, Y)
          WRITE(9,50)T,Y(3),Y(4)
100    CONTINUE
C
C      QUIT IMSL, DELETE WORK SPACE, ECT...**************************
C
       IDO=3
       CALL DIVPRK (IDO, NEQ, FCN, T, TEND, TOL, PARAM, Y)
       CLOSE(UNIT=9)
C
50     FORMAT(1X,3(1PD20.13,2X))
C
       END
C
C      SET UP EQUATIONS*************************************************
C
       SUBROUTINE FCN (NEQ, T, Y, YPRIME)
       IMPLICIT REAL*8 (A-H,O-Z)
       REAL*8 MU, IMPULSE, M
       DIMENSION Y(NEQ), YPRIME(NEQ)
C
       IMPULSE = 900.0
       VJ = 9.80665 * IMPULSE
       MU = 3.98619E14
       BETA = 126.0
C
C      Y1 = radial velocity
C      Y2 = anglar velocity
C      Y3 = radius from center of earth
C      Y4 = phi - the polar angle
C      Y5 = mass of vehicle
C
       YPRIME(1) = -MU/(Y(3)**2.0) + Y(2)**2.0*Y(3)
       YPRIME(2) = -2*Y(1)*Y(2)/ Y(3) + VJ*BETA/ Y(5)
      &  / Y(3)
       YPRIME(3) = Y(1)
       YPRIME(4) = Y(2)
       YPRIME(5) = -BETA
C
       RETURN
       END
```

NTRDOSE.FOR

```
C     NTRDOSE.FOR
C
C     THIS PROGRAM READS THE TRAJECTORY DATA FOR THE NTR VEHICLE
C     AND CALCULATES SEPARATION DISTANCE BETWEEN IT AND SFF.
C
C     INITIALIZE VARIABLES**************************************
C
      IMPLICIT REAL*8(A-H,O-Z)
      PARAMETER (PI=3.141592654, R_EARTH = 6378150.0)
      CHARACTER*1 LAG
      DIMENSION TIME(0:25),R_NTR(0:25),PHI_NTR(0:25)
C
C     INITIALIZE PARAMETERS FOR DOSE CALCULATION
C
      OPER_DR = 225714.0                    !(Sv/s @ 1m)
      R_SS = R_EARTH + 450000.0
      OMEGA = 1.11899E-3
C
C     READ NTR TRAJECTORY DATA
C
      OPEN(UNIT=9,FILE='NTRTRAJ.DAT',STATUS='OLD')
      DO 10 I=0,23
         READ(9,*)TIME(I),R_NTR(I),PHI_NTR(I)
10    CONTINUE
      CLOSE(UNIT=9)
C
C     READ VALUES OF INITIAL SEPARATION AT LAUNCH
C
      READ(5,*)SDINIT,SDFINAL,DELSD
      READ(5,1000)LAG       !- FOR SSF LAGGING, + FOR SSF LEADING
      SDINIT = SDINIT * 1000.
      SDFINAL = SDFINAL * 1000.
      DELSD = DELSD * 1000.
C
C     BEGIN LOOP FOR DIFFERENT INITIAL SEPARATIONS
C
      SEPDIST = SDINIT
100   PHI0 = DACOS(-(SEPDIST**2 - 2*R_SS**2) / (2.0*R_SS**2))
      DI_2 = SEPDIST**2
      CUM_DOSE = 0.0
C
      ALT_NTR = (R_NTR(0) - R_EARTH) / 1000.
      REV_NTR = PHI_NTR(0) / (2*PI)
      REV_SS = 0.0
      SD = SEPDIST / 1000.
      IF(LAG.EQ.'-')WRITE(6,1100)SD
      IF(LAG.EQ.'+')WRITE(6,1200)SD
      WRITE(6,1300)
      WRITE(6,1400)TIME(0),ALT_NTR,REV_NTR,REV_SS,SD,CUM_DOSE
C
C     PRINTOUT EVERY MINUTE FOR MINUTES 0 - 23
C
      DO 300 I=1,23
          IF(LAG.EQ.'-')THEN
            PHI_SS = OMEGA * TIME(I) - PHI0
```

```
          ELSE
            PHI_SS = OMEGA * TIME(I) + PHI0
          ENDIF
          DELX = (R_SS*DCOS(PHI_SS)) - (R_NTR(I)*DCOS(PHI_NTR(I)))
          DELY = (R_SS*DSIN(PHI_SS)) - (R_NTR(I)*DSIN(PHI_NTR(I)))
          DF_2 = DELX**2 + DELY**2
          D_2 = (DF_2 + DI_2)/2.0
          D_INCR = (OPER_DR/D_2) * 60.0
          CUM_DOSE = CUM_DOSE + D_INCR
          DI_2 = DF_2
200       CONTINUE
          ITM = I
          ALT_NTR = (R_NTR(ITM) - R_EARTH) / 1000.
          REV_NTR = PHI_NTR(ITM) / (2*PI)
          REV_SS = PHI_SS / (2*PI)
          SD = DSQRT(DF_2) / 1000.
          TM = TIME(ITM) / 3600.
          WRITE(6,1400)TM,ALT_NTR,REV_NTR,REV_SS,SD,CUM_DOSE
300     CONTINUE
C
        SEPDIST = SEPDIST + DELSD
        IF(SEPDIST.LE.SDFINAL)THEN
          GO TO 100
        ELSE
          STOP
        ENDIF
C
1000    FORMAT(A1)
1100    FORMAT(/1X,'INITIAL SEPARATION DISTANCE: ',F6.1,' km'/
       $        1X,'(SSF LAGGING THE NTR VEHICLE)'/)
1200    FORMAT(/1X,'INITIAL SEPARATION DISTANCE: ',F6.1,' km'/
       $        1X,'(SSF LEADING THE NTR VEHICLE)'/)
1300    FORMAT(/1X,'  TIME (hr)',4X,'ALT (km)',4X,'REV_NTR',5X,'REV_SS',
       $        6X,'SEP DIST',3X,'DOSE (Sv)'/1X,52X,'(km)'/)
1400    FORMAT(1X,6(1PE11.4,1X))
C
        END
```

NASA
National Aeronautics and Space Administration

Report Documentation Page

1. Report No.	2. Government Accession No.	3. Recipient's Catalog No.
NASA CR - 185185		

4. Title and Subtitle
A Radiological Assessment of Nuclear Power and Propulsion Operations Near Space Station Freedom

5. Report Date
March 1990

6. Performing Organization Code

7. Author(s)
Wesley E. Bolch, J. Kelly Thomas, K. Lee Peddicord, Paul Nelson, David T. Marshall, and Donna M. Busche

8. Performing Organization Report No.

10. Work Unit No.

9. Performing Organization Name and Address
Department of Nuclear Engineering
Texas A&M University
College Station, Texas 77843

11. Contract or Grant No.

13. Type of Report and Period Covered
Contract Report
1/88 - 1/90

12. Sponsoring Agency Name and Address
National Aeronautics and Space Administration
Lewis Research Center
Cleveland, Ohio 44135-3191

14. Sponsoring Agency Code

15. Supplementary Notes
Project Manager, Steve M. Stevenson, Advanced Space Analysis Office, NASA Lewis Research Center

16. Abstract

This study was conducted to identify scenarios involving the use of nuclear power systems in the vicinity of Space Station Freedom (SSF) and to quantify their radiological impact on the SSF crew. Several of the scenarios developed relate to the use of SSF as an evolutionary transportation node for lunar and Mars missions. In particular, radiation doses delivered to SSF crew were calculated for both the launch and subsequent return of a Nuclear Electric Propulsion (NEP) cargo vehicle and a Nuclear Thermal Rocket (NTR) personnel vehicle to low earth orbit. The use of nuclear power on co-orbiting platforms and the storage and handling issues associated with radioisotope power systems were also explored as they relate to SSF. A central philosophy in these analyses was the utilization of a radiation dose budget, defined as the difference between recommended dose limits from all radiation sources and estimated doses received by crew members from natural space radiations. Consequently, for each scenario examined, the dose budget concept was used to identify and quantify constraints on operational parameters such as launch separation distances, returned vehicle parking distances, and reactor shutdown times prior to vehicle approach. The results from this study indicate that realistic scenarios do not exist which would preclude the use of nuclear power sources in the vicinity of SSF. The radiation dose to the SSF crew can be maintained at safe levels solely by implementing proper and reasonable operating procedures.

17. Key Words (Suggested by Author(s))	18. Distribution Statement
Space Station - Radiation Radiation Dose Assessment NEP and NTR Vehicles Radioisotope Power Sources	Unclassified - Unlimited

19. Security Classif. (of this report)	20. Security Classif. (of this page)	21. No of pages	22. Price*
Unclassified	Unclassified	108	A06

NASA FORM 1626 OCT 86

*For sale by the National Technical Information Service, Springfield, Virginia 22161